Electrical Lab-on-a-Chip for *Ex Vivo* Study on the Influence of Electric Fields on Pollen Cells

Carlos G. Agudelo

A Thesis
In the Department of
Mechanical and Industrial Engineering

Presented in Partial Fulfillment of the Requirements
For the degree of
Doctor of Philosophy (Mechanical and Industrial Engineering) at
Concordia University
Montréal, Québec

April 2015

CONCORDIA UNIVERSITY

School of Graduate Studies

This is to certify that the thesis prepared

By: **Carlos G. Agudelo**

Entitled: **Electrical Lab-on-a-Chip for *Ex Vivo* Study on the Influence of Electric Fields on Pollen Cells**

and submitted in partial fulfillment of the requirements for the degree of

Doctor of Philosophy (Mechanical and Industrial Engineering)

complies with the regulations of the University and meets the accepted standards with respect to originality and quality.

Signed by the final Examining Committee:

_____Chair
Dr. Luis Rodrigues

_____Examiner
Dr. Lyes Kadem

_____Examiner
Dr. Rama B. Bhat

_____External to Program
Dr. M. Zahangir Kabir

_____External Examiner
Dr. Anja Geitmann

_____External Examiner
Dr. Krishnan Venkatakrishnan

_____Supervisor
Dr. Muthukumaran Packirisamy

Approved by _____
Chair of Department or Graduate Program Director

_____ 2015

_____
Dean of Faculty

Abstract

Electrical Lab-on-a-Chip for *Ex Vivo* Study on the Influence of Electric Fields on Pollen Cells

Carlos G. Agudelo, Ph.D.
Concordia University, 2015

Pollen tubes are polarly growing plant cells that are able to respond to a combination of chemical, mechanical, and electrical cues during their journey through the flower pistil in order to accomplish fertilization. How signals are perceived and processed in the pollen tube is still poorly understood and evidence for electrical guidance, in particular, is vague and highly contradictory. To generate reproducible experimental conditions for *ex vivo* pollen cell cultures, here we present a low-cost, reusable Electrical Lab-on-a-Chip (ELoC) for investigating the influence of electric fields on growing cells. Viability of pollen growth using a structured microfluidic network is first investigated and validated. Then the integration of microelectrodes into the device is addressed in detail. Characterization of the pollen growth medium conductivity and simulation of the ELoC electrical configuration were carried out to define the experimental conditions. Reusability of the microdevice is achieved by structuring the design into two separate rebondable modules: a microfluidic module and a microelectrode module. Two experimental approaches were realized: a batch design for exposing simultaneously a large number of cells to a global electric field, and a single-cell design in which a localized electric field is applied to individual cells. Extensive batch results indicate that DC fields were inhibitory above 6 V/cm. However, switching to AC fields re-established pollen tube growth at frequencies above 100 mHz, suggesting a significant role of the

medium conductivity in controlling the cellular response. Unlike macroscopic open-assay experimental setups, single-cell tests further indicate no reorientation of pollen tube growth, suggesting that previously reported tropic behavior was caused by ion movement in the substrate rather than by a direct effect of the electric field on the cell.

Acknowledgments

I would like to express my deep appreciation and gratitude to my advisor, Dr. Muthukumaran Packirisamy, for his invaluable guidance and continuous support.

Very special thanks to Dr. Anja Geitmann and her lab team at the Botanical Garden for their priceless collaboration and caring encouragement.

I also wish to express my great appreciation to all my lab-mates in the Optical-Bio Microsystems Laboratory of Concordia University and to the administrative staff in the Department of Mechanical and Industrial Engineering for their support.

To

Beatriz and Claudia

Table of Contents

List of Figures

List of Tables

Chapter 1 - Introduction

1.1 Introduction to Pollen

Reproduction in plants has been a topic of most interest ever since humankind began to grasp how intimate and involved the relationships between every living being on planet earth are. Sexual reproduction, in particular, is only one of the many traits humans share with our far evolutionary cousins, the plants. Since many components and processes at the cellular level are similar across the borders of biological kingdoms, it is clear that any insight into the intricacies of plant cellular behavior is not only an advance of knowledge but a further step into the understanding of our own human complexity.

Flowering plants reproduction is a convoluted process that requires a series of precisely choreographed steps, the details of which vary among species (Geitmann and Palanivelu, 2007). The reproduction cycle of *angiosperms*[1] starts with the production of pollen by the *stamen*, the male reproductive organ of the flower (see Figure 1.1). Each pollen grain represents a male gametophyte and consists of a vegetative *cell*[2] and a generative cell. The latter divides to form two sperm cells, the male *gametes*[3]. The pollen is released by the opening of the anther, the pollen producing part of the stamen, and transferred to the *pistil*, the female reproductive structure, either by animals (insects, birds, small mammals) or by wind. The pistil of the pollinated flower holds in its ovary

[1] Angiosperms (flowering plants) are the most dominant group of land plants.

[2] Cell: the structural and functional basic unit of life.

[3] A gamete is a cell that fuses with another cell during fertilization in organisms that reproduce sexually.

the ovules that produce the female gametophyte, a multicellular structure that comprises the *egg cell*.

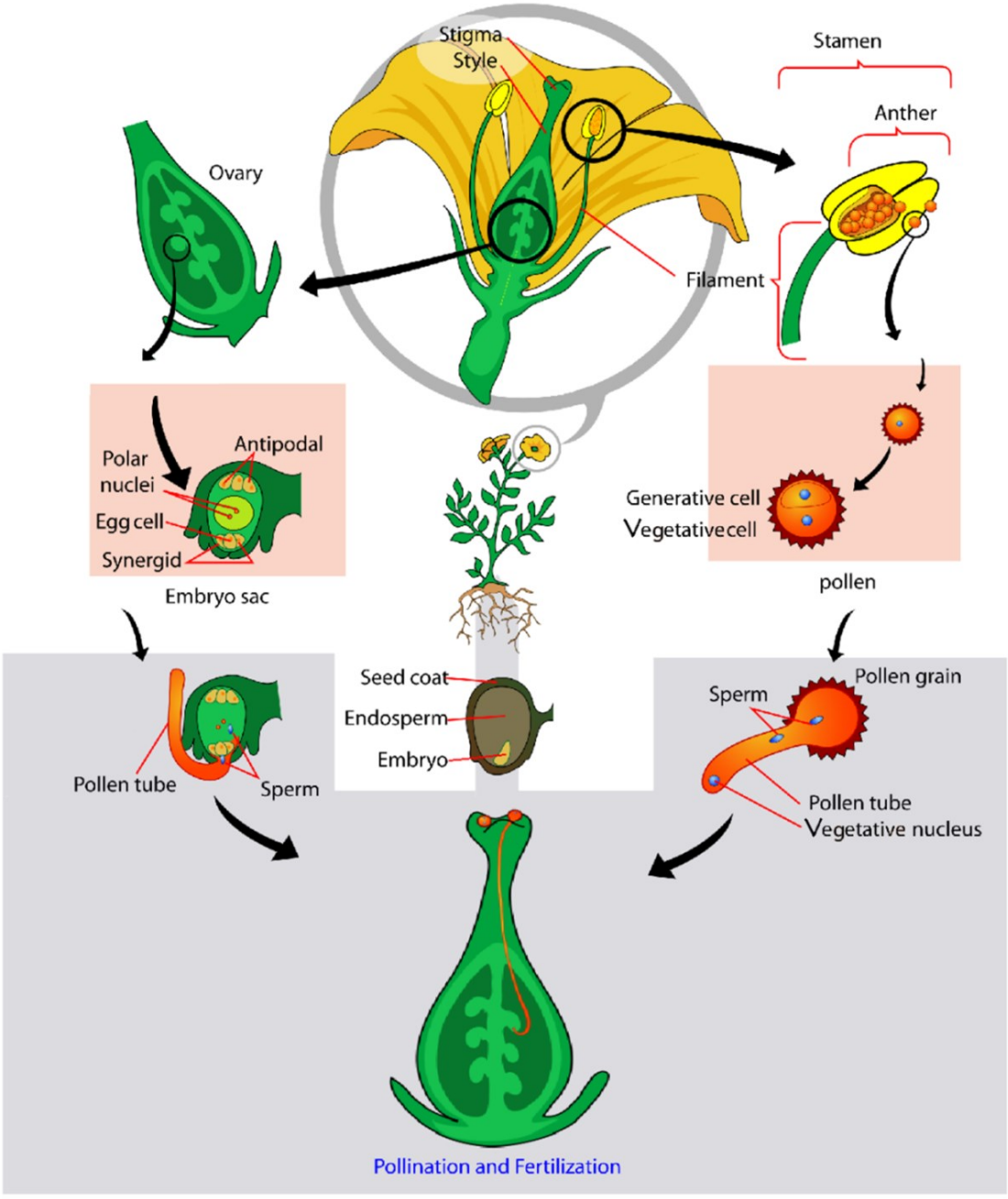

Figure 1.1 Angiosperm life cycle[4].

[4] Figure taken from the Wikimedia Commons.

Once a pollen grain lands on a compatible pistil, it germinates in response to a sugary fluid secreted by the mature *stigma*. The vegetative cell then produces the pollen tube (Figure 1.2), which carries the sperm cells within its *cytoplasm*[5]. This tube is the transportation medium of the immobile male gametes to reach the ovule. To attain the ovule, which is nestled deep within the pistil, the pollen tube must drill its way through a series of tissues all the while following guidance cues emitted by the pistil tissues and by the female gametophyte. Once the pollen tube successfully penetrates an ovule, it injects the two sperm cells by bursting its tip. One of the male gametes fertilizes the egg cell to form an embryo (the future plant), and the other one fuses with both *polar nuclei* of the central cell to form the *endosperm*, which serves as the embryo's food supply. Following this double fertilization, the ovary develops into a fruit and the ovules into seeds.

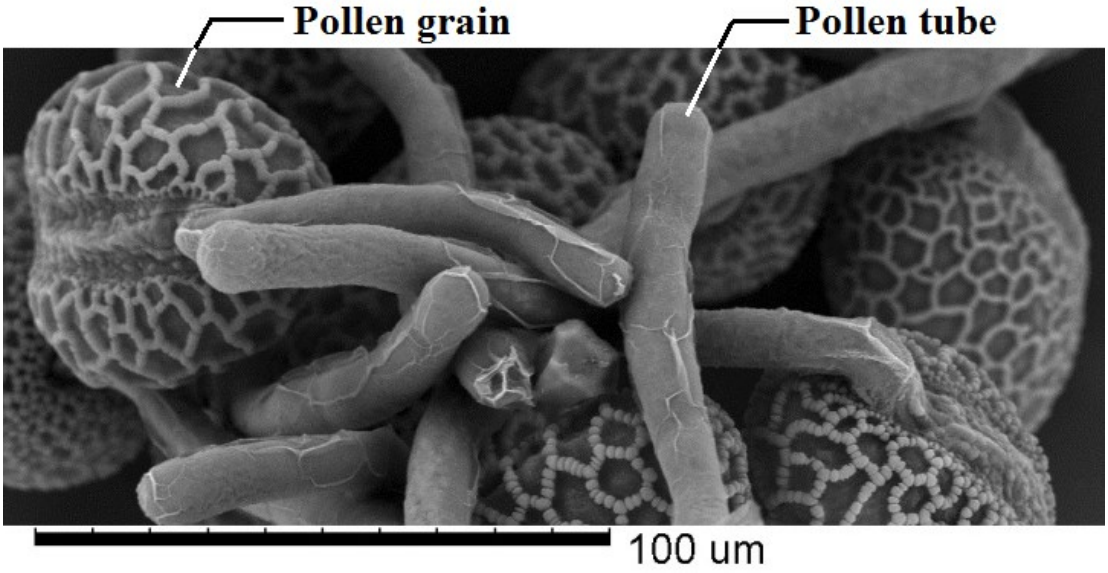

Figure 1.2 Scanning electron microscope (SEM) image of pollen tubes growing from lily pollen grains.

[5] The cytoplasm is the aqueous contents of a cell, enveloped by the plasma membrane. It contains the cell organelles, structural proteins, and surrounds the nucleus and the vacuole.

Pollen tubes are an excellent experimental model for the understanding of plant cell behavior (Malhó, 1998). They are easily cultured *in vitro*[6] and have a very dynamic *cytoskeleton*[7] that *polymerizes*[8] at very high rates, providing the pollen tube with interesting growth properties (Gossot and Geitmann, 2007). Unlike most other plant cells, the pollen tube focuses its cellular growth activity on a very small surface at the extremity of the cell. Interestingly, this kind of tip growth is analogous to the apical extension of axons in animal neuron cells which has the purpose of forming synaptic connections. Both pollen tubes and axons share striking similarities in their quest for reaching remote targets with remarkable reproducible precision (Palanivelu and Preuss, 2000).

The pollen tube accomplishes this tip growth through a coordinated transport process that transfers material from distributed sites of synthesis (numerous *Golgi*[9] located over the entire cytoplasm) to the site of release at the localized growing apex. The

---

[6] A procedure performed *in vitro* (latin: *within the glass*) is performed in a laboratory environment, such as in a test tube or Petri dish, on a partial or dead organism, in contrast with a process that occurs *in vivo*, which takes place in a whole living organism.

[7] The cytoskeleton is a cellular skeleton contained within the cytoplasm that provides the cell with structure and shape. In plant cells the cytoskeleton is composed of microfilaments (or actin filaments) and microtubules.

[8] Polymerization is a process that binds monomer molecules together in a chemical reaction to form three-dimensional networks or polymer chains.

[9] The Golgi apparatus is an organelle composed of stacks of membrane-bound structures that specializes in modifying, sorting, and packaging macromolecules for cell secretion (exocytosis) or use within the cell. Important for plant cells, the Golgi apparatus is the site of polysaccharide synthesis.

microfilaments are used as railways by secretory *vesicles*[10] dispatched and filled with precursor material. These secretory vesicles carry the precursor molecules that are added to the *cell wall*[11], whereas the vesicle membrane itself is inserted into the expanding plasma membrane. Growth is sustained by the continuous delivery of secretory vesicles along the periphery of the tube (in the forward direction) into an annulus-shaped region at the shoulder of the apex (Bove et al., 2008). Excess secretory vesicles and *endocytotic*[12] vesicles coming from the extreme apex are circulated backwards by a rearward flow mediated by microfilaments in the center of the tube. This vesicle flow pattern creates a cone-shaped vesicle pool in the apical region (Figure 1.3). A change in growth direction is preceded by a re-orientation of the cone-shaped vesicle pool which in turn is governed by differential polymerization within the actin array (Bou Daher and Geitmann, 2011).

[10] A vesicle is a small organelle consisting of a lipid bilayer membrane that is able to enclose a variety of cell materials.

[11] The cell wall is the tough layer that surrounds the plasma membrane in plant cells. It provides structural support and protection, and acts as a filtering mechanism. It also acts as a pressure vessel, preventing over-expansion when water enters the cell. It is mainly composed of cellulose, pectin, and, in the case of the pollen, callose. Animal cells do not have cell walls.

[12] Endocytosis is a process by which cells absorb large molecules that cannot pass through the plasma membrane by engulfing them. The opposite process is exocytosis.

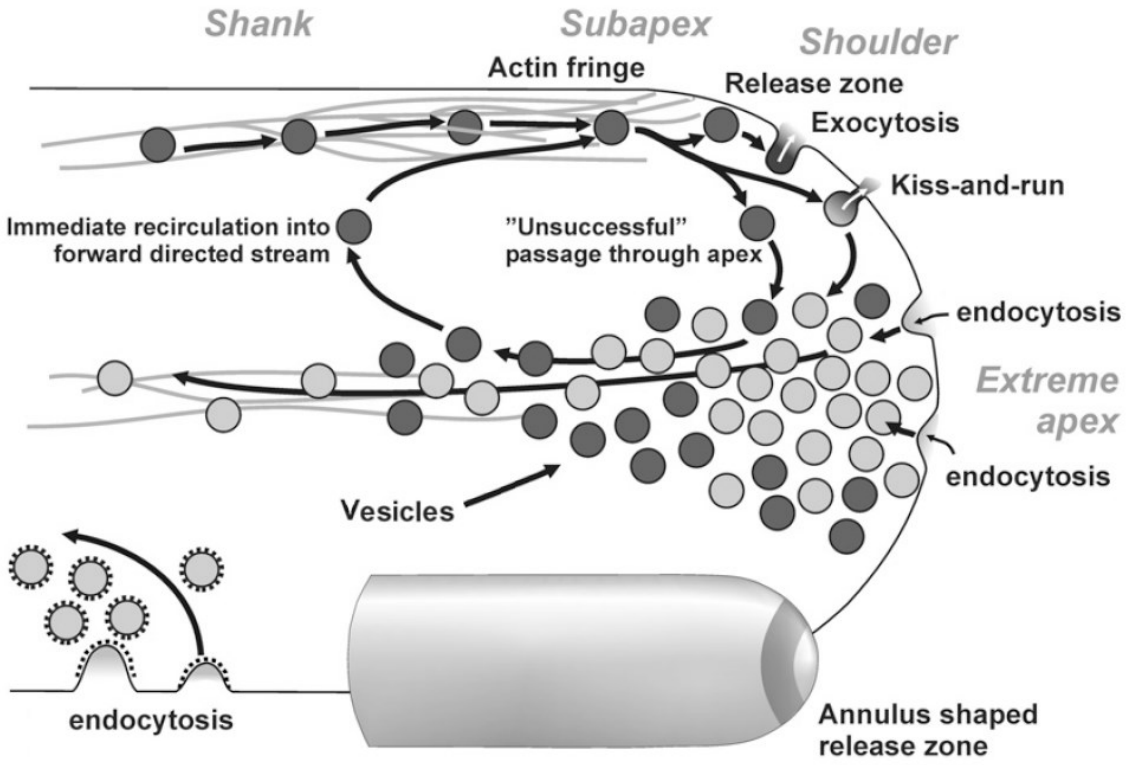

Figure 1.3 Schematic illustrating the principal directions of vesicle flow in the apical region of a pollen tube[13]. Secretory vesicles (dark gray) carry material to the apex, whereas endocytotic vesicles (light gray) carry materials from the apex.

This tip growth mechanism allows the cell to perform two important functions: mechanical invasion of a substrate and tropism (response to directional guidance cues). The invasive force of the pollen tube is generated by the high internal hydrostatic pressure (or *turgor* pressure, typically in the range of a few standard atmospheres) which is allowed by the presence of the tough cell wall (Benkert et al., 1997). Only at the apex, the cell wall is compliant and yields to internal pressure, therefore exerting an effective force against the invaded substrate. *Pectin* plays an important role in producing a soft tip

[13] Figure modified from (Bove et al., 2008).

and the later stiffening of the cell wall below the apical dome (Parre and Geitmann, 2005; Fayant et al., 2010). The combined effect of stretching the cell wall by turgor pressure and the assembly of new soft wall material enables pollen tip growth. Additionally, by extending the cell wall only at the tip, the friction between the tube and the invaded tissue is minimized (Sanati Nezhad and Geitmann, 2013).

The target towards which the pollen tube grows can be tens of centimeters away from the location of the pollen grain when the latter adheres to the stigma (Malhó, 1998). Therefore the precision with which the cellular elongation occurs requires a complex guidance process and continuous communication between the male and female partners (Geitmann and Palanivelu, 2007). On the other hand, as growth rate is a direct selection factor for fertilization success, the pollen tube is also the fastest growing plant cell with up to 2 $cm \cdot h^{-1}$ in some species. Remarkably, the pollen tube's journey through the style can result in depth-to-diameter ratios above 100:1 and up to 1000:1 in certain species, whereas classic mechanical drilling is often only effective up to 15:1 ratios. This extreme growth and the ability to follow guidance cues make the pollen tube an extraordinary model system for investigating growth behaviour (Malhó, 2006).

Extensive work has been dedicated to comprehend how the pollen tube responds to extracellular guidance signals to achieve fertilization (Geitmann and Palanivelu, 2007; Malhó, 2006; Okuda and Higashiyama, 2010). It is believed that pollen tubes react to a combination of chemical, mechanical, and electrical cues during its journey through the pistil (Chebli and Geitmann, 2007; Mascarenhas and Machlis, 1964; Robinson, 1985). However, it is not clear how these external cues work or how they are processed internally. Moreover, sensory receptors for any external cue have not been identified yet.

Nevertheless, several aspects have already been identified as central in the process of pollen tube guidance.

Chemical cues have been studied in detail (Cheung et al., 1995; Lush, 1999; Malhó, 1998; Mascarenhas and Machlis, 1964; Palanivelu and Preuss, 2000), and calcium, for example, is known to act as a chemotropic agent for pollen tubes (Mascarenhas and Machlis, 1964), whereas nitric oxide (NO) is a repulsive agent (Prado, 2004). Proteic signals emitted by the pistil or female gametophyte have been identified to guide the pollen tube *in situ* (Okuda and Higashiyama, 2010). Mechanically, the actin[14] filaments in the cytoskeleton, the peculiar cell wall, and secretory vesicle dynamics, to name a few, are some of the fundamental features readily identified as crucial, but whose role has not yet been completely elucidated (Chebli and Geitmann, 2007; Geitmann and Palanivelu, 2007). The potential role of electrical stimuli for pollen tube growth or guidance, on the other hand, is poorly understood. It is clear that the presence and transfer of ions[15] to and from the cell are important to sustain a healthy cell and particularly to control pollen tube growth (Holdaway-Clarke and Hepler, 2003). However, the very nature of the interaction between pollen tube and electrical charges is unknown, which brings forward the fundamental question on the general effect of electric fields on pollen tube growth.

---

[14] Actin is the monomeric unit of the *microfilaments*, one of the major components of the cytoskeleton.

[15] An *ion* is an atom or molecule in which the total number of electrons is not equal to the total number of protons, giving rise to a net positive or negative electrical charge.

1.2 Literature Review

A turning point in pollen research was the work of Brewbaker and Kwack (1963). Almost every subsequent *in vitro* study on pollen tube growth employs a culture medium based on the one described in this work. Brewbaker and Kwack (1963) also stressed the importance of calcium ions in pollen tube growth, which has been consistently confirmed in the literature ever since.

Investigation of the electrical phenomena in pollen tubes started with the work of Weisenseel et al. (1975). They explored the *endogenous* electric fields[16] around lily pollen tubes growing *in vitro* with a vibrating electrode interfaced by a lock-in amplifier. Based on Ohm's law, the developed probe enabled them to measure current densities as low as a few nanoamperes per square centimeter near individual cells. They found that there exists a steady flow of ions that enters the growing end of the pollen tube with a peak of approximately 500 nA/cm^2, and leaves through the grain with a maximum value of 350 nA/cm^2. This phenomenon was found to occur in pollen grains even before germination and persisted as long as the tube grows. The authors suggest that the electric behavior observed around the pollen tube may be compared with a "current dipole" (which might be a misnomer since it is not a standard term in electromagnetics phenomena[17]). Finally, a train of discrete current pulses were found in some of the pollen tubes that were about to die.

---

[16] Endogenous refers to electric fields produced within the cell, as opposed to exogenous electric fields which are externally applied to the cell.

[17] Incidentally, Weisenseel et al. (1975) mentions in the discussion section: "It is therefore difficult to imagine how the field produced by this current density could have much effect on the cell's growth…".

To perform these experiments, Weisenseel et al. (1975) reported the use of a standard growth medium, with an average resistivity of 1600 Ω-cm (625 uS/cm), on top of an ion-permeable 3-µm thick cellulose membrane employed to hold the pollen tubes underneath. No further details are given about the conductivity of the growth medium, which is considered constant. The electrode was set to vibrate at 200 Hz in a horizontal plane between two extracellular points 30 µm apart. The voltage drop measured was in the order of 150 nV. The reference electrode was typically positioned 400 µm away from the vibrating electrode. Figure 1.4 shows a sketch of the setup used by the authors.

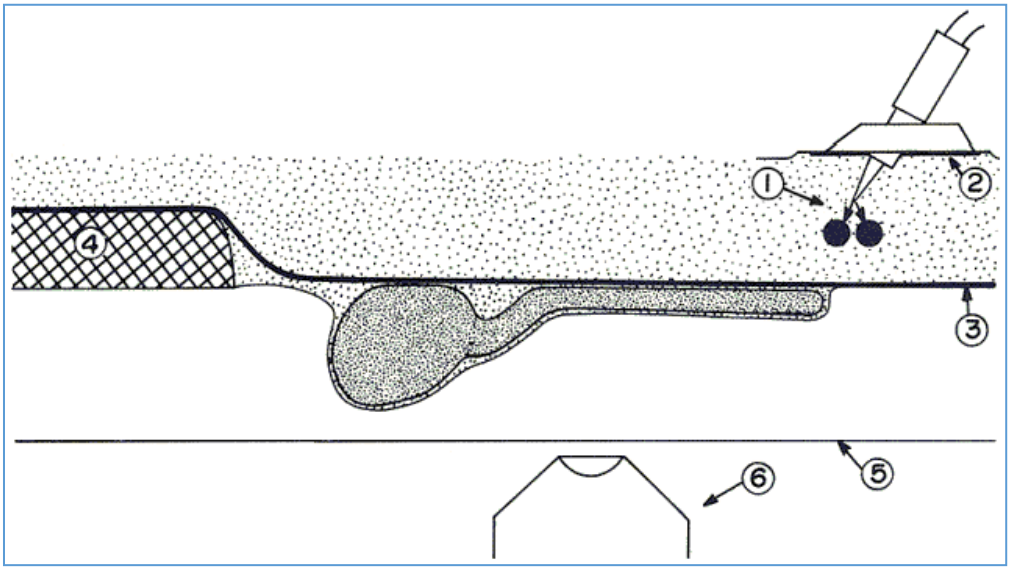

Figure 1.4 Setup used by Weisenseel et al. (1975). (1) Vibrating test electrode. (2) Reference electrode. (3) Ion-permeable cellulose membrane. (4) Nickel frame with 1.4 mm diameter holes. (5) Cover slip which closes air-filled space. (6) Inverted microscope[18].

Most likely the authors mean "electric" field since no mention of any magnetic phenomena is done throughout the paper. A current density does not produce an electric field (technically speaking a varying magnetic field does). This incorrect (and confusing) use of electromagnetic terminology has been found common in the literature.

[18] Figure taken from Weisenseel et al. (1975).

So far the work of Weisenseel et al. (1975) has been the most sophisticated approach to study the electrical behavior of pollen tubes at the micro scale. It comprises the development of a specialized device to measure electric potential in the neighborhood of individual pollen tubes. Still, this approach has several limitations. The main difficulty is the supporting and alignment of the growing pollen tubes so that they would grow horizontally and straight and not be displaced by the flow generated by the movements of the vibrating electrode. The authors somewhat alleviate this issue with the use of a cumbersome setup comprising a nickel frame to support an ion-permeable cellulose membrane. This is indeed a significant problem since flow, especially at the micro scale, would undoubtedly affect the measurements substantially. Another issue is the fact that the membrane has to be ion-permeable since electrical measurements are to be taken. No further discussion was made by the authors to assess the reliability of this membrane. Unfortunately, the membrane prevents measurements to be taken in any other plane or close to the pollen tube. As the authors noted, some uncertainties exist in the measurements, particularly in the vicinity of the grain.

What specific ions constitute the current around the pollen tube and how they affect its growth is still uncertain. However, using a variation of the vibrating electrode with a calcium-specific tip, Kühtreiber and Jaffe (1990) were able to determine that most of the entering current was made of calcium ions (Ca^{2+}), whereas the outward current contained no calcium. This active role of Ca^{2+} in the tip growth of pollen tubes was ratified by Malhó et al. (1992) and later by Pierson et al. (1994), who found a steep, tip-focused intracellular Ca^{2+} gradient from 3.0 μM at the apex to less than 0.2 μM at 20 μm from the

tip. Furthermore, the calcium influx at the tip becomes inactive in non-growing pollen tubes.

More recently, Feijó et al. (1999) employed a proton (H^+) selective vibrating electrode to assert the existence of a proton influx at the extreme apex of the pollen tube and an efflux at the base of the clear zone. The clear zone corresponds to the tip portion of the pollen tube cytoplasm in which large *organelles*[19] are excluded due to *actin* reorganization and high vesicle concentration. The extracellular proton flux pattern results in an intracellular pH gradient with an acidic domain at the tip where the protons enter the pollen tube and a constitutive[20] alkaline band at the base of the clear zone. Inhibition of pollen tube growth eliminates the acidic tip but the alkaline band persists, indicating a correlation between the proton flux and pollen tube growth. Potassium ions (K^+) have also been found to enter the apex of the pollen tube in significant amounts and to exit through the grain (Weisenseel and Jaffe, 1976). However, the role of potassium has barely been studied because of the poor performance exhibited by K^+-selective electrodes (Messerli et al., 1999). Chloride ions (Cl^-) have also been observed to exhibit an efflux at the tip and an influx along the shank (Zonia et al., 2002). Currently, the nature of the electric current measured around the pollen tube and the role of the different ions in pollen tube growth or guidance is still under research (Holdaway-Clarke and Hepler, 2003; Michard et al., 2009).

Remarkably, no further work has been performed regarding the study of endogenous electrical phenomena in pollen tubes even though considerable electric fields have been

[19] An *organelle* is a specialized membrane-bound subunit within a cell that has a specific function.

[20] *Constitutive* refers to a constant activity.

reported to be present in tissues of plants (Jaffe and Nuccitelli, 1977; McCaig et al., 2005; Robinson and Messerli, 2003). For instance, DC Electric fields up to 1 V/cm have been found in plants, mostly locally (e.g., close to wounds), and long-distance (global) bioelectric potentials have been reported to traverse the style of pollinated plants (Spanjers, 1981). Since these bioelectric potentials have the shape of action potentials (Stahlberg, 2006), one could argue that actual in vivo signals can have DC or AC components. Given these facts, it is reasonable to hypothesize that electric fields are involved in pollen tube growth and guidance.

Efforts have already been made to clarify the mechanisms of extracellular electrical signaling in pollen tubes by studying the effects of exogenous electric fields. These studies have mostly been in the form of *electrotropism*[21], which has rather limited the scope of the analysis of the influence of electric fields on pollen cells since the experiments and results are only weighed in terms of growth direction instead of the overall response of the cell as a living interacting entity.

Electrotropism was first studied by Wulff (1935), who reported that *Impatiens* pollen grew toward the anode. Later Marsh and Beams (1945) reported that *Vinca* pollen oriented toward the cathode as did Zeijlemaker (1956) for *Narcissus* pollen. However these reports were contradictory or unclear at best, which is why Wang et al. (1989) set out to reinvestigate the response of pollen to applied electric fields. Wang et al. (1989) cultured tomato and tobacco pollen tubes in a standard Brewbaker-Kwack medium with

[21] *Tropism* is a biological phenomenon that indicates growth or directed movement of an organism in response to an environmental stimulus. *Electrotropism* refers to an electrical stimulus in particular.

agar[22], which is a common method in previous works to obtain a solidified medium in open assays. A constant electric current was provided to the mixture, which was contained in a chamber made with three cover slips on a Petri dish connected to Ag-AgCl electrodes through agar-medium bridges. The authors observed that, for electric fields higher than 0.2 V/cm, the direction of growth changed toward the positive electrode for both tomato and tobacco pollen tubes after 1 h. They also reported that tobacco grains, which have three possible germination apertures, showed a tendency to germinate on the side facing the positive electrode. The tube response increased with increasing electric field strengths until 2.3 V/cm. The authors were surprised to find that the growth rate was equally decreased for tubes growing towards the negative electrode as for those growing towards the positive electrode (20% for an electric field of 0.7 V/cm).

The authors suggested that it is the voltage drop across the tube (about 0.2 mV for 5 μm diameter pollen tube) that produces the effect. It is argued that the voltage drop most certainly acts mainly on the membrane, probably by redistributing the ion channels electrophoretically, especially those for calcium, which is considered the most important chemotropic agent for pollen tubes (Mascarenhas and Machlis, 1964). In any case, the authors conclude that the understanding of electrotropism in pollen tubes will remain elusive until more detailed processes are identified.

Even though the work of Wang et al. (1989) has been central in the subject of pollen electrotropism, the experimental conditions are not clearly defined. For instance, the turning response is measured as the difference of the tube's final direction (at the end of

[22] Agar is a sugar-based polymer mostly used in desserts and microbiological work to provide a solid substrate.

the experiment) and its initial direction (upon germination), but only angles from 0° to 180° are used (the lower limit 0° is inferred since the exact range is never mentioned). How the authors interpreted the turning response is difficult to assess since their angle method already introduces a bias with respect to the electrodes. For instance, if all tubes initially emerged perpendicularly aligned to the electrodes (90° and 270°) and they all reoriented towards the cathode (180°) then the difference method would yield zero, a value that is supposed to be reserved for random growth. Perhaps the authors assumed some symmetry and only tested pollen tubes whose both initial and final angles remained between 0° to 180°, but such assumptions and methods were not clearly stated. Obviously this adds a bias to the measurements. On the other hand, the measured response is described as "statistically significant", but there is no clear figure of a significant amount of tubes in a batch turning, only a picture of 5 pollen tubes. No mention of the effect on the final tube length was done. Electrical parameters, such as the input constant current or the conductivity of the mixture, are neither provided nor discussed. There is no sketch of the setup that was employed. Moreover, since a current source is used instead of a voltage source, no discussion is provided on the electric field measurement. Verification of the homogeneity of electrical variables within the long chamber and the electrical bridges is not considered. The possible effect of the electrodes configuration is not considered either. Discussion of possible different behaviors of pollen tubes in different locations along the chamber is not done. This last issue is particularly important when the electric field is applied to a whole population of pollen tubes at once[23], that is, in a batch mode. Uncertainties about measurements or inferred values of variables are not

[23] Pollen tubes have been reported to behave differently when close to electrodes (Malhó et al., 1992).

addressed, especially those concerning individual pollen tubes. For instance, the actual voltage drop across a pollen tube is by no means measured, only inferred. Moreover, the voltage does not drop only along the tube diameter. Actually, if the pollen tube is aligned with the electric field, the voltage drops solely along the growth axis. Furthermore, since there is no control on the initial pollen grain position or initial pollen tube orientation, the initial voltage drop along the diameter varies among the different pollen tubes, hence the initial tropic response should vary as well. This is not considered either.

It is also noted that the chamber dimensions are larger than the studied object, namely the pollen tube, by orders of magnitude. Accuracy in the description of pollen tube dynamics is seriously limited if measurements are not taken in a proper spatial resolution and focal plane. Even if global tropic behavior is just an extension of individual pollen tube behavior at the micro scale, it still remains to be verified. This point is generally overlooked in the literature. It should be noted that explorations at the micro scale in almost every other discipline has either revealed phenomena otherwise unknown or, at least, permitted a deeper insight or understanding.

Intriguingly, the response of pollen tubes to magnetic fields was among the initial reports. Sperber et al. (1981) exposed growing lily pollen tubes to the strong magnetic field generated by a *Bitter magnet*[24]. The pollen tubes grew strongly oriented and almost parallel to a 14 Tesla homogeneous magnetic field, with equal tendency to grow toward the north or south pole. The effect diminished with decreasing fields and became unnoticeable at 3 Tesla. When exposed to a non-uniform magnetic field, the pollen tubes

[24] A *Bitter magnet* is a magnet made of circular metal plates and insulating spacers stacked in a helical configuration, rather than coils of wire. Invented in 1933 by the American physicist Francis Bitter.

grew preferentially toward the region of decreasing field strength. Although the physiological process is not addressed by the authors, they suggest that magnetic fields may act like other stimuli that can affect local growth. However, a 3 Tesla magnetic field is a very strong field not readily found in living organisms. Therefore whether the reorientation of pollen tube exposed to these conditions is due to true tropism or to material magnetic properties is still unclear. Worthy of note, the behavior in non-uniform fields described by Sperber et al. (1981) resembles the properties of dielectrophoresis (Jones, 1995; Morgan and Green, 2003), which is a well-known phenomenon in cells (Wang and Liu, 2010). Later, Sperber (1984) reported that under an electric field elongating pollen tubes grew towards an electrode, parallel to the applied field, but showed no preference to either the positive or the negative electrode, similarly to those grown in a magnetic field.

Later, Nakamura et al. (1991) reported that pollen tubes of *Camellia japonica*, *Erythrina* and tulip grew toward the negative electrode when exposed to a constant electric field. On the other hand, *Lycoris*, *Hedychium* and *Eriobotrya* pollen tubes grew towards the positive electrode. However, other species such as *Lilium* and *Gladiolus* did not exhibit electrotropism. The authors attribute this contradiction to the probable "unsuitableness of various experimental conditions". Nakamura et al. (1991) reported that the electrotropism effect increased with the applied electric field, with a maximum effect at 1 to 2 V/cm. A field strength of 0.13 V/cm provided the first detectable response. The tube extension of all tested species decreased as the intensity of the electric fields increased, consistent with Wang et al. (1989), who reported a decrease in growth rate. The tube response was measured as the inclination angle from a pollen-grain line, which

the authors call “curvature” even though it does not include any information on the radius of curvature. The percentage of pollen tubes that actually turn in response to the electric field is not quantified, but from the pictures shown it is inferred that more than 50% of the population, especially the longer tubes, showed a response. The final length of pollen tubes is plotted; however the values often exceed the dimensions of the setup (10mm), which is not discussed in the text. The authors also mention a difference in behavior between tubes located within the medium from those on the surface of the medium. In general the report is based on the tubes that grow within the medium since tubes on the surface did not exhibit an appreciable response.

Pertinently, the authors verified the inversion of direction of growth when the polarity of the electric field was changed. Nakamura et al. (1991) also showed that there is an optimum calcium concentration in the growth medium for pollen tubes, which was found to be around 3 to 4 mM. Not surprisingly, the authors state concerns about the experimental conditions to properly place, control, and measure pollen tube response. This is supported by the fact that the chamber is considerably long (approximately 20 cm), hence individual response is difficult to assess quantitatively. The electrical setup is barely described and electrical parameters, such as the medium conductivity, are not reported. Additionally, the use of four additional vessels besides the pollen chamber is not explained nor justified (Figure 1.5). Homogeneity of the agar medium as an electrical conductor was conjectured by Nakamura et al. (1991) to explain the difference between pollen growing within the medium from those on the surface; however no sound explanation is advanced. Misuse of terms like “current intensity” instead of “current density” or “voltage” instead of “voltage per meter” is often misleading. It is noted that if

electric field strengths of 1 V/cm were used, then the applied voltage was at least 20 V. Even though the electric field value is within the biological range, the voltage level is far from being physiologically relevant, which raises concern about the aptness or relevance of the results. This caveat, in particular, applies to most works in the area.

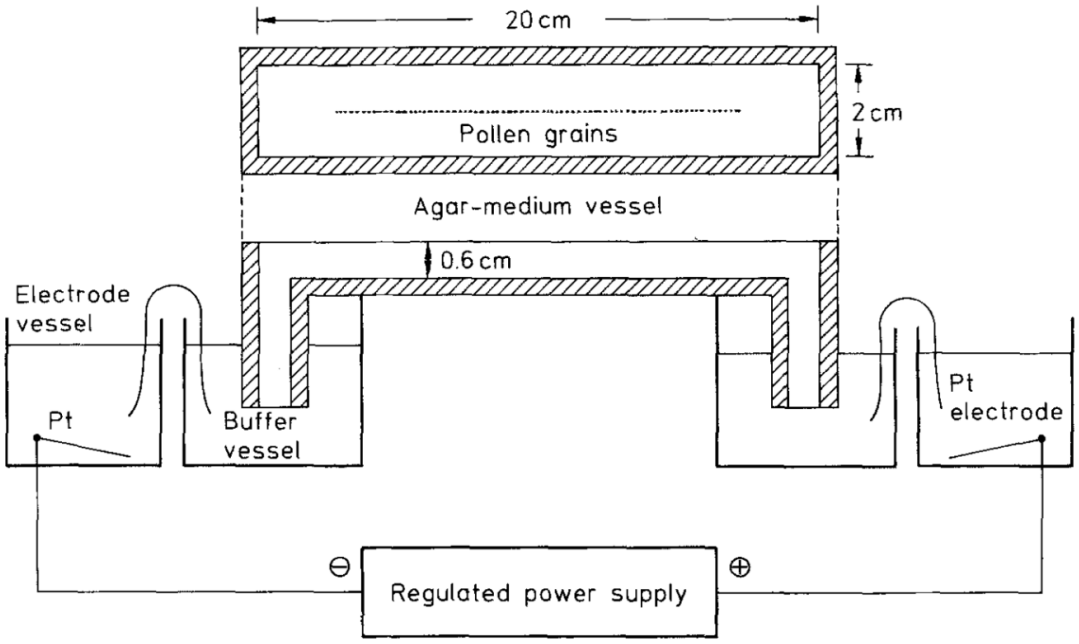

Figure 1.5 Apparatus for growing pollen tubes employed by Nakamura et al. (1991).

There is one particular interesting detail in Nakamura et al. (1991) that the authors failed to comment upon: the maximum curvature effect around 1.5 V/cm (Figure 1.6). According to Nakamura et al. (1991), the electrotropism response decreases at higher field strengths, while the tube length markedly plummets. This raises the question: to what extent does the measured curvature depend on tube length? How could they be related? This remains an open question.

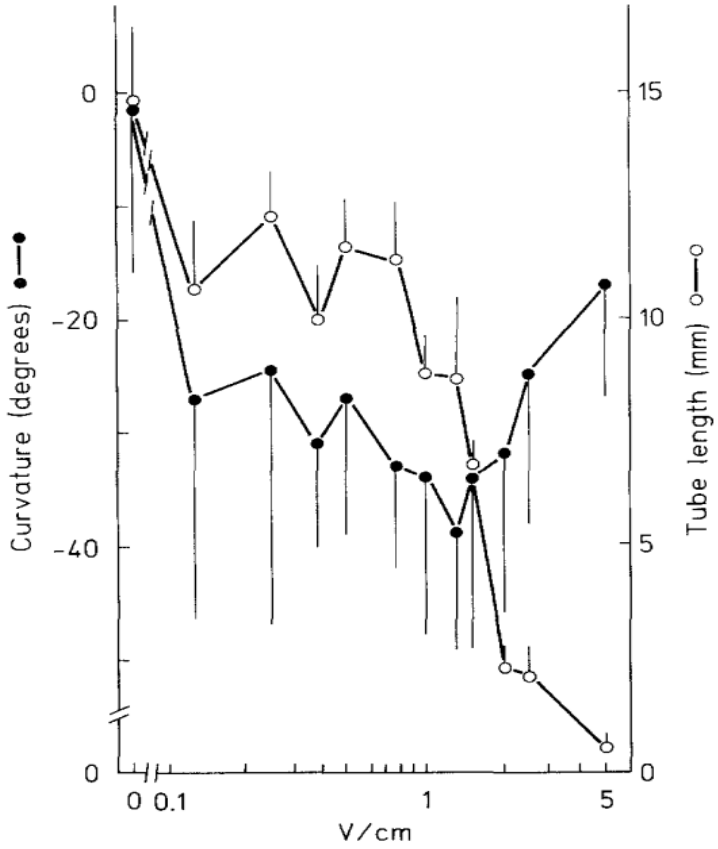

Figure 1.6 Effect of electric field on *Camellia japonica* pollen tubes curvature.[25]

The authors argue that, if the mechanism for pollen tube electrotropism is the redistribution of calcium in the growing tip due to an external electric field, then how to explain the fact that different species grow toward different electrodes. Thus, further work is required. Despite the shortcomings, Nakamura et al. (1991) presented more accurate information on the electrotropism of pollen tubes than previously available.

The question of the direction of pollen tube growth in the presence of electric fields became even more unsettled when Malhó et al. (1992) reported that *Agapanthus umbelatus* pollen tubes grew towards the nearest electrode under a constant electric field

[25] Figure taken from Nakamura et al. (1991).

of 7.5 V/cm, resembling the description given by Sperber (1984). However, when the pollen grains were placed at an equidistant position the authors described a random growth, as opposed to an aligned growth. 82% of the pollen germinating near the cathode presented an orientation alignment with the electric field whereas only 55% of the pollen germinating near the anode did. The experiments were done in batch mode for one hour in a 15 cm long electrophoresis plate and pollen was sown at three equidistant points: near the anode, in the center, and near cathode. Since the electric field has just one homogeneous direction, the reported growth pattern cannot be explained only by the electric field polarity. The authors advance then "that the electric field effect is mediated by ionic currents, resulting in an asymmetric ionic distribution throughout the germination plate." The authors suggest that electrotropism could indeed be caused by a cell membrane electrophoresis induced by exogenous ionic currents and gradients (in relative influences as $Cl^- < Mg^{2+} < K^+ < Ca^{2+}$) that affect the internal gradients along the tube. The authors report that pH (H^+ concentration) and sucrose concentration do not change any result, hence it is argued that these charged molecules are not the main actors. Still, the physiological connection of the facts is still unclear since the concentrations of the same ions along the actual plant style are likely to be significantly higher than those in the experiments.

Once again the description of the electrical setup was limited as much information is not available. A large electrophoresis plate (15 x 5 cm^2), and hence high total voltages (greater than 70 V), are used. Descriptions like "stabilized in potential and current" are confusing as to what electrical variable was indeed regulated in the test. Although the duration of the test (one hour, less than any other work) is given, no mention of pollen

tube length or growth rate is reported, not even in the form of figures. The authors mention a water flow monitored by neutral dyes but it is not clear if they refer to water in the medium or buffers or how it is physically transported. Conductivity is not mentioned nor measured. The role of bridges and buffers (along with their ions: Na^+ and Cl^-) are not discussed. From the pictures, it is evident that tube-tube interaction was neglected. Their tests show that ion composition in the medium and buffers affect the orientation results (experiments 14-17 in the report) to the extent of reversing orientation (experiments 8 and 9), supporting the role of ion currents in electrotropism. The order of influence of ions albeit very relevant is not explained.

Not so long afterwards Nozue and Wada (1993) reported the exposure of tobacco pollen to a constant current. After stating the lack of study in the polarity of plant cells in contrast to animal cells, the authors set out to report the electrotropic response of *Nicotiana tabacum* pollen to electric fields. The pollen grains were suspended in a Brewbaker-Kwack medium and placed in a groove. Although not fully explained, the groove was "generated" using a silicon sheet and then topped with a cover slip to allow for planar visualization with the microscope. Then, a constant electrical voltage is applied to the culture with an electrophoresis power supply in a batch mode. Dimensions or relative positions are not given. Once again, details in the electrical parameters and measurements are limited. The measurement of pollen tube direction involved the average of a cosine function, which in theory should yield zero for random orientation, +1 for a population perfectly aligned towards the positive electrode and -1 for a population perfectly aligned towards the negative electrode. However, technically speaking it would also yield zero for a population uniformly aligned perpendicular to the

electrodes (90° or 270°), which again is biased and difficult to interpret. The average growth rate of pollen tubes was measured as 1.47 ± 0.14 μm/min with no significant difference towards any electrode. The authors reported an average polarization of 0.4 towards the positive electrode when an electric field of 3.8 V/m was applied. The tropic response increased with increasing electric fields, from appreciable at approximately 0.2 V/cm to saturated at 1.8 V/cm. For electric fields greater than 7 V/cm, pollen tubes showed a tendency to burst. The authors report that the tropic response gradually increased with increasing duration to exposure. It is noted that no distinction was made for different initial directions of different pollen tubes and that the measurement of the response is difficult to assess in general because the polarization is measured in a batch mode, that is, an increased effect in tropic response is deduced from the fact that more pollen tubes turn in a given direction, not because one pollen tube is turning more rapidly. This distinction, for instance, could be better studied in a micro environment.

Nozue and Wada (1993) pursued the suggestion made by Malhó et al. (1992) and tested the response of pollen tubes when the electric field was turned off after exposure. The authors did not observe any increase or decrease in the average polarization and the direction of growth was fairly constant. However, no further test for inversion of polarity was done, which might have showed a preferential behavior according to the polarity of the electric field. The authors indicated that the tropic response is due to the electric field and not to a field-induced gradient in constituents of the medium. However, due to the use of agarose blocks in their experiments this issue is not settled. Finally, they suggest that even though it is not known how a pollen tube senses an electric field, the electrotropism in pollen tubes might be explained by an electrophoretic redistribution of

membrane proteins, such as calcium channels, or by a forced intracellular electrophoresis of secretory vesicles that contain wall materials. Worth mentioning is that no picture of the setup is shown and no batch picture of the pollen is provided. The only picture of pollen is that of a couple of pollen tubes turning, which as an individual event is a common occurrence in pollen cultures even when they are not exposed to any stimulus. No control image was shown to demonstrate the significance of the phenomenon in the exposed samples.

The external electrical signal for electrotropism has usually been considered as constant (DC) in the literature. Alternatively, Platzer et al. (1997) applied an AC electric field of low frequency and low amplitude to *Lilium longiflorum* pollen tubes. It was found that the growth rate of pollen tubes was affected by both frequency and amplitude of the AC field. The growth rate incremented by a factor of 1.58 in a narrow window with a maximum at 10 Hz and 20 mV/cm and decreased for higher frequencies and higher field strengths. It was observed that pollen tubes tended to burst at field strengths greater than 50 mV/cm. The range of frequencies and electric fields tested in the experiments was from 1 to 100 Hz and 1.75 to 100 mV/cm (peak to peak) respectively. The effect was found to be independent of the initial orientation of the pollen tubes. The growth direction of pollen tubes was not influenced by the AC electric field.

The work of Platzer et al. (1997) shows, at least, that different electrical stimuli might cause different responses. DC and AC signals are just two of the many types of signals that may exist in nature. It is surprising that AC signals had not been used in experimental assays before. However, it is noted that the field strengths reported were very low in comparison to the typical values found in the literature, although the authors

claim that the strengths are well above the thermal noise limit (Weaver & Astumian, 1990). Platzer et al. (1997) barely mention the setup employed and no description or sketch was provided. Although the authors mention the use of video imaging, there is not a single picture of a pollen tube to illustrate the described response under electric fields. Almost no details of the culture chamber were given, although platinum electrodes were mentioned to be 1 cm apart in a Perspex chamber. Electrical parameters were not mentioned except for the conductivity of the medium, which was reported to be 119 μS/cm. It is also noted that the window where the pollen tube growth is found to increase is considerably narrow in frequency and field strength (approximately ±10 Hz and ±10 mV/cm respectively), which makes it difficult to assess if this increment is really due to the AC electric field or to a random deviation caused by experimental or statistical inaccuracy. Unfortunately, there is no other work in the literature to compare with.

More recently, Bou Daher and Geitmann (2011) used electric fields as a directional trigger to study the internal workings of pollen tube growth in *Camellia japonica*. The authors found a significant reduction in the percentage of pollen tubes responding to an electrical trigger when polymerization of the actin cytoskeleton is partially inhibited. The study also details the important role of calcium in pollen tube growth and redirection. It was found that the target site of secretory vesicles tilts before tube redirection, indicating that a redirection of *exocytosis* activity is responsible for a reorientation of growth. It is argued that the reorientation under electric fields may be due to different types of voltage activated calcium channels at the tip. A constant electric field of 1.5 V/cm was used to make the pollen tubes turn towards the negative electrode. Lower field strengths did not trigger any appreciable effect and higher field strengths caused the pollen tubes to burst.

Description of the electrical setup was minimal and tube response was limited. Only a very small range of redirection was observed (19.95±4.15°) and few tubes (35%) actually changed direction when the electric field was applied. It is noticed that the average response time was found to be 209 seconds, a parameter not measured before in the literature. Also, growth rate (control average was 12 μm/min) was found to be independent of the electric field, contrary to previous works where the growth rate tends to decrease.

Further work on electrotropism or any kind of effect of exogenous electric fields on pollen cell growth has been rare even though most works in the field emphasize the lack of understanding and strongly recommend additional work. This might be explained by the lack of techniques at the micro scale, which might have encouraged the extensive use of fluorescent microscopy in the study of pollen tubes in the last decade. This technique has proved to be very successful in life science, and particularly in pollen tubes, in providing the possibility of labeling specific cell components while observing their dynamics with high resolution images. Several internal processes of the pollen tube have been revealed using this technique such as the pulsating growth of the tip (Messerli et al., 2000) and the secretory vesicle trafficking (Bove et al., 2008), among others.

Despite the fact microfluidics has proved to be a functional tool for cell research at the micro scale (Nahmias, 2009; Vanapalli et al., 2009), it was not until recently that Cooper et al. (2009) and Yetisen et al. (2011) demonstrated how microfabrication techniques can offer more realistic environments for pollen. Cooper et al. (2009) developed a microsystem-based open assay for testing the attraction of pollen tubes by ovules. Such test cannot be properly done in usual isotropic plate essays where there is no control over

growth direction or placement of physical microbarriers. The device consists of a microgroove and two opposite chambers (hence offering an anisotropic configuration) formed in a polymer-based substrate using a SU-8 mold. The minimum feature size reported was 250 µm. A cut pistil with a cluster of pollen tubes fanning out is manually placed and aligned in the microgroove as shown in Figure 1.7. By placing ovules in one chamber and leaving the opposite chamber empty, the authors found that approximately 67% of pollen tubes oriented their growth towards the chamber with ovules.

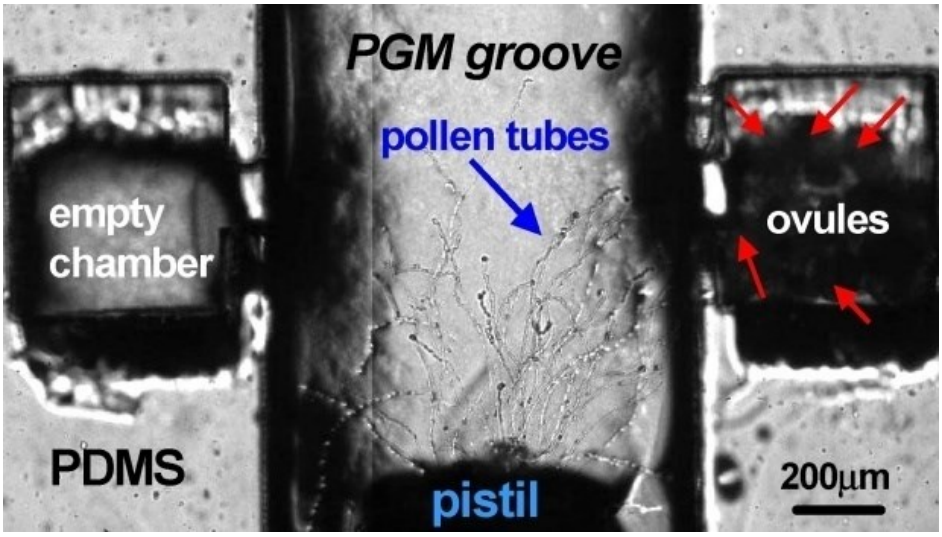

Figure 1.7 Microdevice developed in Cooper et al. (2009). Most pollen tubes grow towards the ovule-containing chamber[26].

Even though the device manufactured by Cooper et al. (2009) fulfills its purpose in showing the efficiency of ovule attraction *in vitro*, the accurate manipulation of individual pollen tubes with microfabrication techniques requires further development. For instance, the placement of the pollen tubes by means of a cut pistil is completely manual. In addition, the fixing and alignment of pollen tubes require delicate handling

[26] Figure taken from Cooper et al. (2009).

which might compromise the reproducibility and accuracy of the experiments. Furthermore, germination of the placed pollen tubes fanning from the pistil occurs at a different focal plane, which complicates the imaging system. Also, since the micro groove is essentially an open channel with a width of 500 μm, their device has to be placed in a Petri dish in order to be covered by growth medium so as to keep the device from drying out, making the microsystem dependent on the larger plate assay. On the other hand, the minimum feature size is still orders of magnitude above the size of the cell and would have to be considerably reduced in order to achieve single pollen tube growth in a controlled manner. Finally, no specific features such as mechanical or electrical components are considered for further testing.

Most importantly, in order to realistically replicate the confined, resource-limited milieu in which pollen tubes actually perform growth to achieve fertilization, an enclosed environment must be offered by the testing microdevice. A limitation shared by every previous work. Nevertheless, the work by Cooper et al. (2009) has been an essential intermediate step towards realizing a targeted device for pollen tube growth research using a Lab-on-a-chip (LoC)[27] platform.

1.3 Statement of the Problem

The fact that cells respond to exogenous electric fields has important implications for developmental processes involved in embryogenesis, wound healing, polarity, differentiation, and motility (McCaig et al., 2005; Jaffe and Nuccitelli, 1977; Li and Lin,

[27] A lab-on-a-chip is a device that integrates laboratory functions on a single chip. Lab-on-a-chip devices are a subset of microelectromechanical systems (MEMS) or microsystems.

2011; Campetelli et al., 2012). In particular for pollen cells, *in vitro* experimentation in open assays has led to numerous insights. However, how the electrical stimulus is perceived and translated into a cellular response is poorly understood in most cellular systems. There is a general lack of understanding of the electrical phenomena in pollen tubes. There is no consensus in the literature on how pollen tubes behave under electric fields and most works in the field emphasize the lack of understanding and strongly recommend further work.

On the other hand, most works have focused solely in pollen tube electrotropism instead of tackling the more general question of the influence of electric fields on pollen tube growth. No systematic application of different types of electric fields has been carried out. For instance, no comprehensive description of pollen tube growth under DC and AC electric fields has been reported for the same pollen species. Furthermore, no single pollen tube approach has been advanced, which could readily assist the investigation of the electrical cue on pollen tube growth as a guidance signal.

A critical constraint has been the difficulty in providing a testing environment that mimics key aspects of the *in vivo* growth environment of the pollen tube. In all studies reported above the application of electric fields has always been done using an open essay configuration. An *ex vivo*[28] approach in which the pollen cell is provided an environment that realistically resembles its natural milieu can yield more relevant results. So far no microdevice for the electrical testing of pollen tubes has been considered in the

[28] *Ex vivo* refers to experimentation with cells from an organism under a minimum alteration of natural conditions, which offers more controlled conditions than is possible in *in vivo* experiments and more realistic results than experiments performed *in vitro*.

literature even though sophisticated microsystems such as LoC are now available. Such technology has already proved useful in biological applications (Vanapalli et al., 2009; Velve-Casquillas et al., 2010). It is therefore of fundamental importance to establish consistent experimental design specifications including a description of the electrical conditions, and the geometry of the setup.

Additionally, the literature review shows that one major issue in previous studies is related to the reported experimental conditions, which raises concerns on the conclusions drawn from the tests. Setup descriptions are often poorly detailed or justified, which seriously affects the repeatability of the tests, especially given the little knowledge of the phenomenon and the vast amount of variables involved. Actual designs or pictures of the experimental setup are rarely provided and sometimes even sketches are missing all together. Moreover, concerns about the suitability of the experimental conditions for controlled pollen tube growth have been reported (Nakamura et al., 1991). Also, quantification of the pollen tube response is often obscure or subjective. For instance, the use of difference angles (Wang et al., 1989) or curvature with no radius information (Nakamura et al., 1991) might be misleading. In addition, the electrical parameters are usually overlooked in the literature and loose terminology is often used, which further obscures the discussion. Moreover, most results have not been confirmed by others. A better elaboration on the design, the electrical conditions, and the setup used to carry out the experiments will ensure improved reproducibility and has the potential to shed more light on the actual influence of electric fields on pollen tube growth.

Since statistical determination of behaviour in biology requires numerous repeats of an experiment, the ability to easily and reliably reproduce test conditions is highly

important. Yet, most compact microdevices do not address the issue of reusability directly; instead the device is usually disposed of after a single use (Nahmias, 2009). Although a single-use approach may be inevitable when toxic compounds are involved, a reusable approach helps save time and resources while reducing costs. If the LoC (or at least part of it) can be reused, the device can be employed in a more efficient way, which, albeit a design challenge, makes the LoC more versatile.

1.4 Thesis Objectives

This work aims to elucidate the role of electric fields on pollen tube growth by systematically exposing pollen to controlled electric fields in a LoC environment that is simple, yet properly defined and reproducible in design.

More specifically, the objectives of this work are:

1. To design, fabricate, and test a LoC that enables the growth of pollen tubes in a structured microenvironment.
2. To design, fabricate, and test a LoC with integrated microelectrodes that enables the systematic application of electric fields to pollen tubes.
3. To characterize the behavior of pollen tubes under global DC and AC electric fields.
4. To apply and assess the effect of localized DC electric fields to individual pollen tubes.

1.5 Thesis Contribution

This work will contribute to the understanding of the influence of electric fields on pollen cells growth. The proposed LoC will assist to the development of pollen cell analysis by offering a specific platform capable of manipulating either populations of cells or single pollen tubes. By providing a controlled *ex vivo* environment that has features similar to the one *in vivo*, the responses of the pollen tube to external signals can be better studied. On the other hand, implementation of the reusability aspect directly in the fabrication will certainly promote wide-spread use of LoC technology in day-to-day applications (Whitesides, 2011), particularly in out-of-the-lab instances. This will offer an efficient platform for experimentally studying and manipulating the growth behavior of pollen tubes for various applications such as cytomechanics, toxicology, drug development, drug diagnosis, drug discovery, among others.

A comprehensive study of the influence of electric fields on pollen tubes at the micro scale will help bring consensus in the literature on how pollen tubes behave under electrical stimulus. Furthermore, the application of localized electric fields to individual pollen tubes will clarify aspects of the dynamics of their growth not possible before. Until now, the use of a microsystem to study individual pollen tubes during electric field exposure has not been reported. The development of such a systematic approach to experimentation will also benefit research on other cell types reported to respond to electric fields (Chen and Jaffe, 1979; Ishikawa and Evans, 1990; McGillivray and Gow, 1986; Peng and Jaffe, 1976; Robinson, 1985; Stenz and Weisenseel, 1993). This can enable the development of methodologies for prevention or treatment of many disorders

and diseases which could potentially benefit areas such as agriculture and medicine, among others.

1.5.1 Publications

Publications stemmed from this Ph.D. research are listed below:

Published articles:

1. Agudelo, C.G., Sanati Nezhad, A., Ghanbari, M., Packirisamy, M., and Geitmann, A. (2012). A microfluidic platform for the investigation of elongation growth in pollen tubes. Journal of Micromechanics and Microengineering. *22*, doi:10.1088/0960-1317/22/11/115009.

   Contribution: Concept. Experimentation. Writing (All sections). Editing. Material from this article is included in chapters 2.

2. Agudelo, C.G., Sanati Nezhad, A., Ghanbari, M., Naghavi, M., Packirisamy, M., and Geitmann, A. (2013). TipChip: a modular, MEMS-based platform for experimentation and phenotyping of tip-growing cells. Plant Journal for Cell and Molecular Biology. *73*, 1057–1068.

   Contribution: Concept, Sections: Design, Metal Biocompatibility. Editing. The Metal biocompatibility section is included in chapter 3.

3. Agudelo, C.G., Packirisamy, M., and Geitmann, A. (2013). Lab-on-a-Chip for studying growing pollen tubes. In: Plant Cell Morphogenesis: Methods and Protocols, Series "Methods in Molecular Biology", eds. Žárský V, Cvrčková F, Springer, pp 237-248.

   Contribution: Concept. Experimentation. Writing (All sections). Editing. Material from this book section is included in chapters 2 and 3.

4. Sanati Nezhad, A., Ghanbari, M., Agudelo, C.G., Packirisamy, M., Bhat, R.B., and Geitmann, A. (2013). PDMS microcantilever-based flow sensor integration for Lab-on-a-Chip. IEEE Sens J. *13*, 601–609.

   Contribution: Concept, Editing, Lab support. This article is only cited. No material is included in the thesis.

5. Sanati Nezhad, A., Ghanbari, M., Agudelo, C.G., Naghavi, M., Packirisamy, M., Bhat, R.B., and Geitmann, A. (2013). Optimization of flow assisted entrapment of pollen grains in a microfluidic platform for tip growth analysis. Biomed Microdevices. *16*, 23–33.

Contribution: Concept, Editing. This article is only cited. No material is included in the thesis.

6. Ghanbari, M., Sanati Nezhad, A., Agudelo, C.G., Packirisamy, M., and Geitmann, A. (2014). Microfluidic positioning of pollen grains in lab-on-a-chip for single cell analysis. Journal of Bioscience and Bioengineering. *117*, 504–511.

   Contribution: Concept, Editing. This article is only cited. No material is included in the thesis.

Articles in review:

7. Agudelo, C.G., Geitmann, A., and Packirisamy, M. (2015). Influence of electric fields and conductivity on pollen tube growth assessed via Electrical Lab-on-Chip.

   Contribution: Concept. Experimentation. Writing (all sections). Editing. Material from this article is included in chapters 4, 5, and 6.

Conference papers:

8. Agudelo, C.G., Sanati Nezhad, A., Ghanbari, M., Naghavi, M. Packirisamy, M., and Geitmann, A. (2013). Combining live cell imaging and MEMS technology. Meeting of the Microscopical Society of Canada, Victoria, Jun 18-20.

9. Agudelo, C.G., Packirisamy, M., and Geitmann, A. (2014). Assessing the influence of electric cues and conductivity on pollen tube growth via Lab-on-a-Chip technology. Biophysical Society 58th Annual Meeting, San Francisco, California, Feb 15-19.

10. Chebli, Y., Agudelo, C.G., Sanati Nezhad, A., Ghanbari, M., Naghavi, M. Packirisamy, M., and Geitmann, A. (2014). Tipchip or MEMS-based platform for experimentation with tip growing cells. Nagoya, Japan. Sep 10-11.

11. Agudelo, C.G., Sanati Nezhad, A., Ghanbari, M., Naghavi, M. Packirisamy, M., and Geitmann, A. (2013). MEMS technology in combination with high resolution live cell imaging. 18th International Microscopy Congress. Prague, Sep 7-12.

12. Agudelo, C.G., Sanati Nezhad, A., Ghanbari, M., Packirisamy, M., and Geitmann, A. (2015). Navigating a Maze - Sensing and Responding to Mechanical Obstacles during Cellular Invasive Growth. Biophysical Journal. Volume 108, Issue 2, Supplement 1, 27 January 2015.

1.6 Description of the Work

The proposed LoC is based on an *ex vivo* microfluidic platform that offers individual pollen tubes a microenvironment where their growth can be monitored microscopically and experimentally studied. The device was designed for *Camellia japonica* pollen tubes but it can be adapted to any other species in a straightforward manner. Chapter 2 introduces the LoC architectural design and describes the microfluidic approach. It also presents microfluidics simulations and details the LoC fabrication. The LoC is exemplified with a simple collision test.

Next, microelectrodes are integrated into the LoC. Chapter 3 describes the Electrical LoC (ELoC). Design considerations such as reusability are discussed. Fabrication is also presented in detail. In order to apply global and local electric fields, two variants of the ELoC are introduced: Batch and Single-cell. Electrical characterization of the ELoC in the presence of growth medium (an electrolyte) is also addressed.

The effects of global DC and AC electric fields on pollen tube growth are covered in Chapter 4 and 5 respectively. Data are systematically collected on pollen tube length, growth rate, germination, and bursting. Pollen tube orientation is also measured and discussed. Chapter 5 further investigates the effect of electric field frequency and electrode material on pollen growth.

The application of subcellular electric fields using the single-cell ELoC is presented in Chapter 6. The role of electric fields as a potential guidance cue is also covered therein. Finally, Chapter 7 presents the conclusions and future work.

Chapter 2 - Growing Pollen Tubes by Means of a Microfluidic Platform

In the present chapter, a LoC based on an autonomous microfluidic platform is developed with the aim to expose individual pollen tubes to a growth environment that is able to test their response to various mechanical challenges. A published presentation of this chapter can be found in Agudelo et al. (2012). A detailed fabrication procedure with materials, methods, annotations and lab tips can be consulted in Agudelo et al. (2013a).

The design of the LoC had to meet several criteria: 1) The microchannel setup was to be designed to allow for several single pollen tubes to grow simultaneously in individual channels; 2) Ungerminated pollen grains had to be injected in such a manner that they would be positioned in front of microchannels into which the pollen tubes could grow; 3) The device would have to allow culture medium to flow through continuously to supply the growing pollen tubes with fresh nutrients and oxygen; and 4) Optical compatibility needed to be ensured in order to measure pollen tube growth by image analysis.

2.1 LoC Design

The proposed LoC design is based on a microfluidic network that permits the controlled manipulation of pollen grains suspended in a liquid growth medium. It is composed of an inlet, a linear distribution chamber, two series of symmetrical microchannels (top and bottom), and two outlets. Figure 2.1a shows a schematic of the proposed LoC. The diameter of a pollen tube is species dependent with typical values in the order of a few micrometers. Here, the device is designed for pollen tubes from species with relatively large tubes such as *Lilium longiflorum* or *Camellia japonica.* The tubes

from these species grow rapidly with a large diameter (typically between 10 to 20 µm) and relatively straight, making them an ideal model system for the investigation of biomechanical behaviour (Bou Daher and Geitmann, 2011).

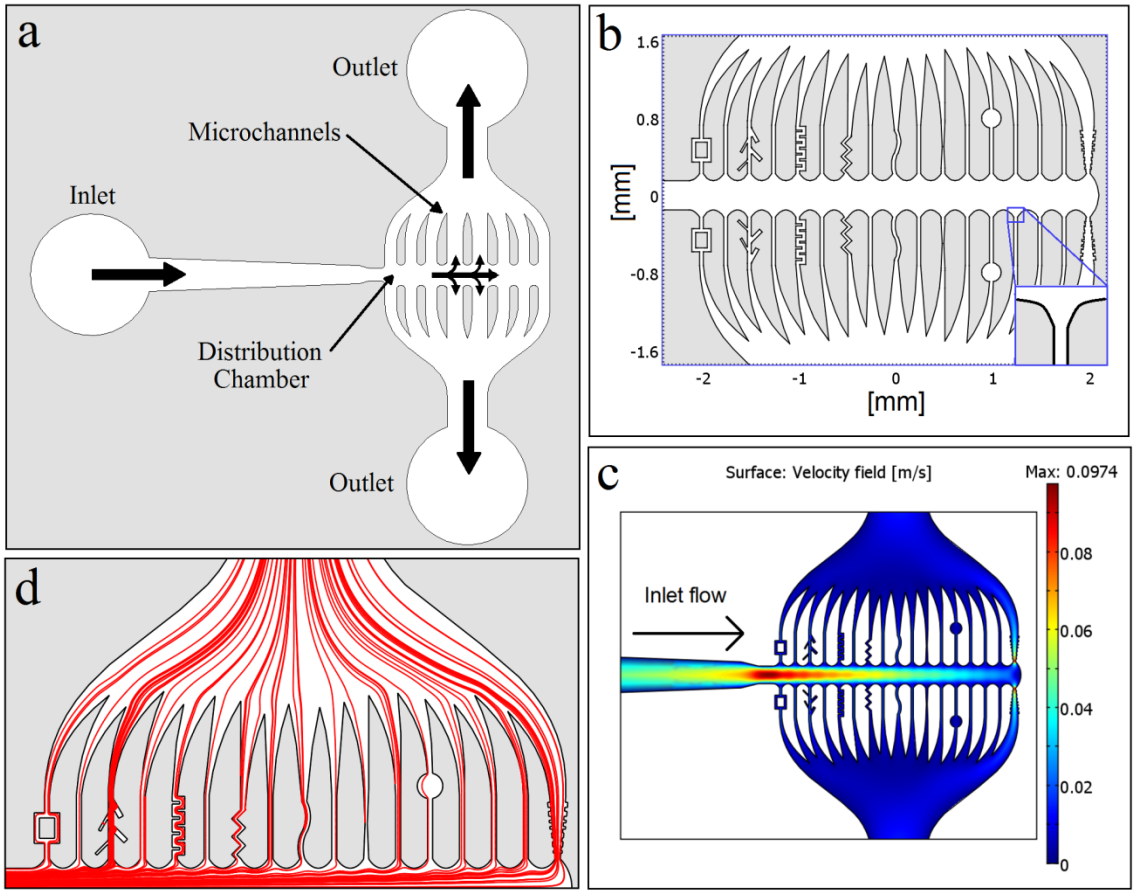

Figure 2.1 Overall design of the LoC. (a) Schematic. (b) Detailed layout of the microchannels. Curved notch at the entrance of a microchannel is zoomed in. (c) Velocity field simulation of the microfluidic platform. (d) Flow simulation for half of the microfluidic network.

The whole platform is conceived to be planar with a limited thickness in order to avoid the accumulation of pollen grains into stacks that would represent a mechanical impediment to germination and a visual obtrusion preventing microscopical observation. The limited thickness also restrains the pollen grain interactions to a two-dimensional space and ensures that all growth occurs in the same focal plane. Considering that

Camellia pollen grains vary from 50 μm to 60 μm in diameter, the thickness of the microfluidic network was set to 80 μm to allow for unimpeded motion of the grains. The configuration encloses pollen from all sides thus preventing, by definition, the evaporation of the growth medium, a phenomenon which has proved difficult to deal with in open assays (Yetisen et al., 2011).

The microfluidic network is designed in such a way that the suspended pollen grains are transported by the medium flow from the inlet, through a *distribution chamber*, to the entrances of the *microchannels*. The microchannels are narrow conduits through which pollen tubes are guided to grow and that expose the elongating tubes to a variety of mechanical obstacles and constraints. The entrances of the microchannels are designed to be sufficiently narrow to block the pollen grains from entering but allowing the elongating tubes to pass through. This is achieved by setting the width of microchannels to 40 μm, a distance shorter than the pollen grain diameter. In addition, the transition between the distribution chamber and the microchannels is designed as a curved notch to promote the trapping of pollen grains at the entrances of the microchannels along the smooth flow streamlines. Once the pollen grains are properly positioned within the microdevice, the flow of the culture medium can be set to a minimum to maintain a nutrient-rich environment for the pollen tubes while exploiting the fluid force to assist in the trapping of the pollen grains at the entrances of the microchannels. Finally, the liquid medium exits the microfluidic network through the outlets.

It is noted that since the typical diameter of *Camellia* pollen tubes ranges between 10 and 20 μm, more than one pollen tube can fit inside a given microchannel. Even if the microchannel width was reduced, the height of the microchannel (80 μm) would still

allow for multiple pollen tubes. However, the main purpose of the microchannel entrance in the present design is to prevent any pollen grain from slipping in. Reducing the cross section of the microchannel to allow the entry of exactly one pollen tube would require determining the minimum volume of medium surrounding the pollen tube and more advanced microfabrication techniques, which is subject to future investigation. Nonetheless, the multiple microchannel configuration ensures that in any given experiment at least several microchannels are invaded by a single pollen tube. The probability of a double invasion of a microchannel depends on the quantity of grains trapped at the microchannel entrance. It is, therefore, desirable to limit the number of grains trapped at the entrance. On the other hand, the direction in which a pollen grain produces a tube is essentially arbitrary and from a geometrical point of view, the probability that the tube emitted from a single grain grows into a channel is low. Hence, the ideal number of grains in front of each channel would be anywhere between 3 and 6, taking also into account that not all grains germinate in the first place.

The shape of each microchannel is intrinsically related to the intended test to be carried out on the pollen tube. For instance, straight microchannels can be used to study the unobstructed elongation rate in the presence of various growth media or simply to enforce a direction on the pollen tube for further testing; or a curve or zigzag shape can be used to study the motility of pollen tubes under different conditions or their capacity to overcome obstacles. In the present design, differently shaped microchannels are included to assess the feasibility of individual experimental approaches. Individual channels are shaped to be straight, curved, zigzag, or serpentine, among others. Figure 2.1b shows a

detailed layout of the microchannels. Two sets of identical microchannels (top and bottom) are included in the design for redundancy.

The platform is conceived in such a way that sophisticated tests can be realized on single pollen tubes. To do so, each microchannel could be followed by a test chamber which would contain a variety of features specific to the intended test. A vast choice of micro sensors or micro actuators could be placed inside the test chamber due to the flexibility offered by the microfabrication technique used to implement the proposed LoC. For instance, simple fixed mechanical obstacles (as explained below in section 2.8) or movable structures (such as cantilevers) could be embedded in the test chamber to measure forces or stresses in the pollen tube. Even electrical-based features (such as microelectrodes) could be easily integrated within the microfluidic network in order to test different biological parameters characterizing pollen tube growth. Lastly, though various types of microsensors can be used, the planar nature of the microdevice makes microscopical observation and image analysis the main tool used to assess and quantify cellular responses.

2.2 Microfluidics Analysis

In order to predict the fluid flow behavior within the microfluidic network, and particularly the movement of pollen grains along the streamlines, a 2D Finite Element Method (FEM) fluid analysis implementing the incompressible Navier-Stokes and continuity equations was carried out using COMSOL Multiphysics (Figure 2.1c,d). A velocity of 0.02 m/s was selected as the boundary condition at the inlet to reflect typical medium injection by syringe, and the outlets were set to atmospheric pressure. Since the liquid medium used here consists mostly of water (Brewbaker and Kwack, 1963), the

density (ρ) and the dynamic viscosity (μ) are set to 10^3 kg·m^{-3} and 10^{-3} Pa·s respectively. A variable mesh size was employed as to use finer elements in areas where the feature size was smaller (e.g. at the microchannels). The mesh size was consistently reduced until further mesh refinement would not result in appreciable change in the simulated pressure and fluid velocity. Triangular elements with qualities always greater than 0.4 were used[29]. These settings apply to every simulation in this work unless stated otherwise. This particular simulation uses 65172 triangular elements with a minimum element quality of 0.48, which yielded 308631 degrees of freedom.

Figure 2.1c shows the simulated velocity field which reveals that the velocity is higher at the entrance of the linear chamber, mostly caused by the narrowing of the inlet. This in itself is desirable because it pushes the suspended grains towards the outlet of the linear distribution chamber, ensuring a relatively homogeneous distribution of pollen grains along the series of microchannel entrances. However, if the entry velocity is too high then most of the grains will be thrust to the outlet of the linear chamber, leaving the first microchannels unoccupied. To accurately determine the optimal velocity would require a detailed flow-particle interaction analysis, which in turn would necessitate precise information on pollen grain density. In practice, the flow velocity can be adjusted empirically by increasing or decreasing the size of the linear chamber width. Furthermore, a different shape other than linear could be used for the distribution chamber to ensure a more homogeneous flow velocity towards the entrances of the microchannels, for example to accommodate pollen grains from different plant species that might have a different size or shape.

[29] COMSOL states that a mesh quality greater than 0.3 should not affect the solution's quality.

From Figure 2.1c it is also observed that the flow through the different microchannels is kept uniform except for the microchannel furthest away from the inlet where a higher flow velocity is observed, consistent with its larger diameter. Figure 2.1d shows how this imbalance of microchannel shapes affects the distribution of the streamlines among the microchannels. This indicates that in order to obtain a homogeneous distribution among the microchannels, the constriction given by their shape should be designed to not differ considerably. A trivial solution would be the use of identical microchannels, yet an optimized design should take this aspect into account.

The flow simulation (Figure 2.1d) using COMSOL Finite Element Method shows how the trajectories of the pollen grains depend on their initial location at the inlet cross section. A grain close to the wall is predicted to be trapped at the entrance of microchannel closest to the inlet whereas a grain at the center will end up at the outlet of the linear chamber. Note however, that when a microchannel entrance is partially blocked by a positioned pollen grain, subsequent pollen grains are likely to bounce off the trapped grains, resulting in an increased flow towards the outlet of the linear chamber.

It is noted that at the microscale, the Reynolds number becomes small (usually less than one), resulting in a well-defined laminar fluid motion, which allows us to assume that the grains follow the streamlines accurately (Melling, 1997). To verify this assumption, the Reynolds number is calculated for a straight microchannel. In order to do so, the characteristic length L is computed as the ratio between the cross section area A and the cross section area's perimeter P of the microfluidic feature as follows:

$$\mathrm{Re} = \frac{\rho \mathrm{v} L}{\mu} = \frac{\rho \mathrm{v} A}{\mu P} = \frac{\rho \mathrm{v} (w \cdot d)}{\mu \cdot 2(w + d)}$$

Where v is the mean fluid velocity on the cross section area, *w* is the section width, and *d* is the section depth. Note that *d* is already set to 80 μm by design. Given the straight microchannel width (40 μm) and the mean velocity at this point (approximately 0.02 m/s from Figure 2.1c), the Reynolds number can be computed as 0.26, which confirms the laminar flow assumption. For completeness, the maximum value of the Reynolds number throughout the design is located at the entry of the distribution chamber, where the flow velocity is highest, with a value of 3.06, which is still very close to unity and very far from turbulent flow conditions.

2.3 Fabrication

Conventional planar microfabrication techniques and soft lithography are used to fabricate the microfluidic platform (Ziaie et al., 2004). This well understood process makes redesign loops and integration of design modifications straightforward since it can be systematically implemented. Furthermore, the fabrication recipe can be easily modified to include more sophisticated structures, layers, or features.

Initially, the LoC is drawn in a CAD software and reproduced on a transparent film using digital printing. Then the design is used to pattern a Silicon/SU-8 mold through photolithography. The microfluidic network is fabricated from polydimethylsiloxane (PDMS) by creating a replica using the Silicon/SU-8 mold. The mold allows for several copies of the platform to be easily made in a batch mode. The choice of PMDS as material is motivated by its bio-compatibility (nontoxicity), optical transparency, relative low cost, and ease of use. The fabrication process is illustrated in Figure 2.2a and it proceeds as follows:

1) The process starts with the fabrication of a Silicon/SU8 mold by means of photolithography. Initially a silicon wafer (WRS materials) is cleaned with a Piranha bath, followed by HF etching to eliminate any native oxide (this step is critical in order to ensure a good Silicon/SU8 adhesion).
2) Negative photoresist SU-8 (MicroChem Corp.) is deposited on top of the silicon wafer. To reach the thickness of 80 μm, SU-8 2035 is spin-coated at 1500 rpm. The SU-8 is then soft-baked for 5 min at 65ºC and 10 min at 95ºC on a hotplate to harden the photoresist.
3) Next, the photoresist is cooled down to room temperature and exposed to UV light using a photo mask. Post-exposure bake is then carried out first for 5 min at 65ºC and then for 10 min at 95ºC in order to cross-link the SU-8. The SU-8 layer is then developed to obtain the final SU-8 pattern and hard-baked at 150ºC for 10 min to solidify the remaining photoresist and reduce mechanical stresses in the structure. Next the mold is silanized to prevent the PDMS replica from sticking to the mold.
4) The microfluidic network is fabricated by pouring (1:10 polymer base/curing agent ratio) PDMS onto the Silicon/SU-8 mold. The total thickness of this PDMS layer is not critical, usually 2 to 3 mm, as long as inlet and outlet drilling can be done properly. The PDMS is then degasified in a vacuum desiccator for 15 min and cured in an oven at 80ºC for 1 hour.
5) The PDMS replica is then peeled off from the mold and diced (multiple devices are usually cast on a single mold).
6) Next inlet and outlet ports are drilled.

7) Finally, the device is bonded to a glass slide using oxygen plasma bonding (Harrick Plasma PDC-001) to seal the microfluidic network.

Since the microdevice is planar by design, the attachment of inlet and outlet PVC tubes is made from the top of the structure. Figure 2.2b shows the actual fabricated LoC.

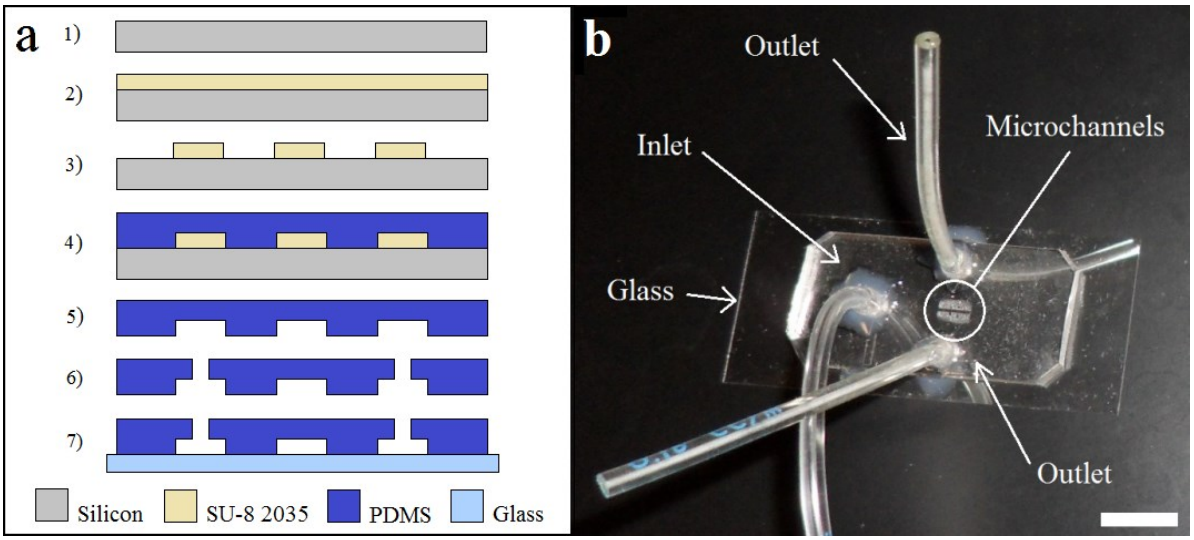

Figure 2.2 (a) LoC fabrication process: 1) Silicon wafer cleaning, 2) SU-8 2035 Photoresist spin coating, 3) Photolithographic patterning and photoresist development, 4) PDMS pouring and curing, 5) PDMS layer detachment, 6) Microfluidic access drilling, 7) PDMS-glass bonding. (b) Fabricated LoC. Scale bar = 1 mm.

2.4 Growth within the LoC

To validate the predictions made by the flow model and to test whether the microchannel device is conducive for pollen tube growth, we used *Camellia japonica* pollen. The pollen is collected and then dehydrated on silica gel before storage at -20ºC. Prior to experimentation, few micrograms of the pollen are thawed and rehydrated in humid atmosphere for 30 min and subsequently suspended in 1 mL liquid growth medium (Brewbaker and Kwack, 1963; Bou Daher and Geitmann, 2011). All tests are performed at room temperature.

2.4.1 Pollen grain distribution

To test the flow-driven distribution of pollen grains within the microfluidic platform, the grain/medium suspension is carefully injected through the inlet with the aid of a syringe. Depending on the amount of pollen injected, the entrances of many microchannels hosted small clusters of pollen grains as desired (Figure 2.3a). However, at the inlet of the distribution chamber several microchannel entrances remained unoccupied. This distribution pattern was consistent with the predictions of the FEM model for high entry flow velocity. Broadening the linear distribution chamber or modifying its shape to conical would likely yield a better distribution of the grains.

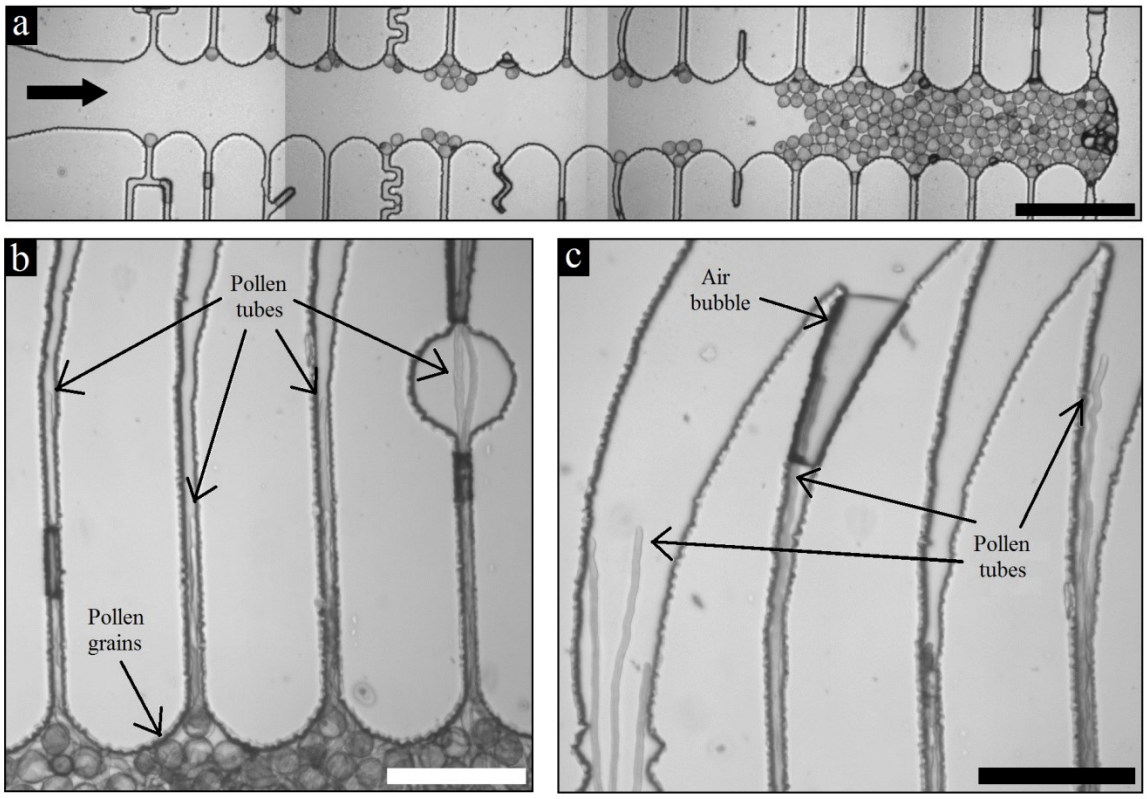

Figure 2.3 Pollen tube growth within the LoC. (a) Initial pollen grain distribution. The inlet flow enters the distribution chamber from left and exits symmetrically through the top and bottom microchannels. Overview image is stitched from high magnification micrographs. Scale bar = 500 μm. (b) Growth of pollen tubes within the microchannels. Scale bar = 250 μm. (c) Growth after 2 hours. Scale bar = 250 μm.

It was also noticed that many pollen grains accumulated at the outlet of the linear distribution chamber, a situation that is not desired. Accumulation occurred because of an excess of pollen grains in the injected suspension. This is consistent with the predictions by the FE model and confirms that controlling the amount of injected pollen is important to obtain optimal distribution. In addition, including a drain outlet at the outlet of the distribution chamber would help removing excess pollen grains.

Once pollen grains are positioned, they are left to germinate. Tests have shown that a continuous flow of medium from the inlet promotes pollen tube growth without displacing the pollen grains. On the other hand, the experiments demonstrated that continuous flow is not a necessary condition in the present setup since even under no-flow conditions germination and pollen tube growth occurred at satisfactory rates. This indicates that the nutrients and oxygen contained in the liquid growth medium filling the microfluidic network is sufficient to sustain pollen tube growth for the duration of an experiment. The fact that the closed chamber prevents evaporation is believed to be an important factor in successful germination and growth.

2.4.2 Pollen tube growth

In bulk *ex vivo* conditions, *Camellia* pollen grains usually start germinating after 30 min imbibition in growth medium; approximately the same time was observed for pollen injected into the microchannel device. The germination rate observed within the microdevice was consistently above 80%, agreeing with *Camellia* plate assays (Bou Daher and Geitmann, 2011). In the description of the results given in this section, time zero is used to indicate the moment when most pollen tubes are germinated.

Figure 2.3b shows that pollen tubes successfully grew into the microchannels. In most cases, the tubes reached the end of the narrow microchannels at about 2 hours after germination, demonstrating that they easily grow more than 1 mm in length under the LoC experimental conditions used here (Figure 2.3c). However, the validation experiments carried out revealed a number of potential problems which should be taken into consideration in future implementations of the platform. Firstly, air bubbles occasionally remained in the device after injection of the pollen suspension (Figure 2.3c). Since contact of a pollen tube with an air bubble may influence its behavior, these should ideally be eliminated through improved design. Furthermore, the use of low resolution (low cost) ink-jet printed masks in the fabrication of the Silicon/SU-8 mold resulted in relatively rough inner channel surfaces with features in the dimension of the pollen tube diameter. Since testing the pollen tube's capacity to respond to mechanical cues is one of the ultimate goals of the present approach, such unspecific mechanical features should be eliminated.

In order to measure the pollen tube growth rate within the microfluidic network, twelve representative trajectories were chosen and quantified by image analysis (Figure 2.4a). Their average growth history with its standard deviation is shown in Figure 2.4b. For comparison purposes a linear fit is used to determine the average growth rate, which was found to be 8.62 μm/min. This value is consistent with the average growth rate reported in the literature for *Camellia* pollen tubes in plate assays (about 12 μm/min) (Bou Daher and Geitmann, 2011).

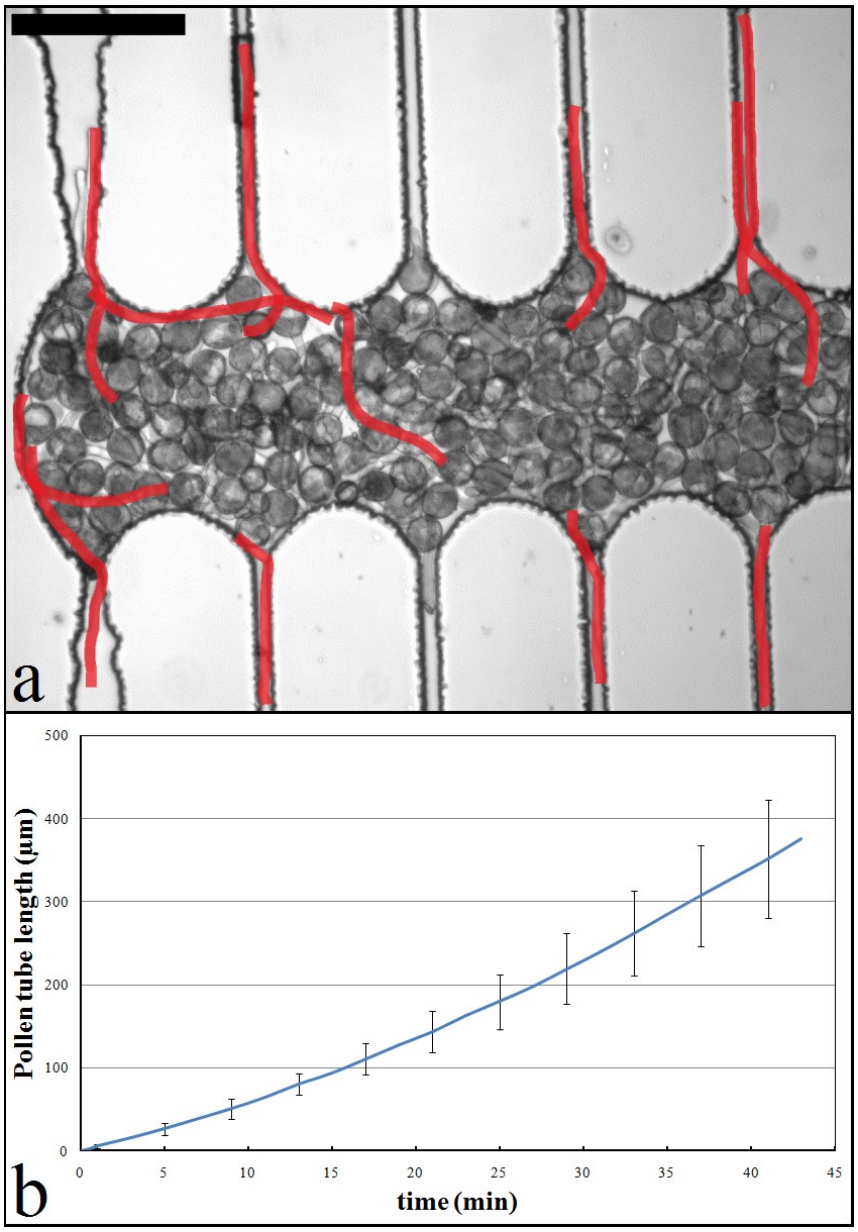

Figure 2.4 (a) Representative trajectories of pollen tube growing within the LoC. Scale bar on top left = 250 µm. (b) Average growth history (n=12). Error bars represent the standard deviation.

A systematic study to investigate the behavior of pollen tubes in differently shaped microchannels is subject of a future study, but the preliminary data shown here revealed that tubes follow the direction imposed by the microchannel regardless of the shape. To

illustrate this, Figure 2.5 show two different pollen tubes easily navigating the 90° angles imposed at 100 μm intervals by a serpentine-shaped microchannel in a similar way.

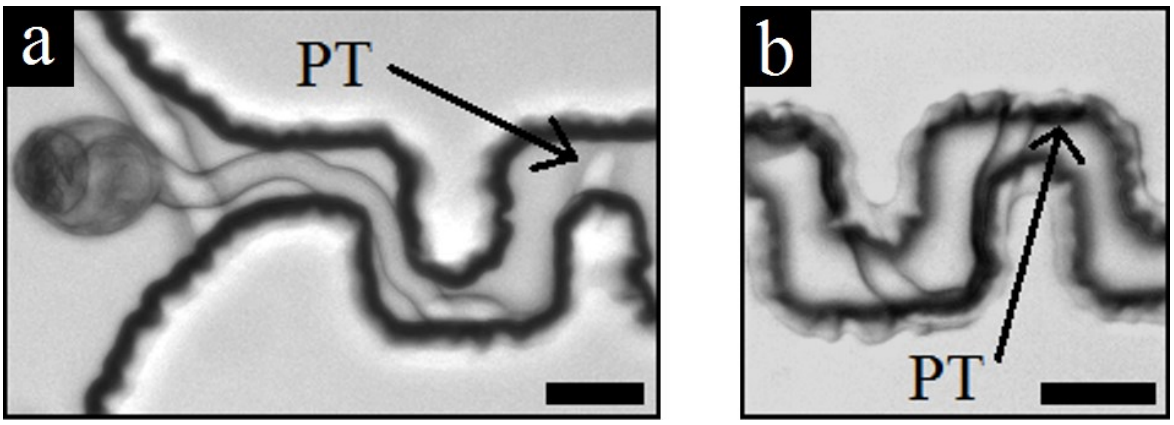

Figure 2.5 Pollen tube (PT) growth along serpentine-shaped microchannels. Scale bars = 50 μm.

2.5 Pollen Tube Collision Test

During the initial tests we noted that the instantaneous growth rate varies considerably when the pollen tube advances unimpeded, or crosses other tubes, or encounters other obstacles in its way. To assess whether this behavior was the result of a physical constraint on growth caused by crowding or the consequence of a touch response, a simple collision LoC was designed (Figure 2.6). A 2D Finite Element Method (FEM) fluid analysis implementing the incompressible Navier-Stokes and continuity equations was also carried out for this design under the same conditions as described in Section 2.2 (Figure 2.6d).

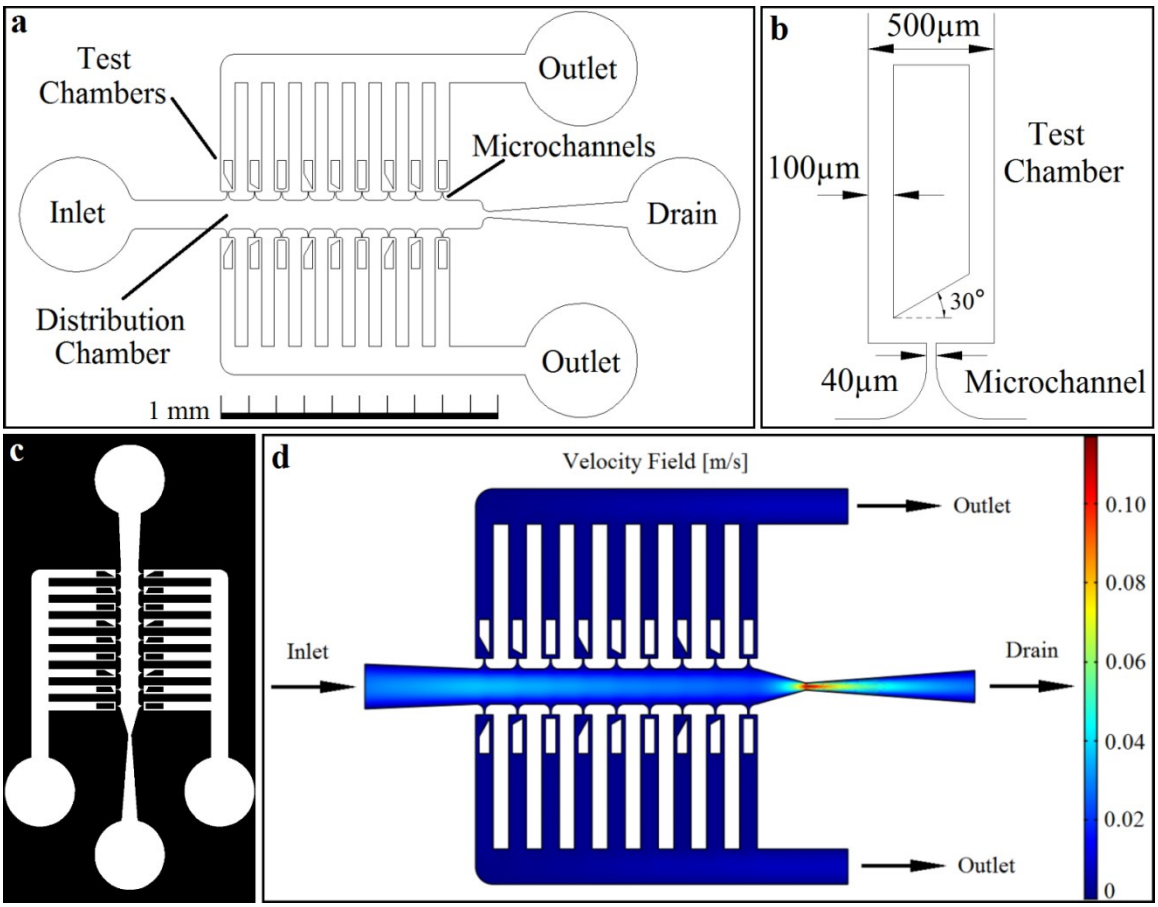

Figure 2.6 Overall design of the LoC. (a) Schematic. (b) Detailed layout of a microchannel and test chamber. (c) Photomask. (d) Velocity fluid field simulation of the microfluidic platform.

This particular device was equipped with a drain outlet at the rear end of the distribution chamber which ensured a more uniform distribution of grains over the microchannel entrances and absence of accumulation at the rear end (Figure 2.7a). Only straight-shaped microchannels are used in order to impose an initial direction of growth on the pollen tubes and to obtain a more homogeneous fluid flow among the microchannels. Each microchannel is followed by a test chamber which contains a fixed plane obstacle at defined angles: 0º, 30º, and 60º between the microchannel direction and the plane normal (Figure 2.7b). The direction of a given pollen tube is only approximately parallel to the orientation of the microchannel. Therefore, all collisions

with obstacles are classified into three types according to the collision angle between the pollen tube and the plane normal: i) angles from -15º to +15º are considered as collision type 0º, ii) angles from +15º to +45º are considered as collision type 30º, and iii) angles from +45º to +75º are considered as collision type 60º. The design is fabricated using a direct-write lithography (DWL) system (DWL 66 FS - Heidelberg Instruments) to achieve higher resolution and therefore minimizing wall roughness, which is essential to ensure a predictable collision angle. Finally, redundancy is exploited by placing the three types of obstacles repeatedly on top and bottom microchannel series.

The growth rate before, during, and after collision is computed for 12 pollen tubes from micrographs taken at 10 seconds intervals (Figure 2.8). It is noted that the average growth rate achieved within the collision LoC is higher than that in the previous section, possibly due to less grain crowding in the distribution chamber, which was intended by the enhanced design. The data show that for type 0º collision the growth rate decreases dramatically and can be temporarily as low as zero. Pollen tubes encountering the obstacle in a type 30º collision also exhibit a statistically significant, temporary decrease in growth rate, however less pronounced, whereas type 60º encounters barely result in any decrease at all. This is consistent with the fact that a type 0º collision forces the pollen tube to make a more demanding turn, whereas a type 60º deviates the pollen tube's trajectory only slightly. Consistent with the higher impact on growth rate, the average duration of the temporary slowdown during a type 0º collision was 4 min, whereas the original growth rate is recovered after 2 min for type 30º. The temporary slowdown and subsequent recovery of pollen tube growth upon contact with an obstacle suggests that this behavior is due to a touch response.

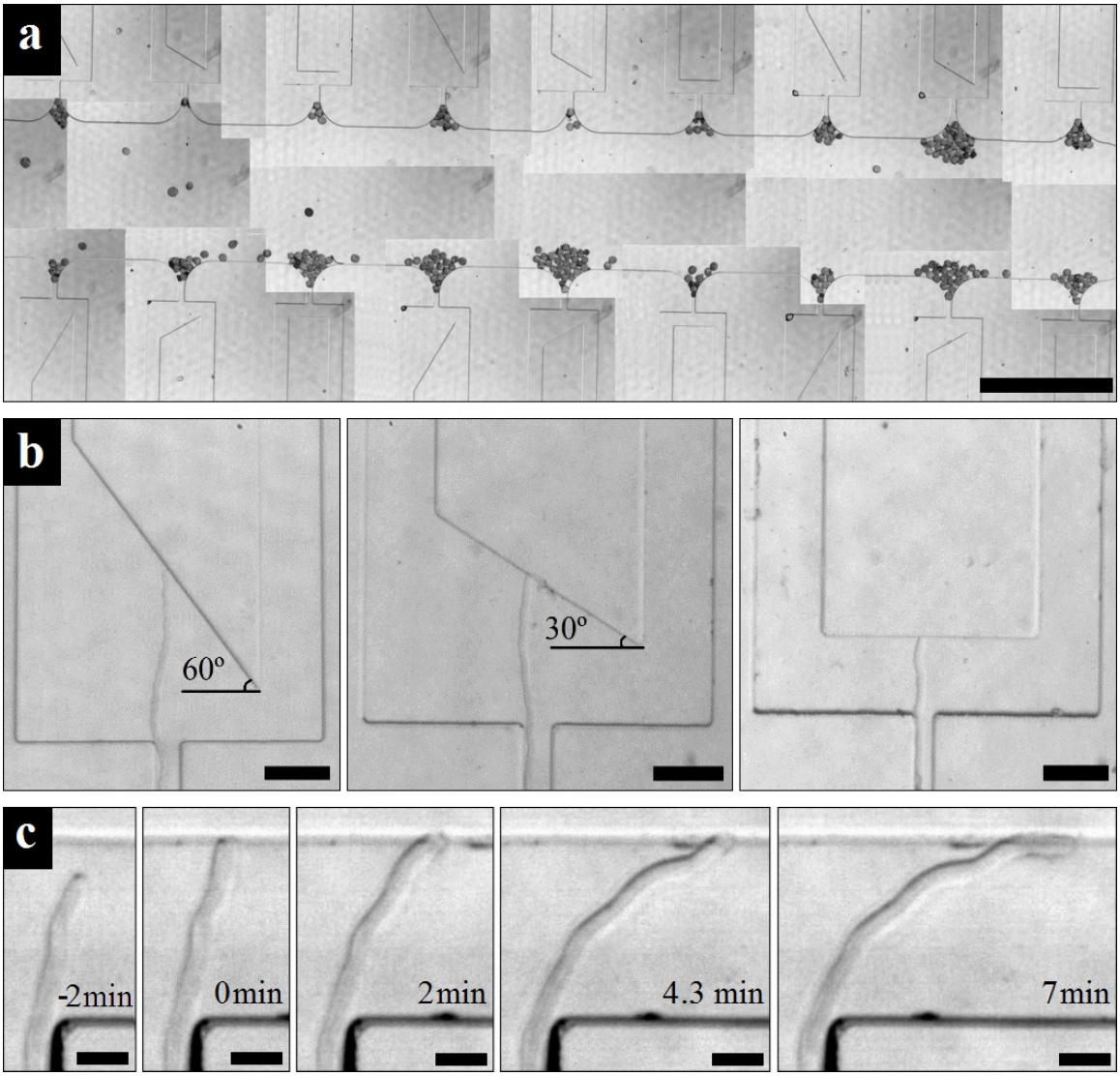

Figure 2.7 Collision test. (a) Initial pollen grain distribution (image is stitched from several high magnification micrographs. Scale bar = 1000 μm. (b) Pollen tubes colliding with predefined obstacles at: 60º, 30º, and 0º. Scale bars = 100 μm. (c) Time lapse sequence of a type 0º collision. Scale bars = 25 μm.

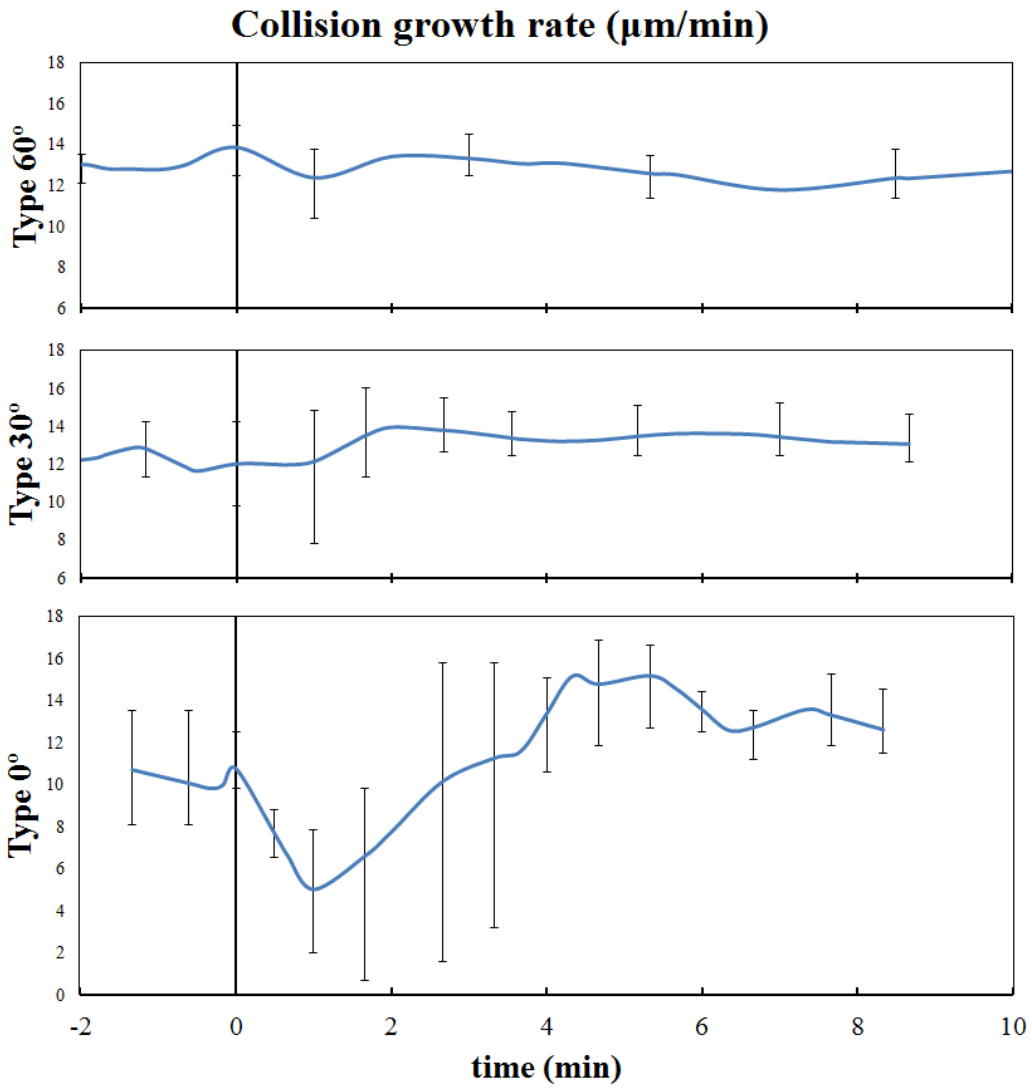

Figure 2.8 Growth rate before, during, and after collision for each collision type. Time zero indicates the moment where collision occurs. Each curve represents the average growth rate for each collision type. Error bars represent the standard deviation.

The finding that higher turning angles are accompanied by longer time-delays for recovery suggests that the apical growth machinery needs to actively change the direction of elongation. It is notable, however, that the pollen tube does not execute an immediate change in direction upon collision. Figure 2.7c illustrates that the pollen tube first resorts to bending and slipping along the obstacle. Only after approximately 4 minutes is the apical region of the tube approximately parallel to the wall, resulting from a reorientation

in the growth direction. Surprisingly, this time point coincides with a temporary increase in the growth rate above that of the original growth rate (Figure 2.8). This behavior might also explain the slight increase of the growth rate for type 30º collisions as soon as 2 min after collision, and for type 60º upon the moment of collision, since in these oblique encounters the pollen tube orientation is closer to parallel to the obstacle. However, a detailed investigation on the role of pollen tube mechanical properties and putative touch response is beyond the scope of this thesis and subject to future investigation.

2.6 Discussion

A LoC for the study of pollen tube growth is presented. The design and fabrication of such platform have been addressed in detail. A microfluidic network has been designed to provide an enclosed environment for pollen tube growth through narrow channels presenting mechanical obstacles. The design ensured that pollen grains are positioned properly at the entrance of the microchannels by simple injection without further manual intervention. Microfluidics simulation has been carried out to support the current design and to predict future, improved configurations.

Experimental testing revealed that *Camellia japonica* pollen successfully germinated and formed elongating tubes. Pollen tube support and alignment was effectively provided by the LoC. Pollen tubes grow along the microchannels in the direction enforced by its shape, often attaining total lengths over 1 mm. Pollen germination and growth rate within the device (*ex vivo*) are consistent with that observed under conventional *in vitro* conditions confirming that the spatial confinement and associated limitation of the volume of the surrounding growth medium does not interfere negatively with cellular behavior.

The interaction of pollen tubes with the microchannel features can elucidate many aspects of pollen tube behaviour as demonstrated with a simple collision test. But, more importantly, the presented microdevice allows for the design and easy integration of different kinds of micro sensors within the microfluidic network to measure various biological parameters of a single pollen tube. This opens multiple new avenues for experimental assays that were not possible in conventional bulk experiments.

Chapter 3 - Microelectrodes and Microfluidic Integration

Herein we propose a microfluidic device, namely ELoC (Electrical LoC), to develop a reproducible assay for the study of *Camellia japonica* pollen tubes subjected to global and local electric fields. It enables positioning of the cells and controlled application of electric fields through microelectrodes. It is compatible with high resolution imaging, and it is reusable. Reusability is integrated into the ELoC by separating the design into two separate bondable modules: a PDMS-based microfluidic network module that houses the cells and the liquid medium, and a metal-based microelectrode module through which electric fields are applied.

3.1 ELoC Design

The microdevice offers a simple way to introduce and position the cells, to allow accurate exposure to electric fields during growth, and afterwards to remove them as well as any traces of growth medium. This last feature is particularly challenging since pollen is notoriously difficult to remove or dissolve because of its extreme resilience to chemical reactions, pollen is often the only plant remnant in fossil records (Gray et al., 1985; Langdon et al., 2004), particularly in tightly enclosed environments where the tubes might easily get entangled. Additionally, the integration of microelectrodes into the ELoC is simple and versatile, yet compact and accurate. The trade-off is not straightforward as these properties are not necessarily positively correlated.

In order to address these specifications, a modular design was conceived based on two components: i) a microfluidic network that positions and immobilizes the cells, and ii) an

electrical interface that permits the application of an electric field (Figure 3.1). The microfluidic network layer is set to a height that is determined by the size of the pollen grains plus a margin for free movement (80 μm for *Camellia japonica* pollen). This is meant to avoid clogging while allowing free, fluid-flow driven motion of the cells. Additionally, the planar arrangement ensures compatibility with optical imaging. The electrical module consists of a metal layer that is used to apply a voltage signal on the microelectrodes, thus generating a desired electric field. The geometry of the metal electrodes determines the exact electric field pattern, providing a great level of control.

The ELoC is designed to be opened, cleaned, and closed again for reuse by enabling the detachment and reattachment of the two modules without damaging or destroying the inner features. This approach lends itself to a point-of-care operation since the ELoC can be recycled in a reduced laboratory environment, as only rebonding is required. To ensure reusability, a SU-8 layer is patterned on top of the metal layer as to expose only the microelectrodes and to function as a protective top layer. This arrangement ensures that the metal layer never touches the microfluidic module, providing a longer life to the microdevice.

Each module of the ELoC is fabricated separately. In general this approach offers the following practical advantages: i) since each module is independent, the fabrication of the ELoC is decoupled, maximizing fabrication yield and minimizing costs in case of fabrication defects; ii) the design of one module can be used along with different designs of the other module, increasing versatility without the need for further fabrication.

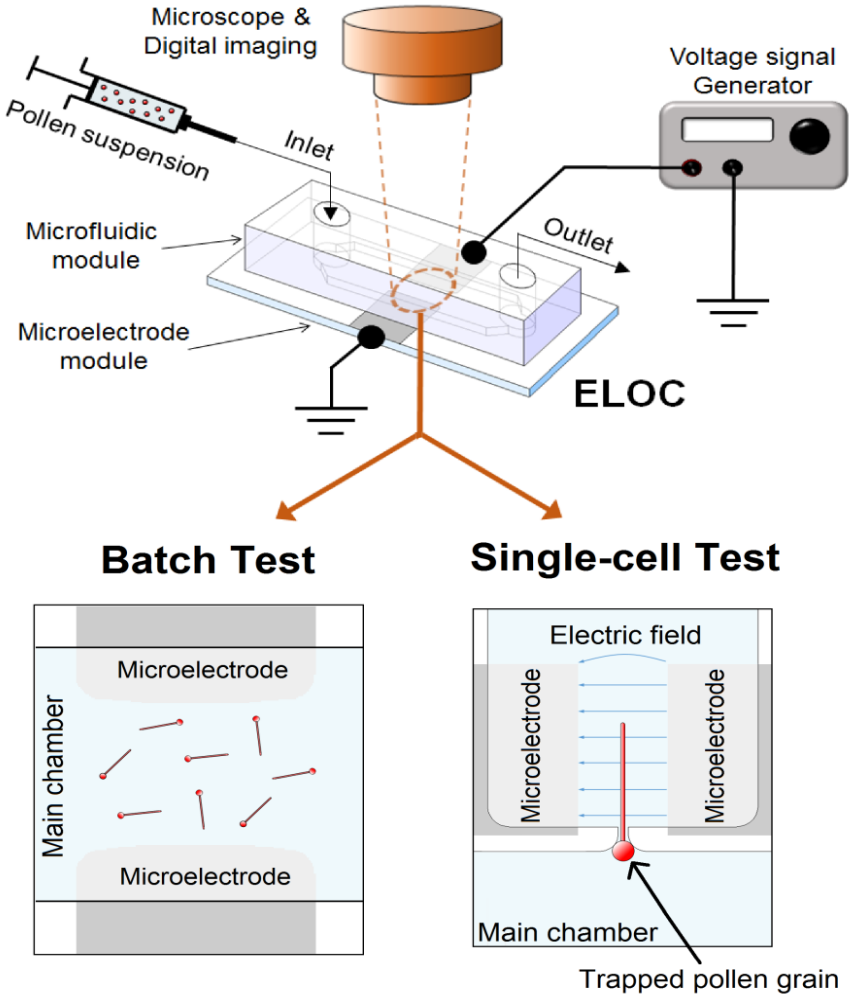

Figure 3.1 Schematic view of the ELoC setup. The ELoC can be configured to perform both types of tests: Batch and Single-Cell.

3.2 Microfluidic Network

In order to expose pollen tubes to global and local electric fields, two different versions of the ELoC were considered. The microfluidic network and electrical layout for both batch and single-cell ELoC's are shown in Figure 3.2. The basic microfluidic layout for tip-growing cells has been described previously (Agudelo et al., 2012). Briefly, the pollen grain suspension is first injected into the microfluidic network through an inlet into a main chamber. The batch approach uses such a main chamber to apply a global

electric field to populations of pollen tubes whereas the single-cell approach employs adjacent electrical test chambers to apply a localized electric field to single pollen tubes. A set of microchannels connects the test chambers to the main chamber. Fluid flow in the main chamber distributes the grains towards the entrances of the microchannels within which pollen tube growth is guided to the electrical test chambers. Each microchannel is 45 μm wide in order to trap pollen grains while allowing passage to the pollen tube only. An outlet drain is placed at the far end of the main chamber to evacuate excess pollen grains preventing their accumulation at the entrances of the microchannels. Additionally, any mechanical sensor or relevant structure could be included in the microchannels as required by the test. For instance, barriers, shaped microchannels (Sanati Nezhad et al., 2013a, 2013b), additional chambers, or even microcantilevers can be employed (Sanati Nezhad et al., 2013c). Finally, outlets are placed at the end of the microfluidic network to provide an exit for the medium flow.

The shape of the traps was designed to capture several pollen grains rather than single grains (Figure 3.2b). This design feature exploits a phenomenon that has not been investigated systematically in pollen grains: *quorum sensing*[30]. Our preliminary tests have shown that when only a single *Camellia* pollen grain was trapped at the entrance of a microchannel, germination rarely occurred; whereas when a group of grains were clustered at the entrance, most of them produced healthy tubes. This improved performance by clustered cells has been observed in bacteria (Boedicker et al., 2009), and seems to apply to the species of pollen used here. The exact conditions and proper quantification of this growth behaviour warrants further research but for the present

[30] Quorum sensing refers to stimulus and response correlated to population density.

approach the trapezoidal microfluidic network was optimized to always obtain groups of pollen grains.

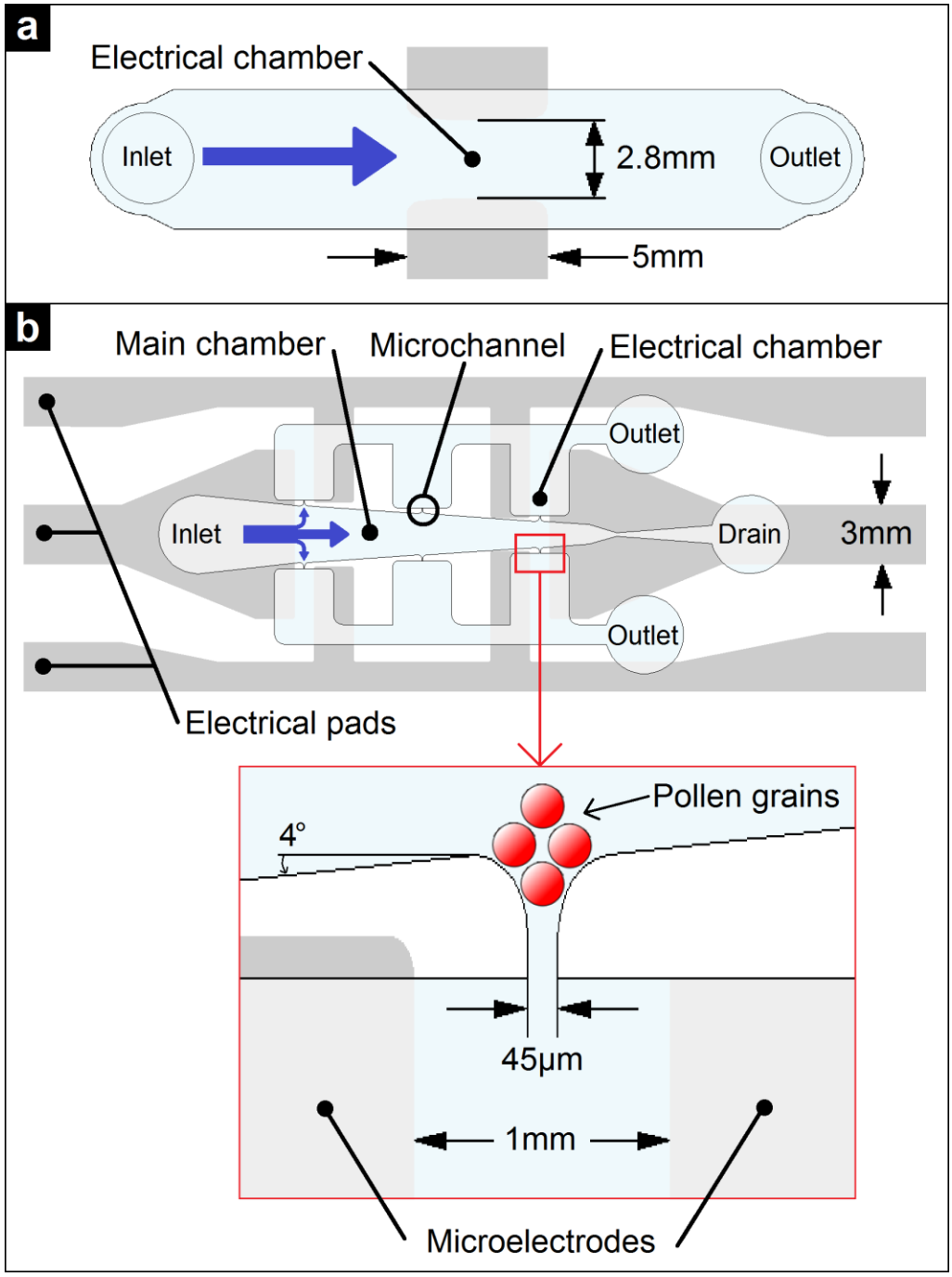

Figure 3.2 ELoC design. a) Batch ELoC. b) Single-cell ELoC.

Since the positioning of the pollen grains at the entrances of the traps is achieved by fluid flow, the geometry of the main chamber is crucial. To achieve uniform distribution of pollen grains over the serially arranged traps, here we propose a trapezoid-shaped main chamber. By widening the inlet of the main chamber the inlet streamlines are better spread between the traps, improving cell distribution, as opposed to using a rectangular configuration (Sanati Nezhad et al., 2013d).

To experimentally assess the performance of different angles of the trapezoid shape of the main chamber, we experimentally evaluated the efficacy of cell trapping at the traps with 4°, and 8° inclinations of the main chamber shape and compared them to a rectangular (linear) shape (0°) (Figure 3.3). As shown previously, a rectangular main chamber resulted in greater grain accumulation at the traps located at its far end (Agudelo et al., 2012; Sanati Nezhad et al., 2013d). An 8° inclination reversed the trend by yielding a greater grain accumulation in the traps located close to the inlet. By choosing an intermediate 4° inclination, however, the distribution of pollen grains among the trap entrances was rendered nearly even. It is worth noting that the distribution pattern also depends on the geometry of the inlet and of the shapes of the traps and therefore needs to be optimized if the overall chamber geometry is altered.

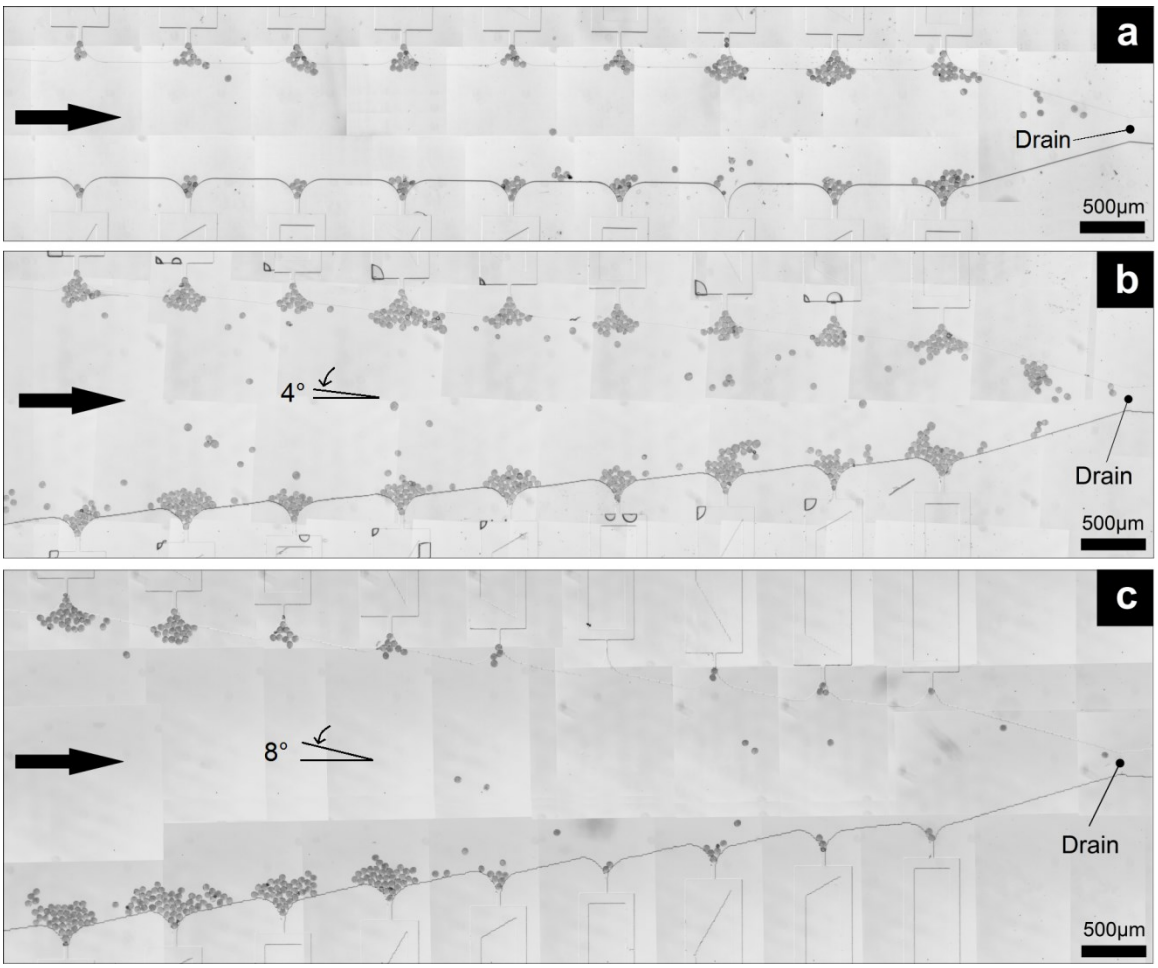

Figure 3.3 Microfluidic network design after pollen grains injection. a) Trapezoid-shaped chamber at 0°, b) at 4°, c) at 8°. The arrow indicates the direction of fluid flow upon injection of the pollen tube suspension.

3.3 Biocompatibility of Materials

Pollen tubes are highly sensitive to chemical agents, hence their use in toxicity assays (Kristen and Kappler, 1995). PDMS is conventionally used in MEMS fabrication, and has been demonstrated to be conducive to pollen tube germination (Agudelo et al., 2012). However, advanced MEMS-based approaches require various types of materials to be included in the LoC, for example for fabrication of electrodes, actuators and sensors. Therefore, we tested the behavior of pollen tubes suspended in a drop of growth medium

in direct contact with thin layers of various MEMS materials: PDMS (1:10 polymer base/curing agent ratio), single-crystal silicon wafer, sputtered gold, aluminum film and laminated copper.

Pollen germinating in contact with PDMS, silicon, aluminum and gold exhibited growth, but the presence of metallic copper almost completely suppressed pollen germination and tube growth (Figure 3.4). The physiological reason for this inhibitory effect of copper warrants further research, but may be related to the electrophysiology of the pollen tube (Feijó et al., 1995) or the toxicity of copper ions released by the metal (Sawidis and Reiss, 1995). To assess this further, we fabricated a PCB-based LoC in which a copper layer is present at the bottom of the chamber immediately adjacent to and at the same height as a PDMS layer (Figure 3.4c). Pollen grains were placed in all parts of the chamber by injection and germinated under 'no flow' conditions. Quantification of the pollen tube length of grains located at various distances from the copper substrate revealed a clear long-distance inhibitory effect, probably caused by the toxicity of copper ions released into the medium. This is further corroborated by preliminary findings obtained under constant flow conditions showing that pollen tube growth in the vicinity of the copper layer but not in direct contact with copper was restored to control levels by continuous replacement of the medium. Despite its higher conductivity, the use of copper for fabrication of electrodes in further testing must therefore be evaluated critically, and is not recommended for experiments conceived to be performed under 'no flow' conditions. Instead, aluminum is chosen as the metal layer material.

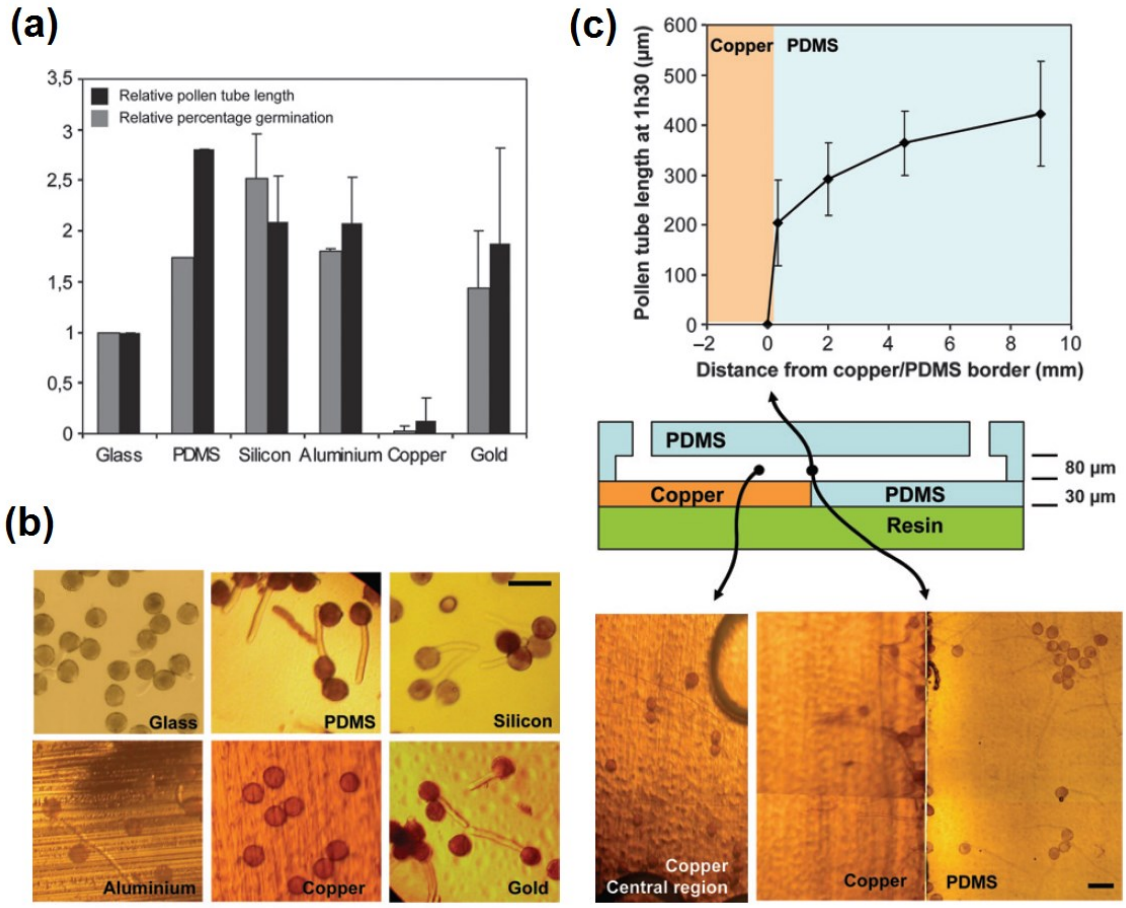

Figure 3.4 Biocompatibility testing of materials. (a) Relative percentage of germinating *Camellia* pollen grains and relative mean length of pollen tubes in the presence of various materials. Values were normalized to the glass sample. Bars are standard deviation errors from three repeats. (b) Stereomicrographs of *Camellia* pollen germinated in the presence of the various materials used in MEMS fabrication. Scale bar = 100 µm. (c) The distance dependence of copper-induced inhibition of pollen tube growth (top) was tested in a specially devised LoC (cross-section shown in the centre; objects are not to scale). Scale bar = 100 µm.

3.4 Microelectrode Integration

The metal layer of the ELoC consists of microelectrodes, electrical routing, and electrical pads. Tests on batches of cells, for instance, can be carried out with as few as two electrodes. However, LoC technology is better used by exploiting redundancy to increase reliability, especially when working with biological samples since these show considerable variation in their response. By incorporating more test sites the probability

for a successful test increases; moreover, control tests can be included directly in the chip. Redundancy in electrical pads also serves the purpose of monitoring the applied electrical signals, which confirms the presence of the electrical stimulus or indicates a failed test, even if it is a simple defect in the electrical routing. These benefits are exploited in the single-cell ELoC.

A variety of metals can be used for the microfabrication of the microelectrodes, each of which is associated with constraints, such as potential toxicity for the living cells (Li and Lin, 2011). For instance, copper was found to be toxic for *Camellia japonica* pollen tubes, whereas aluminium is not (Agudelo et al., 2013b). Other metals such as gold or platinum are often used due to their reduced reactivity (Robinson, 1968), but availability, cost, and ease of use are concerns.

In preliminary tests, deposited layers of metal were considered to build the microelectrodes. These included materials such as gold, indium tin oxide (ITO), and aluminium. Although deposited layers of these materials performed well electrically, they pose a problem for reusability. Because of the small thickness of evaporated or sputtered material (in the order of a few nanometers), the metal layer is scraped and torn apart very easily, making handling, detaching and reattaching of the modules unfeasible in the long term. To find a more viable solution (both in economic and practical terms), thicker layers were considered. As the thickness increases, the mechanical resistance to wear improves. In addition, the deposited metal layer entails high resistance paths between the microelectrodes and pads (>100 Ω), whereas resistances of less than 1 Ω are common with thicker layers. However, the metal layer cannot be too thick, since this would compromise the planarity of the protective SU-8 layer, which would in turn reduce the

bonding between the microfluidic module and the electrical module. As for the material, even though gold has a slightly higher electrical conductivity, aluminium was chosen as the metal element since it is considerably more cost-effective for thick layers, compatible with microfabrication, and bio-compatible with pollen tubes. To ascertain that the layer is sturdy enough, a 15 μm aluminium thickness is used. Glass is chosen as the substrate onto which the metal layer is placed since transparency is required for microscopic visualization.

The following protocol was optimized for reliable fabrication of the ELoC with an integrated patterned aluminium thin film (Figure 3.5).

- The fabrication of the microfluidic platform, is done using principles of soft lithography (Ziaie et al., 2004). The exact details of the technique are detailed elsewhere (Agudelo et al., 2013a). Concisely, the microfluidic layout is used as a mask to reproduce the design on a Silicon/SU-8 mold through photolithography. Multiple PDMS replicas are then cast from the mold, detached, and diced (Figure 3.5-1). Next, the microfluidic inlet and outlet are punched in order to allow the insertion of PVC tubes from the top of the chip (Figure 3.5-2).
- A thin PDMS layer is coated on the glass substrate. 1 ml of PDMS (10:1 polymer base/curing agent ratio) is poured on a clean glass slide and spin-coated at 2000 rpm for 20 s (Figure 3.5-3).
- The aluminium thin film is placed gently on top of the substrate. A larger glass is placed on top of the aluminium as to produce a flat layer. Then the entire assembly is clamped. Trapped air bubbles are evacuated by slight directed pressure and vacuum if necessary (Figure 3.5-4).

- The clamped set is placed in the oven at 65°C for the PDMS layer to cure (at least 1h). Once fully cured, the set is unclamped and excess aluminium around the glass slide is cut away.
- In order to improve the adhesion and homogeneity between the photoresist and the aluminium thin film, plasma treatment is applied to the aluminium layer for 25 s. Immediately afterwards, positive photoresist (AZ1518) is spin-coated on the aluminium layer at 800 rpm for 20 s. The set is let to settle for 2 min to improve homogeneity, then prebaked at 100°C for 2 min, and finally left to settle for 2 min at room temperature to allow hardening of the photoresist (Figure 3.5-5).
- The photoresist is then patterned with a positive mask of the electrode configuration by standard UV exposure (Figure 3.5-6).
- The photoresist is post-baked at 100°C for 2 min so as to fully crosslink, and let to settle for 2 min at room temperature for hardening. Then the photoresist is developed for 3 min. The photoresist is next annealed at 100°C for 2 min to remove residual stresses after development, and let to settle for 2 min at room temperature (Figure 3.5-7).
- The aluminium layer is next wet-etched at 70ºC (on a hotplate) for 1 h. The aluminium etchant is a combination of phosphoric acid (80%), acetic acid (5%), nitric acid (5%), and deionized water (10%), which results in a smooth etched surface. Next the photoresist is easily removed with acetone (Figure 3.5-8).
- Once the aluminium layer is patterned, a layer of SU-8 2035 is coated on top. The SU-8 is spun at 3000 rpm to produce a 40 μm thick protective/insulating layer.

Then it is aligned and patterned as to expose only electrical pads and microelectrodes (Figure 3.5-9).

- Electrical wires are bonded to the metal pads with conductive epoxy to provide electrical access to the electrical chamber (Figure 3.5-10).
- The two modules are aligned and bonded together using oxygen plasma in order to seal the electrical chamber. In our setup (Harrick Plasma PDC-001), activation times between 30 s to 1 min produced satisfactory results. In order to ensure a proper bond and to avoid any leakage, the two modules are clamped together immediately after contact (Figure 3.5-11).

Figure 3.6a shows a fabricated Batch ELoC. Once the ELoC has been used for an experimental assay, it undergoes a simple procedure to make it ready for reuse. This procedure should be performed as soon as the test ends as to minimize contamination of the chip. First, the modules are gently detached by peeling the PDMS bulk from the microelectrode module (Figure 3.6b). Each module can then be thoroughly cleaned and any residue removed. Finally, both modules are rebonded using the procedure described above. The proposed ELoC has been tested in several series of electrical tests and is generally expected to last dozens of reuses with minimum care.

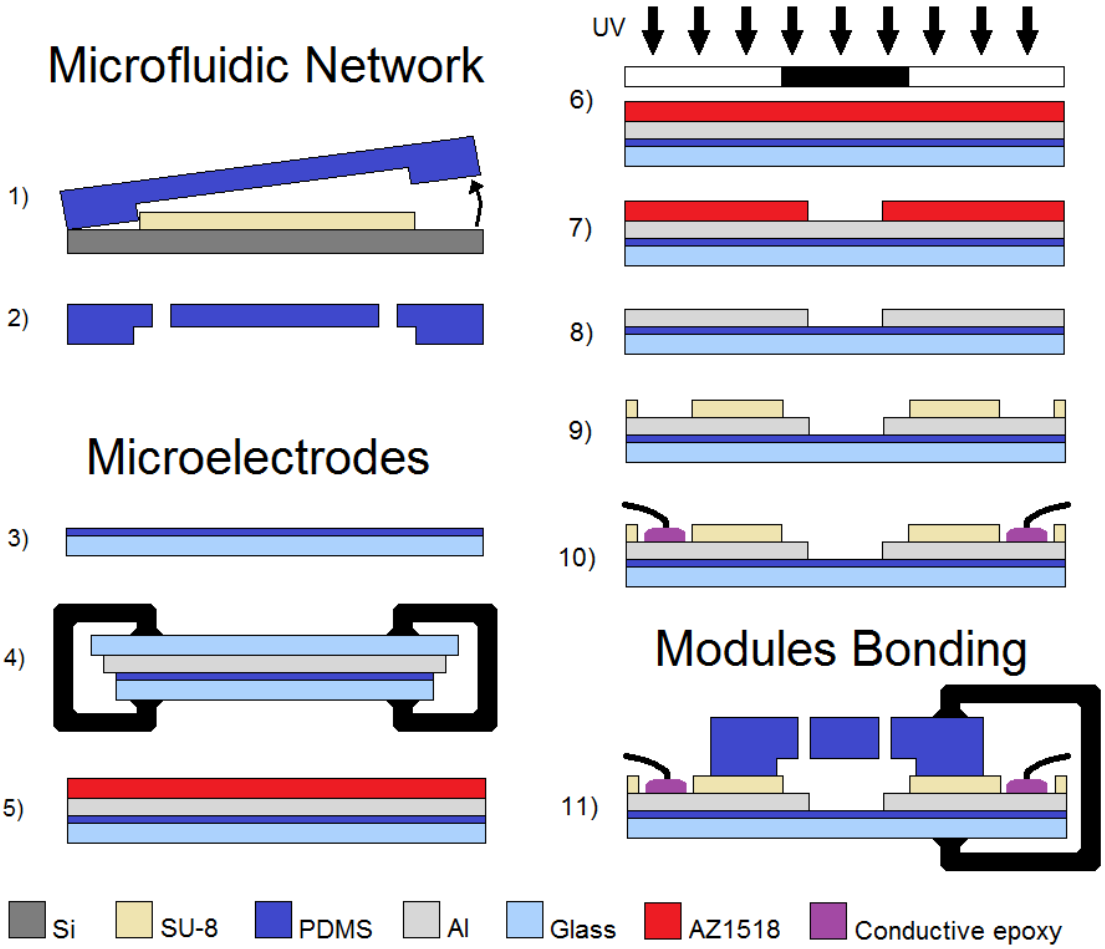

Figure 3.5 ELoC fabrication process: (1) PDMS layer detachment from the silicon/SU-8 mold, (2) microfluidic inlet and outlet punching, (3) thin PDMS layer spin-coating on glass substrate, (4) aluminium thin film clamping, (5) positive photoresist (AZ1518) is spin-coated on the aluminium layer, (6) standard UV exposure with metal layer mask, (7) photoresist developing and annealing, (8) aluminium etching, (9) coating and patterning of the insulating SU-8 layer, (10) wire bonding, (11) bonding of the microfluidic network module to the microelectrode module.

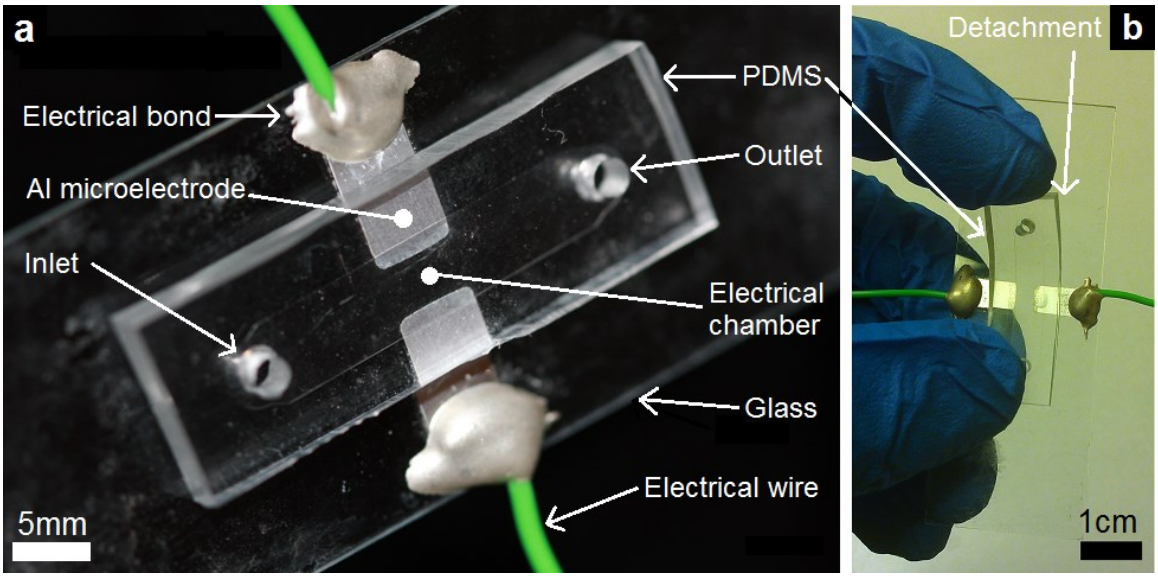

Figure 3.6 Reusability procedure. a) Fabricated ELoC. b) Microfluidic module detachment from the microelectrodes module.

3.5 Medium Conductivity

During experimentation, the microfluidic network is completely filled with liquid growth medium (usually in the range of a few microliters), hence the behavior of this solution in the presence of an electric field needs to be assessed. The growth medium used here was previously optimized for optimal germination and pollen tube growth of the species *Camellia japonica* and contains salts and sugar (1.62 mM H_3BO_3, 2.54 mM $Ca(NO_3)_2 \cdot 4H_2O$, 0.81 mM $MgSO_4 \cdot 7H_2O$, 1 mM KNO_3, 8% sucrose (w/v)) (Bou Daher and Geitmann, 2011), which makes it an electrolyte. Hence, the electrical behaviour of this medium might become considerably complex when an electric field is present. Since this point is generally overlooked in the literature, here we investigated the medium conductivity in the absence of pollen to better understand the electrical behaviour of the tests. A conductivity cell was built to properly assess the bulk medium conductivity (Figure 3.7a).

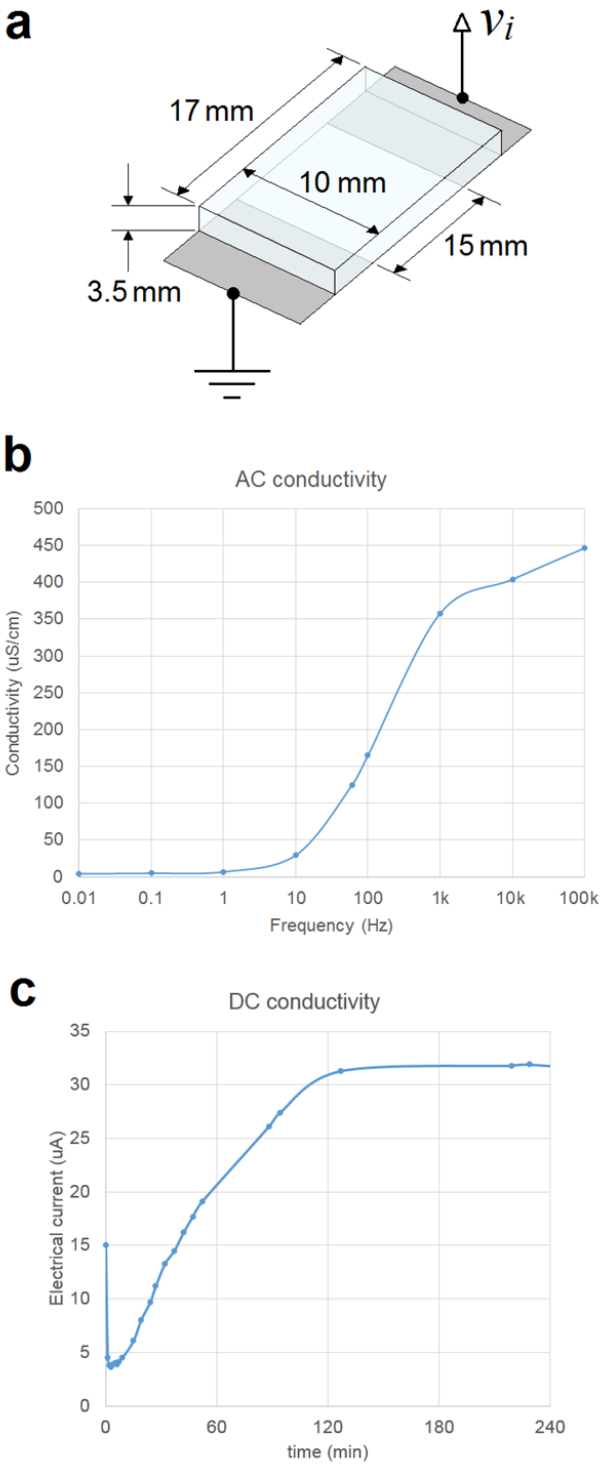

Figure 3.7 Growth medium conductivity. a) Conductivity cell for quantification of growth medium conductivity. b) Dependency of AC conductivity on frequency, c) Dependency of DC conductivity on time.

First, an AC conductivity test was carried out. A sinusoidal voltage input v_i at different frequencies was directly applied to the conductivity cell using an Agilent 33220A waveform generator. The amplitude of the sinusoidal signal was set at 1V. For each frequency the sinusoidal electrical current i was measured using an Agilent 34401A mutimeter and the electrical resistance R was computed as v_i/i. Assuming a purely ohmic behaviour, the growth medium resistivity ρ can be computed as $R(A/l)$, where A is the cross-sectional area of the conductivity cell and l is the length between the electrodes. Figure 3.7b shows the computed growth medium conductivity $\sigma = \rho^{-1}$ in the frequency range considered in this work. This AC conductivity test shows that the medium conductivity is highly dependent on the applied frequency. It is noted that around 1 kHz the conductivity is close to the values reported in the literature, which is consistent with the fact that most standard conductivity meters operate close to this frequency to avoid electrolysis (Platzer et al., 1997; Weisenseel and Jaffe, 1976). Using standard commercial equipment (Hanna HI98129, which uses standard AC voltages) we determined a similar conductivity value for our medium (670 μS/cm). Previous experimental studies on pollen tubes reported the use of similar devices for conductivity measurement, but none of these studies actually applies an AC electric field during experimentation (Malhó et al., 1992; Nakamura et al., 1991; Nozue and Wada, 1993; Wang et al., 1989). Figure 3.7b shows that as the frequency decreases the conductivity drops. Since constant electric fields are fundamental to the present work, a DC conductivity test was carried out next.

Using the same conductivity cell a constant voltage input (3.3V) was applied and the electrical current was measured for several hours. Figure 3.7c shows that the electrical current through the growth medium is not the constant value expected for a purely

resistive medium. Initially, there is a current peak, then the current rapidly plunges, followed by a steady increase until it reaches a plateau after 2 hours. The current values correspond to a range of conductivities from approximately 4.6 to 41.4 μS/cm, which is considerably lower than the typical AC conductivity at 1 kHz. Two hours after the current leveled out it started to slowly decrease (down to 22 μA after 17 h). At 17 hours a scant whitish aggregation had formed along a line parallel to the microelectrodes in the center of the conductivity cell. This aggregation formed gradually and was not observed during the first 4 hours.

3.6 Modeling an Electrical Test Chamber

Compared to macroscopic assays, the ELoC has the advantage of applying an electrical stimulus to cells in a more precise, stable and reproducible way, since the well-defined ELoC geometry reduces complicated boundary conditions for the electric field (Li and Lin, 2011). Due to the planar geometry of our design, the exact electric field distribution produced by the microelectrodes can be accurately predicted by a 2D simulation, and hence used to determine the local experimental conditions at subcellular resolution. We also used these simulations to aid designing microelectrode geometry, for example to minimize fringing field zones and achieve homogeneous electric fields.

For DC tests, where a purely ohmic culture medium with conductivity σ is assumed, the governing equation is the Laplace equation $\nabla^2 V = 0$, where V is the voltage at any particular point in the simulated geometry with respect to ground. The electric field E is uniquely determined by the applied voltage (as $E = -\nabla V$) regardless of the medium conductivity. The simulation of the resulting electrostatic field in the single-cell ELoC electric chamber is performed by Finite Element Methods (FEM) using Comsol

Multiphysics software (Figure 3.8a). Boundary conditions for the left electrode were set as a constant 1V input value, the right electrode is set as ground and the limits of the geometry are set as electric insulation.

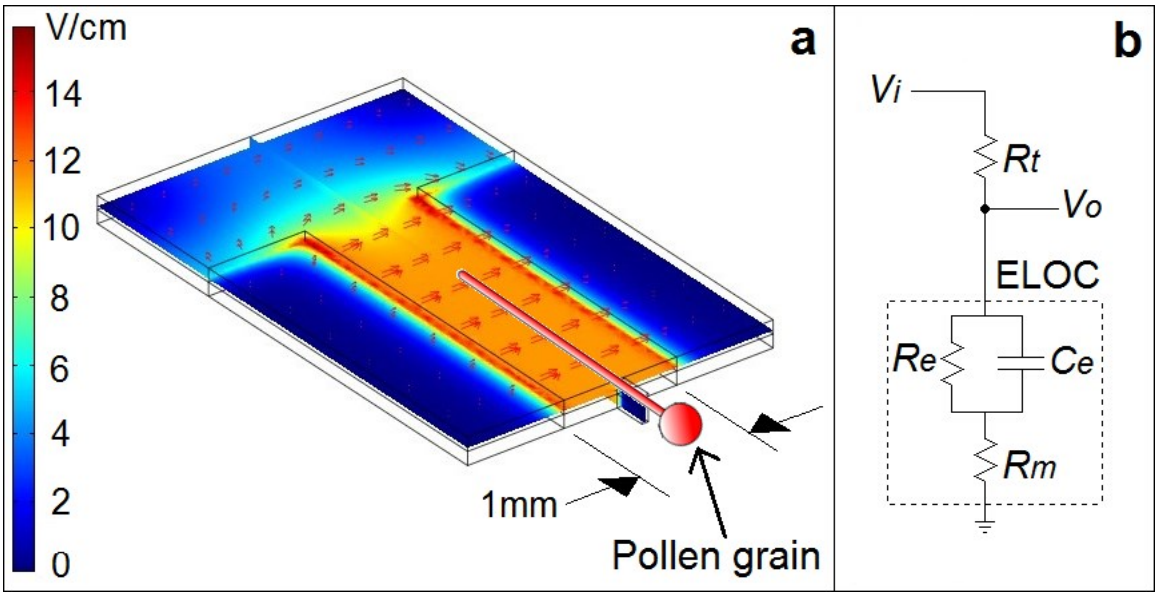

Figure 3.8 ELoC electrical model. a) Simulated electric field norm [V/cm] within an electrical test chamber for a constant 1V input. Arrows: electric field direction and normalized intensity. b) ELoC equivalent circuit.

In order to develop the ELoC's electrical model under any electric field, the role of the electrical double layer that forms at the interface between the metal microelectrodes and the electrolyte solution could also be considered (Robinson, 1968). Although it is beyond the scope of this work to discuss the intricacies of the poorly understood electrochemistry involved, the electrical behaviour of the ELoC can be characterized by the circuit in Figure 3.8b, where C_e is the capacitance of the electrical double layer at the interface, R_e is the leakage resistance across the electrical double layer, and R_m is the resistance of the culture medium between the electrodes.

Electrical tests on cells fall essentially into two categories: DC and AC tests. For DC tests the capacitance C_e can be neglected since the behaviour is mostly ohmic once the

capacitance is fully charged. For AC tests, however, the capacitance cannot be neglected since its reactance becomes relevant with frequency. On the other hand, R_e can be neglected for AC tests since its resistance is much higher than the reactance produced by C_e. The values of these parameters can be estimated by setting the following conditions: first, an AC test was carried out in which a sinusoidal voltage input v_i at different frequencies was directly applied to the ELoC (Agilent 33220A waveform generator). The amplitude of the sinusoidal input signal A_i was set conveniently at 1V. For each frequency the sinusoidal output voltage v_o was measured both in amplitude A_o and in phase ϕ. Figure 3.9a shows the signal attenuation measured in dB as $20\log_{10}(A_o/A_i)$. In steady state, v_o is given by

$$v_o = \frac{R_m - jX_c}{R_t + R_m - jX_c} v_i$$

where $X_c = 1/\omega C_e$ is the capacitive reactance, ω is the angular frequency, R_t is a known resistor (set to $154\ k\Omega$), and the input v_i is considered as the reference at a phase of zero degrees. The amplitude and phase of the output signal can then be deduced as

$$A_o = \frac{\sqrt{[R_m(R_t + R_m) + X_c^2]^2 + R_t^2 X_c^2}}{(R_t + R_m)^2 + X_c^2}$$

and

$$\tan\phi = \frac{-R_t X_c}{R_m(R_t + R_m) + X_c^2}$$

By solving these two equations simultaneously one obtains the values of R_m and C_e at each frequency (Figure 3.9b). As expected for electrolytes, these parameters do not behave as lumped elements of constant value; rather they tend to decrease as frequency

increases (Robinson, 1968). From R_m and the ELoC dimensions the AC conductivity of the medium can be computed (Figure 3.9c). It is seen that the AC conductivity increases significantly with the applied frequency. Given the electrolytic nature of the growth medium, this complex dependency on the frequency is not surprising, rather it is already acknowledged (Chandra and Bagchi, 2000).

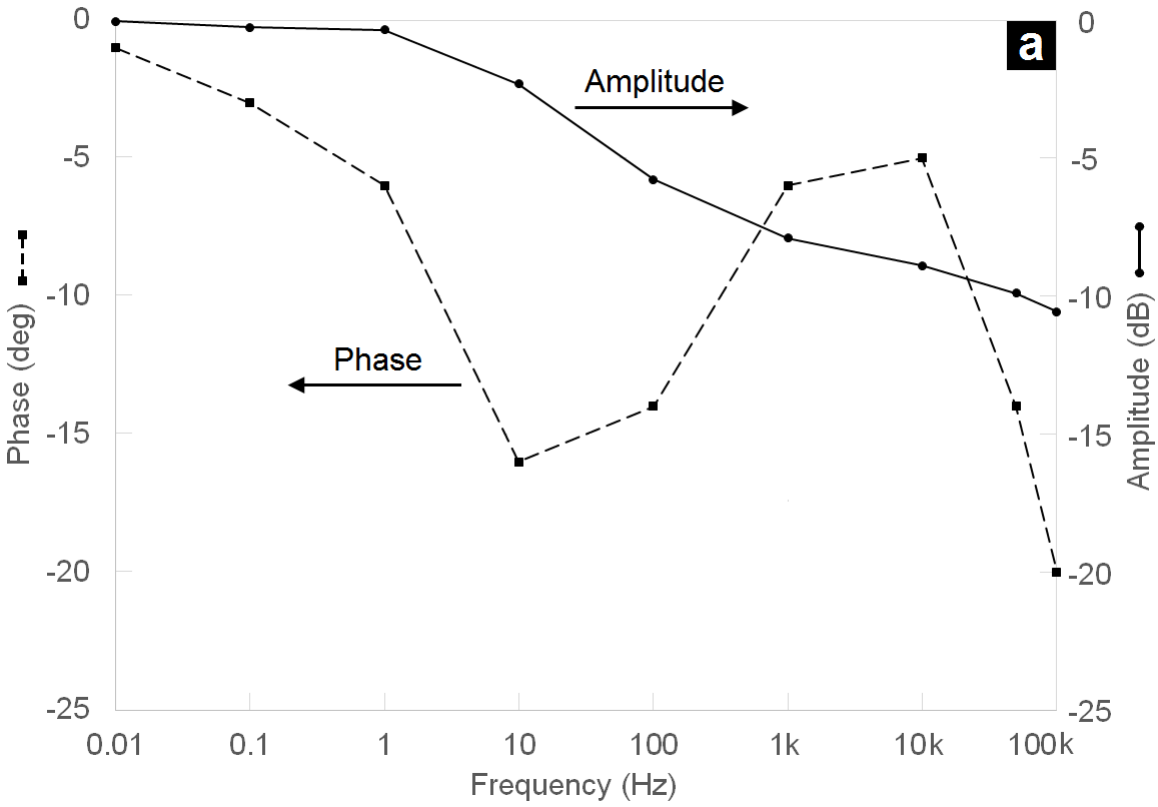

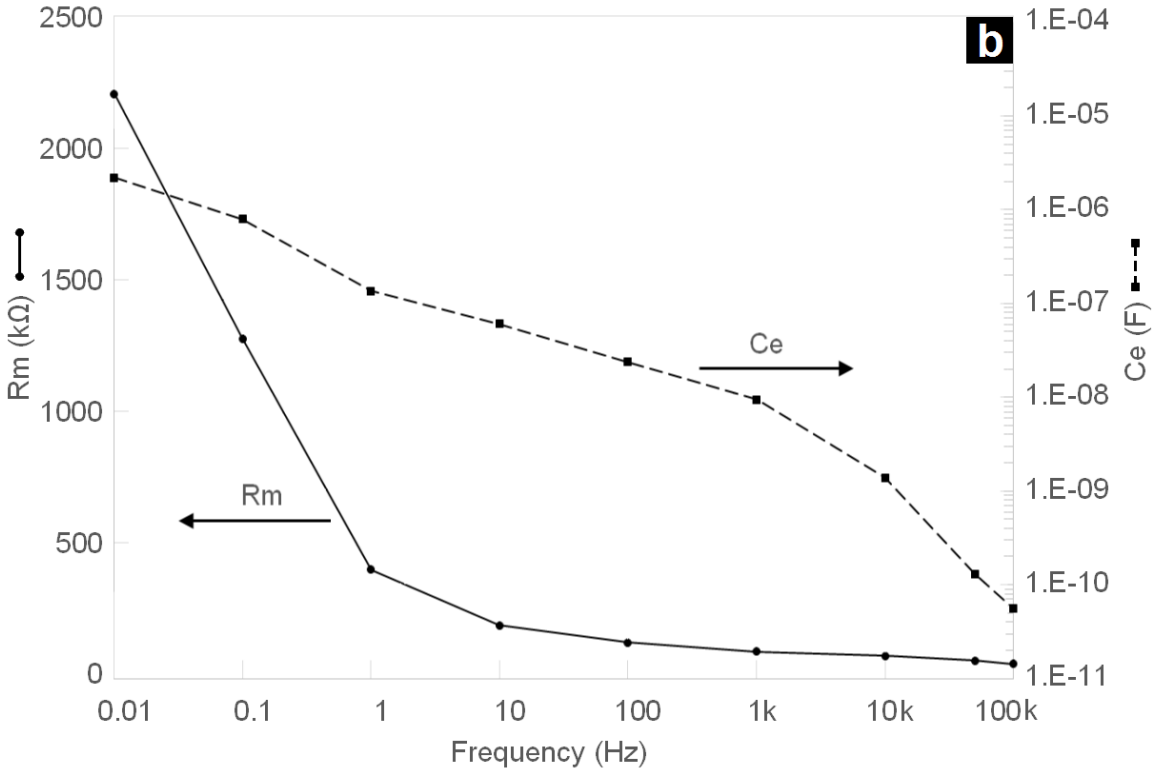
b
2500
2000
1500
1000
500
0
Rm (kΩ)
1.E-04
1.E-05
1.E-06
1.E-07
1.E-08
1.E-09
1.E-10
1.E-11
Ce (F)
Ce
Rm
0.01
0.1
1
10
100
1k
10k
100k
Frequency (Hz)

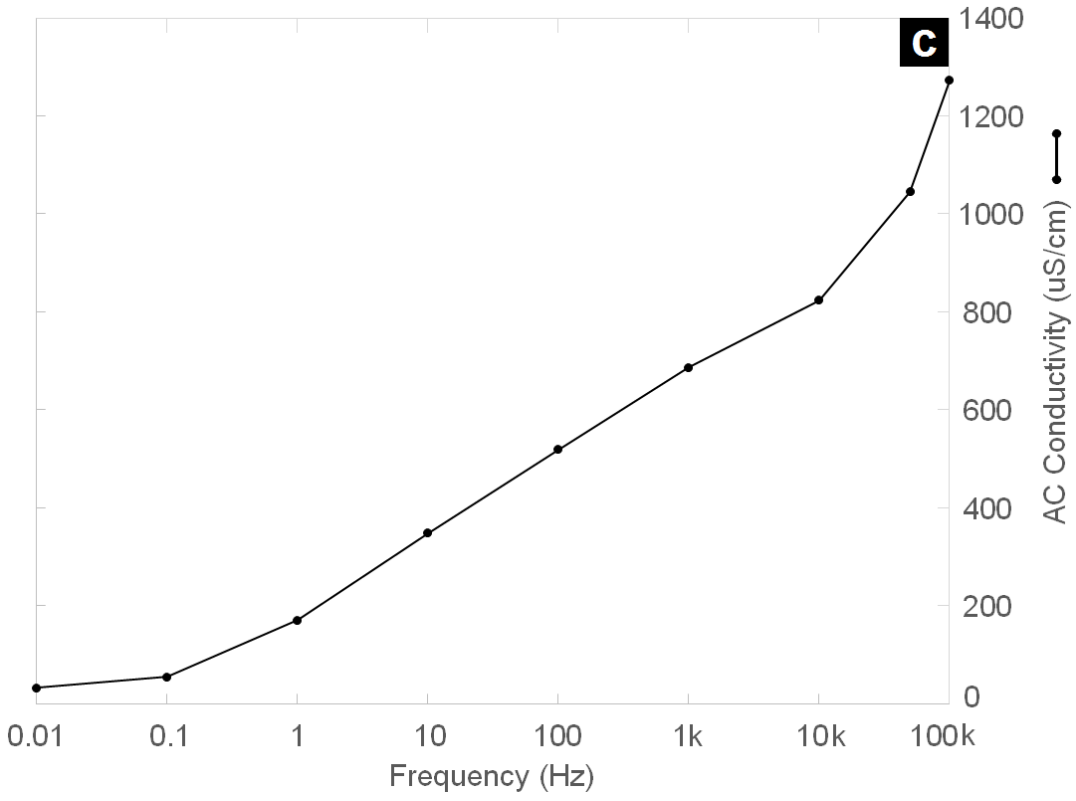
c
1400
1200
1000
800
600
400
200
0
AC Conductivity (uS/cm)
0.01
0.1
1
10
100
1k
10k
100k
Frequency (Hz)

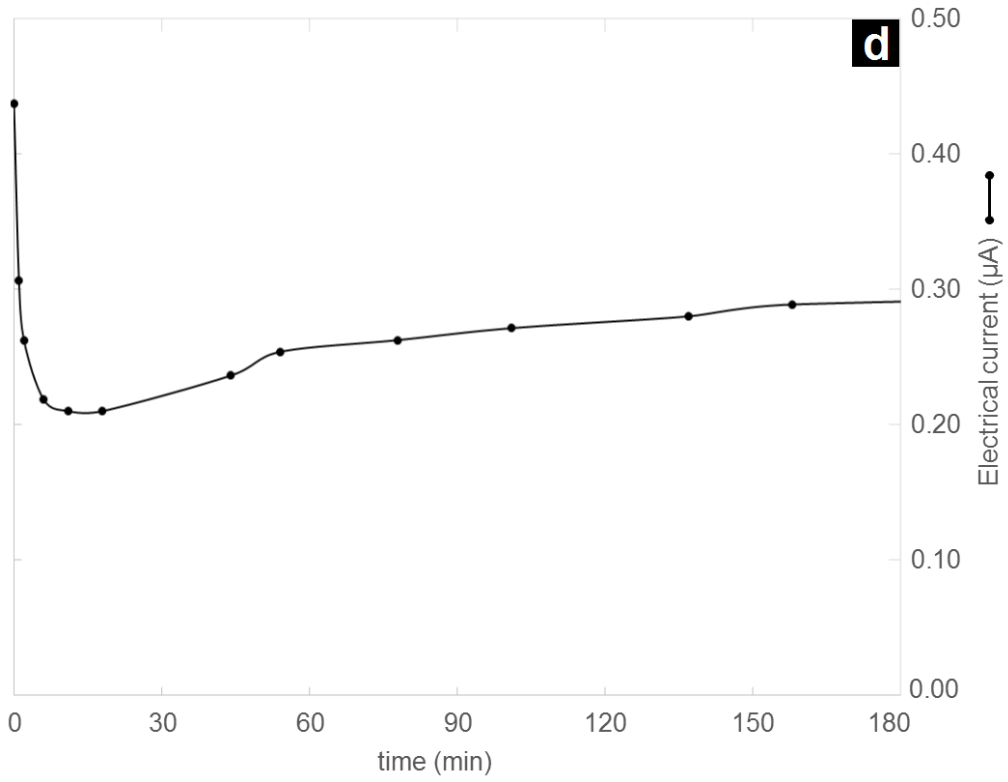

Figure 3.9 ELoC electrical model characterization. a) Measured signal attenuation and phase versus frequency. b) Estimated values of R_m and C_e versus frequency. c) Conductivity versus frequency. d) Current through ELoC measured over time for a constant input voltage (3V).

Next a DC conductivity test was carried out to estimate the value of R_e. Ideally the response to a constant input voltage should be a constant current (purely ohmic behaviour); however, due to the presence of an electrolyte, the electrical current obtained under such conditions deviates from this as it varies over time (Figure 3.9d). Because of electrokinetic phenomena, such as the formation of ionic gradients, the electrical behaviour of the ion charges is not straightforward. Moreover, the use of DC entails electrolysis, further complicating the overall behaviour. Nonetheless, considering that the initial peak lasts a few minutes and the length of a regular electrical experiment on living cells typically takes a few hours, DC behaviour can well be approximated by the sum of R_e and R_m in series once the initial transient is past. The average DC resistance can be

obtained by averaging the steady final current, which yields $0.25\,\mu A$, which in turn corresponds to a total resistance ($R_e + R_m$) of $12.2\,M\Omega$. It must be noted that the average DC conductivity falls between 4.7 and 9.8 µS/cm, which agrees with the trend observed in Figure 3.9c when extrapolating to DC (frequency zero).

Incidentally, the electrical characterization of the electrical test chamber inspired the design of a Bendable 2D Load Sensor (see Appendix-A, page 123).

Chapter 4 - Effect of DC Electric Fields on Pollen Tube Growth

4.1 Biological Material and Experimental Test Conditions

Camellia japonica pollen was collected, dehydrated, and stored on silica gel at −20°C until use. Pollen was thawed and rehydrated in humid atmosphere for one hour before submersion in liquid growth medium and injection into the chip. Once the pollen is positioned in the ELoC, the growth medium flow is stopped and the electric field is turned on. Then the pollen tubes are left to germinate and grow for 2 hours undisturbed. All tests were carried out at room temperature. Since the resulting electrical current is small (nanoamperes in every case), heating of the medium is considered negligible.

To ensure reproducibility of test conditions, the following considerations were made: i) No flow conditions were maintained during testing. ii) The set-up eliminates the use of agarose, buffers, dyes, bridges or additives of any kind thus reducing the complexity of parameters potentially affecting the field. iii) At the end of every test an extreme voltage was applied to visually assert the presence of the electric field by inducing electrolysis, therefore a test series is carried out in increasing order of applied voltage to minimize any possible effect of wear in the microelectrodes due to the application of such extreme voltages. iv) Only pollen from the same plant, same flowering season, and same collection lot was used in a given series to minimize the effect of genetic variation, environmental conditions and grain maturity. v) Complete wetting of each microelectrode by the growth medium is assessed visually to ensure proper electrical conduction. vi) Due to surface tension and the small LoC dimensions, it is difficult to ensure the complete

absence of any trapped air, especially during injection. However, the presence of air bubbles is kept to a minimum to avoid any disruptions in the electric field distribution as a result of differences in the electrical properties of the medium. In particular, bubbles are avoided since oxygen influences pollen tube tropism (Blasiak et al., 2001). vii) Pollen density in the suspension is adjusted to obtain a minimum of 25 pollen grains in each zone of the electric chamber for statistical purposes, but no more than 80 to avoid overcrowding which would compromise imaging and might lead to cell-cell interactions. Tests which did not comply with these criteria were aborted.

4.2 Quantitative Assessment of Pollen Tube Behaviour

Pollen tube growth was monitored using an Olympus BX60M bright-field microscope equipped with a Nikon Coolpix 4500 camera (resolution of 1.28 μm per pixel). Time lapse images of the entire electrical chamber were acquired at regular intervals and stitched. Depending on the test, the following parameters were measured: pollen tube length, percentage of germination, percentage of bursting (tubes and ungerminated grains). As pollen tube orientation plays an important role in the putative effect of an electrical cue, the initial and final orientation of each pollen tube is measured with respect to the orientation of the microelectrodes. For this parameter only pollen tubes longer than twice the diameter of their grain were taken into account. Zero angle was considered to be perpendicular to the electric field (Figure 4.1). Positive (counter clockwise) and negative (clockwise) angles are used, yielding the total range: $[-180°, 180°]$. Any angle computation outside this range is converted to its equivalent angle within the range. Furthermore, germination sites are scored with the value -1 when the pollen tube

germinates towards the bottom microelectrode and +1 when the pollen tube germinates towards the top microelectrode.

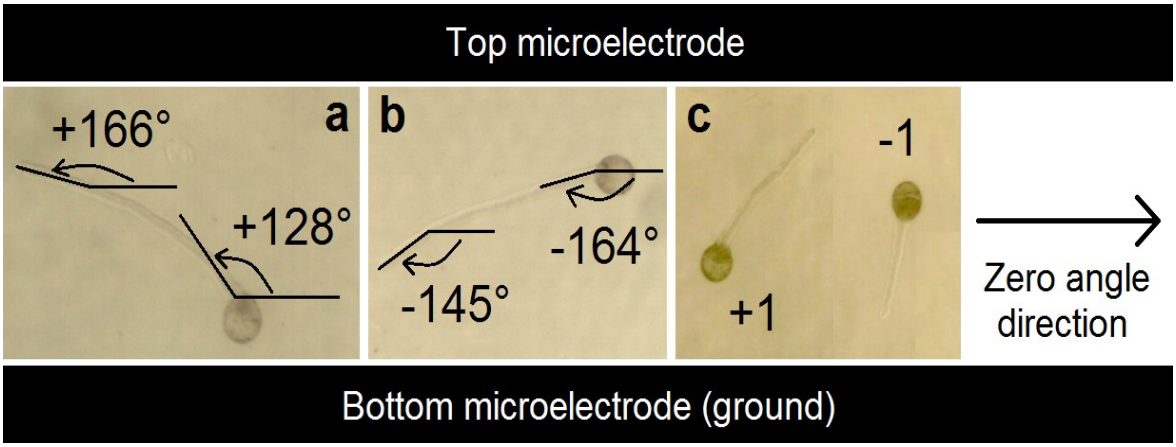

Figure 4.1 Quantification of pollen tube orientation. Angles were determined for the initial and final tube portions with respect to the zero angle direction as indicated by the arrow as positive angles (a), negative angles (b), and the germination site on the grain was scored with respect to its orientation towards either electrode (c).

4.3 Maximum Electric Field Conditions and Simulation in DC Batch Tests

In order to assess the maximum field strength that has an effect on pollen tube growth in our setup, various levels of constant voltage (up to 3.4 V) were applied and pollen tube behavior in different zones of the batch ELoC were considered (Figure 4.2). At high voltages bubbles appeared around the ground electrode (Figure 4.2b). This is a by-product of electrolysis and was dose-dependent. For aluminium electrodes these bubbles started appearing after one hour of applying 3.0 V. No bubbles formed below this voltage threshold. For voltages higher than 6 V, on the other hand, bubbles formed within seconds, completely covering and hence electrically insulating the microelectrode. The threshold voltage was not constant between experiments. It slightly increased as the

microelectrodes were reused, most likely due to the medium-microelectrode interaction as suggested by stains that started appearing on the metal layer after several usages. It is noted that for high voltages a faint aggregation formed along a midline between the microelectrodes, similarly to that observed in the conductivity cell described above.

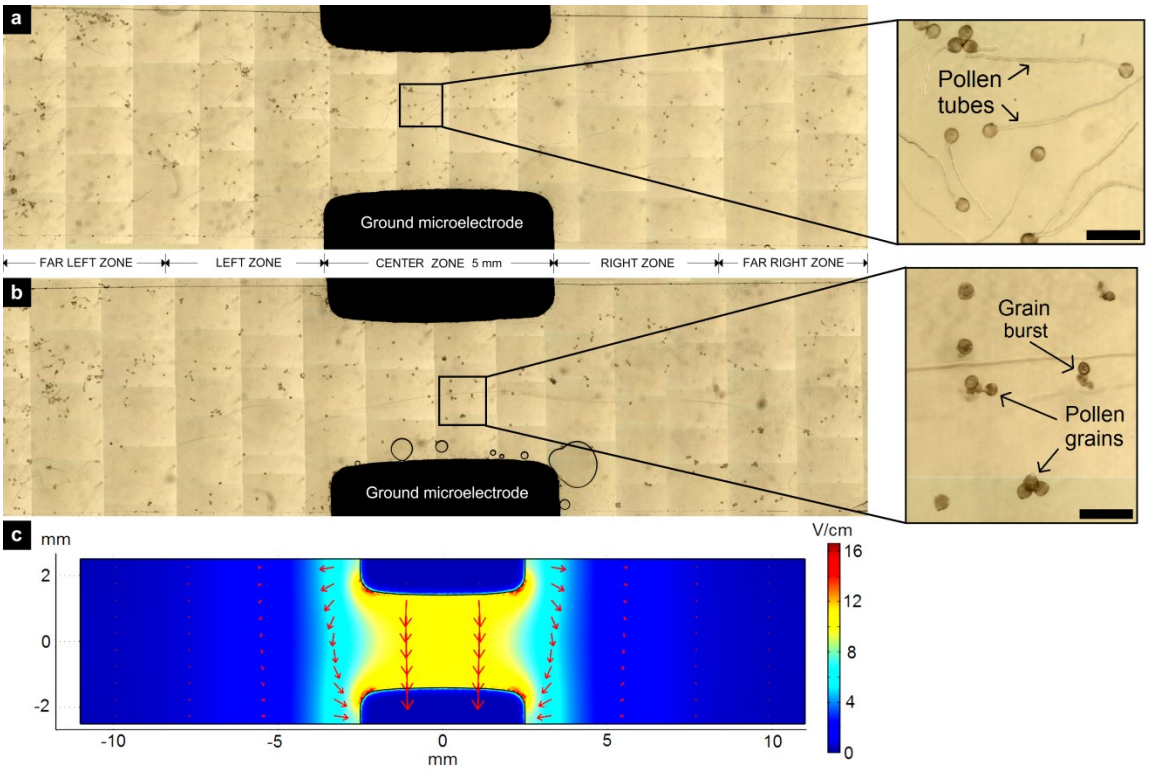

Figure 4.2 Electric field conditions and simulation. a-b) Stitched micrograph of germinated pollen in DC batch electric chamber at 0 V (a), and 3.0 V (b). Scale bars on both zoom-in = 200µm. c) Simulated electric field norm [V/cm] within the electrical chamber for a constant 3 V input. Arrows: electric field direction and normalized intensity.

In order to predict the behaviour of the electrical chamber once it is filled with culture medium, 3D Finite Element Method (FEM) analysis was performed with Comsol Multiphysics. Figure 4.2c shows the simulated electrostatic field in the electric chamber considering the culture medium as a purely ohmic medium with conductivity σ. For a purely ohmic medium, the equation governing the physics is the Laplace's equation:

$$\nabla^2 V = 0,$$

where V is the voltage at any particular point in the simulated geometry with respect to ground. The electric field E is uniquely determined by the applied voltage (as $\mathrm{E} = -\nabla \mathrm{V}$) regardless of the medium conductivity. In Figure 4.2c the boundary condition for the upper electrode was given as a constant 3V input value, the bottom electrode is set as ground and the limits of the geometry are set as electric insulation. Based on simulations, a slightly curved shape was given to the microelectrodes to minimize the fringing field. It is noted that the electric field between the microelectrodes (the center region of the electrical chamber) is fairly homogeneous and can be approximated by $|\mathrm{E}| = \mathrm{V}/\mathrm{d}$, which in this case results in $|\mathrm{E}| = 3\mathrm{V}/0.28\mathrm{cm} = 10.7\ \mathrm{V}/\mathrm{cm}$. Based on this simulation, we categorized five vertically separated zones: the center zone with a homogeneous field that is approximated by $|\mathrm{E}| = \mathrm{V}/\mathrm{d}$; a left and a right zone adjacent to the parallel electrodes where the electric field fringe dominates; and a far-left and a far-right zone where the electric field is relatively small. Data from equidistant zones on the left and right were pooled.

4.4 Effect of Batch DC Electric Fields on Pollen Tube Growth

In the series shown in Figure 4.3 the average pollen tube length throughout the LoC for the zero-voltage test resulted in 721 μm, which amounts to an average growth rate of approximately 8 μm/min (taking into account a typical germination time of 30 min). These values are well within the range reported in the literature, but they are not constant between batches. Therefore, pollen tube lengths were always normalized with respect to the zero-voltage test (721 μm in this case).

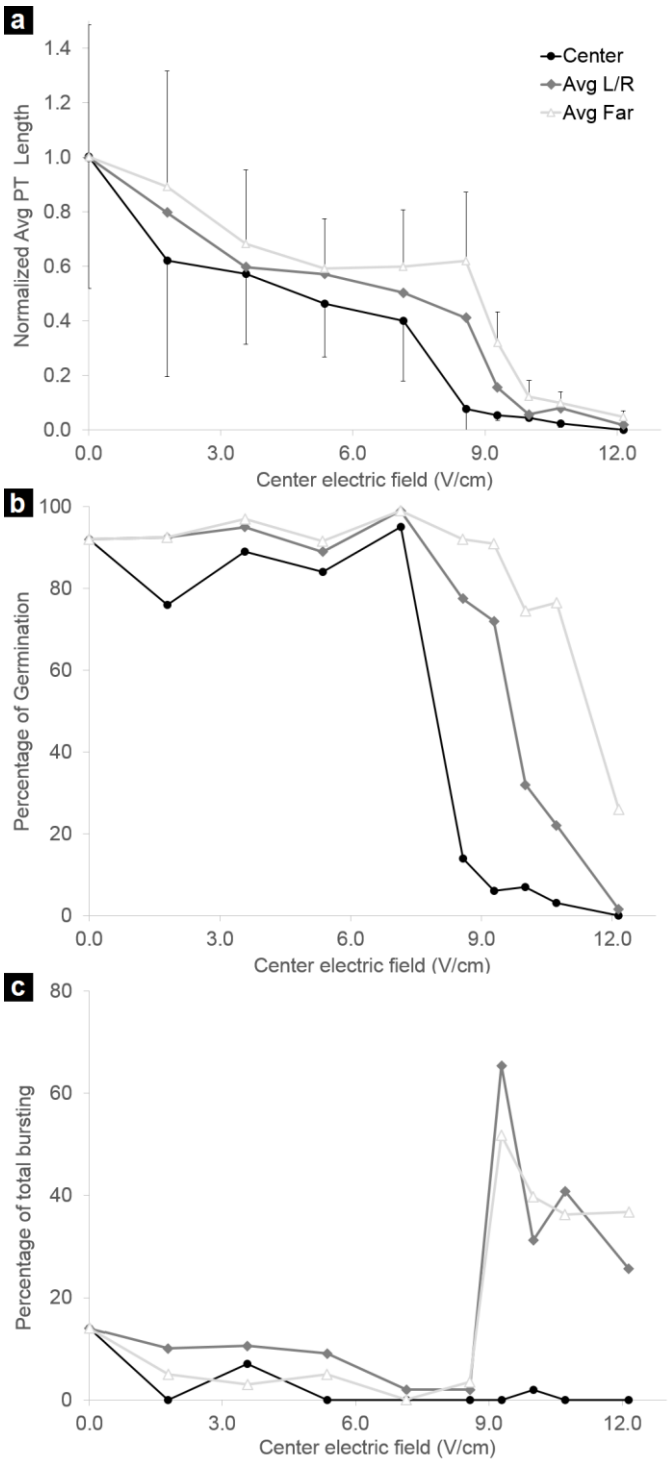

Figure 4.3 Effect of batch DC electric fields on pollen tube growth (n=2572). a) On normalized pollen tube length. b) On percentage of pollen germination. c) On percentage of bursting. The field strength applied between the electrodes is indicated on the x-axis. L/R = pooled data from Left and Right Zones, Far = pooled data from Far left and right zones. For clarity, the standard deviation in a) is only indicated for the Center and Far zones.

Tests run at different constant electric fields showed that pollen tube performance was both dose- and position dependent. In the zero-voltage test (which corresponds to an electric field strength of 0 V/cm) all zones within the electric chamber showed a similar average tube length indicating that the simple vicinity to the aluminium electrode did not affect pollen tube growth (Figure 4.3a). Increasing electric fields decreased the average pollen tube length. At all applied voltage levels the pollen tubes most affected were those in the center zone, where the cells were located directly between the electrodes. The effect was less severe for the Left and Right zones and much reduced for the Far-Left and Far-Right zones. This pattern is consistent with the electric field distribution shown in Figure 4.2c. When the electric field applied was sufficiently high all pollen in the LoC was effectively inhibited from growing (>12 V/cm in Figure 4.3a).

Similarly to the pollen tube length, the percentage of pollen germination also decreased as the applied electric field increased (Figure 4.3b). However, germination remained relatively unaffected for small electric fields but dropped steeply once the electric field was raised past a certain threshold (around 8 V/cm). Again the central zone was more affected than the periphery. The pollen grains located in the center zone did not display much bursting since the percentage of bursting was always below 20% (Figure 4.3c). However, in the adjacent left and right zones, bursting increased dramatically for field strengths above 8 V/cm. The reason for this is elusive, but at least two considerations can be made: i) bursting might require an ongoing germination process, whereas totally inhibited grains that do not initiate the germination process and thus the requisite softening of the cell wall in the aperture region might not burst at all. Consequently, the range of electric field strengths that produces bursting before affecting

germination in the central zone might have been skipped in our tests thus reducing the total percentage of bursting events. ii) The peripheral regions of the field correspond to the nonhomogeneous portion of the field (the fringing field). The fact that bursting occurred more frequently here may indicate that this inhomogeneity has a destabilizing effect on pollen grains or on the ion gradients. In either case, this observation might warrant further investigation.

4.5 Effect of Batch DC Electric Fields on Pollen Tube Orientation

To assess whether the direction of pollen tube growth is influenced by a constant field, we assessed the orientation of pollen tubes upon germination and after 2 hours in the set of experiments described above. Only pollen tubes positioned in the central zone were considered.

In Table I both the applied constant voltage and its corresponding electric field in the center zone, as predicted by the simulations, are specified. Since germination is insufficient at higher voltages, measurements were carried out up to 2.0 V. For each pollen tube the initial angle, final angle, and germination orientation measurements were quantified as explained above. The average of the angle difference in orientation, which corresponds to the final angle minus the initial angle for each pollen tube, is also indicated. Interestingly, no indication of any statistically significant preferred direction was found either upon germination or after two hours. As expected, the average initial degree for each test was close to zero. Given that the total range is from $-180°$ to $180°$, this indicates that the initial direction of the average pollen tube is essentially random. Alternatively, the zero average value could also indicate that most tubes started their growth pointing to the zero-angle direction, but the high standard deviation clearly

indicates an even distribution of the values over the available range. The average final angle for each test was also close to zero, indicating a random final orientation. Measuring the difference between the final and initial orientation of the pollen tube allowed us to estimate how much the average pollen tube changed direction while exposed to the electric field. This difference is also close to zero in average (Table I), indicating that the average pollen tube essentially maintained its direction throughout the whole test. Any changes in orientation seemed to be random. Furthermore, the standard deviation of the difference angle indicates that 68.2% of the pollen tubes deviated only within ±18.95° after germination. Consistent with this, the discrete germination orientation score showed an average close to zero, meaning that pollen tubes germinated randomly towards either microelectrode. To summarize, even though pollen tube length was critically affected, pollen tube orientation was virtually insensitive to the presence of the electric field in our tests.

Table I. Pollen tube orientation under batch DC electric fields in the center zone. The standard deviation is given in parenthesis

Voltage (V)	Electric field (V/cm)	Initial (°)	Final (°)	Difference (°)	Germination Orientation
2.0	7.1	6.80 (103.33)	15.02 (101.92)	15.31 (22.10)	-0.04
1.5	5.4	2.26 (101.97)	-1.43 (109.86)	-3.70 (16.65)	-0.06
1.0	3.6	-4.50 (101.71)	-17.63 (108.21)	-13.12 (11.58)	0.00
0.5	1.8	-0.99 (97.02)	-0.07 (92.95)	0.93 (20.02)	0.03
0.0	0.0	-7.44 (99.65)	-5.11 (103.45)	2.33 (25.26)	-0.08
	Total average	-0.77 (100.74)	-1.84 (103.29)	-1.32 (18.95)	-0.03

4.6 Effect of Batch DC Electric Fields on the Instantaneous Growth Rate

To assess the effect of a batch DC field on the instantaneous growth rate, the length of individual tubes located in the center zone was monitored over time in independent tests

(Figure 4.4a). The growth rates were normalized with respect to the highest average value in the zero-voltage test (10.94 μm/min in this series). Time lapse images were taken every 5 minutes for three hours. The data show that pollen tube growth initiated slowly and accelerated during the first two hours of the experiment, after which it reached a steady value. As the electric field increased, growth rates were reduced both during the acceleration phase and the plateau. Consistent with the previous section, an electric field above 10.7 V/cm completely prevented growth.

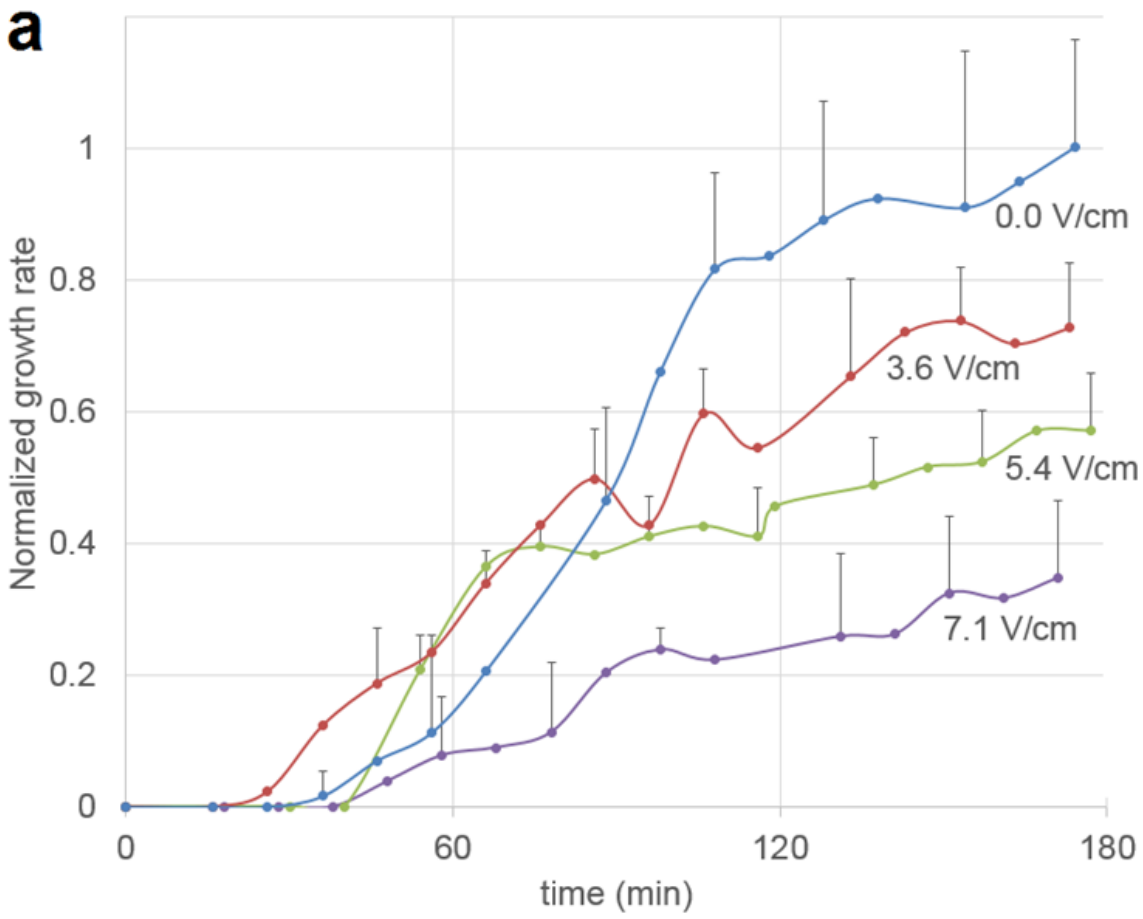

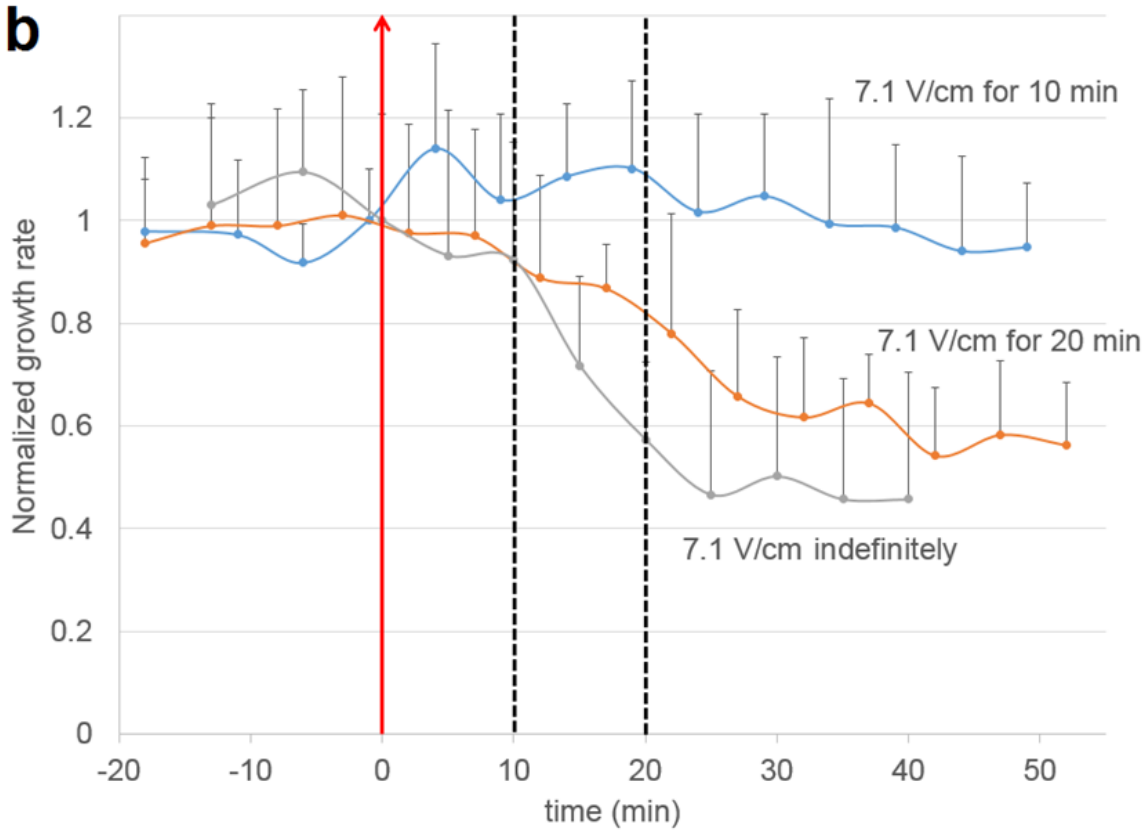

Figure 4.4 Effect of batch constant electric fields on instantaneous pollen tube growth rate. Error bars represent the standard deviation. a) Normalized growth rate for increasing values of the applied constant electric field versus time (n=13). b) Normalized growth rate when a 7.1 V/cm DC electric field is applied for 10 min, 20 min, and indefinitely. Time zero (red arrow) indicates the moment at which the electric field is switched on. Dashed lines indicate the moment at which the electric field is switched off (n=18).

In order to assess the effect of the duration of field application, a new series of tests was devised (Figure 4.4b). First pollen tubes were allowed to grow without any field applied. After 150 min, when a plateau growth rate had been reached, a strong constant field was applied (7.1 V/cm) for 10 min, 20 min, or indefinitely. The growth rate was normalized with respect to the average growth rate just prior to the electric field application: 5.59 µm/min, 6.30 µm/min, and 4.77 µm/min respectively (n=6 tubes for each). The data show that application of the field for 10 min did not alter the growth rate whereas an application for 20 min caused the growth rate to decrease. The growth rate

kept decreasing despite the field being switched off and a new steady value was reached (approximately 30 min after switching on the field). Over the period of observation the growth rate did not recover. When the electric field was kept on indefinitely the growth rate continued to decrease to an even lower steady value. For higher field strengths the growth rate not only decreased more dramatically, but pollen tubes tended to burst.

4.7 Discussion

The DC batch tests detailed in this chapter showed that electric fields inhibited pollen tube growth as determined by both total length and instantaneous growth rate. The effect was dose-dependent since stronger electric fields reduced pollen tube growth more than weaker ones. Moderate fields also caused pollen grains and tubes to burst. In this context it is remarkable that the duration of the application of the electric field seems to be important for the degree of the cellular response, and that the effect lasts beyond the period of exposure. The application of a DC field that upon continuous exposure caused a reduction in growth rate by approximately 50% did not have any visible effect when applied for 10 minutes only. However, the growth rate dropped when the application was for 20 min or longer, and this effect was not reversible upon removal of the field. Also, if a short-lived, strong electric field does not affect the growth rate significantly (as demonstrated by the 10 min applied pulse), might it act by affecting some other physiological parameter? More importantly, is recovery of the growth rate possible under different circumstances? For instance, could a systematic inclusion of medium flow through the microfluidic network re-establish normal growth rates? Is the response time in pollen tube growth rate a purely internal cell mechanism, or could it be also a

consequence of ion redistribution in the medium surrounding the cells? These questions might justify further investigation.

Concerning pollen tube orientation, no statistically significant evidence of a preferred orientation of the average pollen tube was found during the application of any DC or AC electric field when using our device. Nonetheless, sporadically an individual pollen tube exhibited a slight turn when the electric field was switched on, but at an angle well within the standard deviation of the difference angle measured in any zero-voltage test. Also, whenever this slight turn took place, it was always in a "single glitch" manner, that is, the tube slowed growth rate, turned slightly and continued growth; no accumulated turning over time resulting in a curved shape was observed in our work.

The biggest contrast between our data and those observed by Nakamura et al. (1991) on the same pollen tube species is the lack of tropic response in our hands. However, given that studies using electric fields on cells have a high incidence of contradictory findings, this is not surprising. Various pollen species have been reported to turn in different directions: towards the cathode (Nakamura et al., 1991), towards the anode (Wang et al., 1989), towards the closer electrode (Malhó et al., 1992), parallel to the electric field (Sperber, 1984), no alignment at the centre of the field (Malhó et al., 1992). Other organisms exhibit a whole range of differing responses. For instance, maize roots have been reported to grow towards the anode and towards the cathode (Ishikawa and Evans, 1990; Stenz and Weisenseel, 1993). *Funaria* moss spores tend to form rhizoids towards the positive electrode, but when DC electric fields are applied across already developed rhizoids, their subsequent growth is directed towards the negative electrode (Chen and Jaffe, 1979). Out of sixteen, eleven batches of fucoid eggs of the brown algae

Pelvetia responded by initiating rhizoids towards the positive electrode, two batches responded by growing towards the negative electrode, and three had responses of a mixed sort (Peng and Jaffe, 1976). *Neurospora crassa* and *Achlya bisexualis* mycelial fungi grew and formed branches towards the anode whereas *Aspergillus nidulans* and *Mucor mucedo* exhibited tropisms towards the cathode (McGillivray and Gow, 1986). Some animal cells even migrate to the cathode while their axis is aligned perpendicularly to the electric field (Robinson, 1985). Plausible explanations for the discrepancies in the electrically induced orientation, even in the same species, are difficult to assess mainly because the exact electrical, chemical, and mechanical conditions in which the tests are carried out are not clearly described in most articles to allow for reproduction by a different lab. Notably, the physical nature of the medium surrounding the cells might play an important role. While an electric field is likely to induce a certain motion of ions in a liquid medium, a medium stiffened by agarose or other gelling agents may behave different as it prevents the generation of convection.

Chapter 5 - Effect of AC Electric Fields on Pollen Tube Growth

5.1 Effect of Batch AC Electric Fields on Pollen Tube Growth

To assess the effect of a field with nonzero frequency, AC electric fields were employed. The voltage signal applied was of the form $v(t) = A \cdot \sin(2\pi ft)$, where v is the applied voltage as a function of time t, A is the sinusoidal wave amplitude, and f is the sinusoidal wave frequency. The same Batch ELoC and general conditions described for the DC batch tests were used. Three voltage amplitudes were selected: 1V, 2V, and 3V (which correspond to 3.6 V/cm, 7.1 V/cm, and 10.7 V/cm respectively) in order to cover the range of electric field strengths used in the DC batch tests. For each amplitude, tests were run at 0 Hz (or DC), 0.1 Hz, 1 Hz, 10 Hz, and 100 Hz. It is noted that the instantaneous electric field is still determined by the applied voltage as under DC conditions regardless of the time-varying nature of the input signal since the frequencies considered here are well within the electromagnetic quasistatic regime. The AC electric field equivalent to a given DC electric field (in the sense of the same power being delivered) is obtained by dividing the sinusoidal amplitude A by $\sqrt{2}$.

In the series shown in Figure 5.1, the average tube length throughout the LoC for the zero-voltage test was 510 μm (Table II). Therefore, pollen tube lengths were normalized with respect to this value. As expected, all tests at zero frequency resembled the DC behavior described in the previous section. Intriguingly, the application of a nonzero frequency was increasingly beneficial for pollen tube growth. As frequency increased the pollen tube length in all zones approached that of the zero-voltage control (Figure 5.1a).

This does not mean that high frequency AC fields were always without inhibitory effect since at a sufficiently high voltage (8 V amplitude, which corresponds to field strength of 28.6 V/cm) the application of a 100 Hz AC field resulted in complete growth inhibition in the center zone (Table II). It must be emphasized that the pollen is still exposed to the same instantaneous electric field strengths as those of the DC fields (up to 10.7 V/cm); it is the use of a frequency that permitted the pollen to recover its normal growth. Also, Figure 5.1b shows that the percentage of germination in AC fields was indistinguishable from the zero-voltage control for every amplitude and frequency tested, except for the case of a 10.7 V/cm amplitude field at very low frequencies. The same was true for the percentage of bursting (Figure 5.1c). The quantification of pollen tube orientation revealed that pollen tubes neither germinated nor grew into a preferred direction (Table III). It is noted that no electrolysis was observed under any AC field.

Table II. Effect of batch AC electric fields on pollen tube growth at field amplitudes 0 V/cm and 28.6 V/cm. The standard deviation is given in parenthesis. Pollen tube length was normalized with respect to 510 μm (zero-voltage test).

Amplitude	Frequency	Measurement	Center	Avg L/R	Avg Far
28.6 V/cm	100 Hz	Normalized Avg PT Length	0.0 (0.0)	0.0 (0.0)	0.1 (0.1)
		% Germination	0	0	56
		% Bursting	18	34	64
0 V/cm	0 Hz	Normalized Avg PT Length	1.0 (0.3)	0.9 (0.4)	1.0 (0.4)
		% Germination	97	98	97
		% Bursting	3	0	0

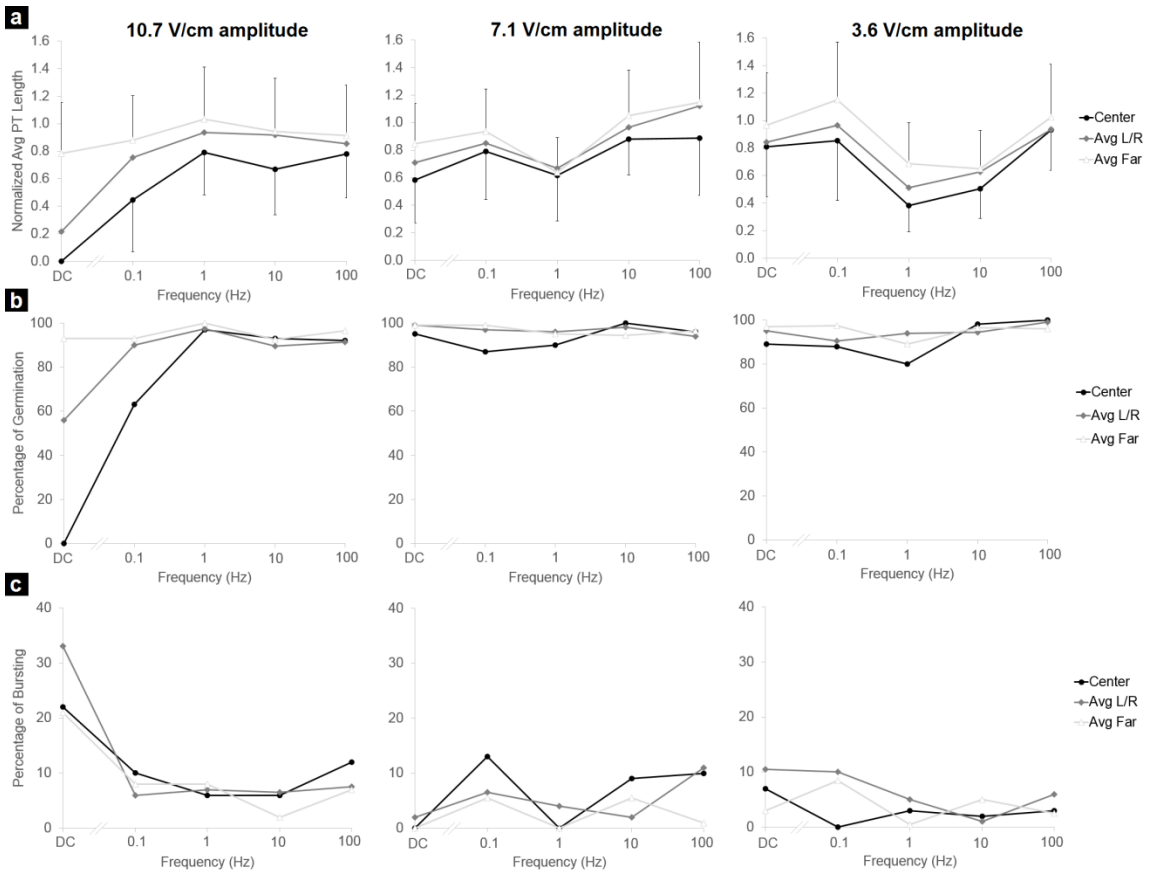

Figure 5.1 Effect of batch AC electric fields on pollen tube growth (n=3362). a) Average pollen tube length in different zones of the chamber normalized to the average control value (510 µm). b) Percentage of germination. c) Percentage of pollen bursting. The frequency applied is indicated on the x-axis. Each column corresponds to a different field amplitude. L/R = pooled data from Left and Right Zones, Far = pooled data from Far left and right zones. For clarity, the standard deviation in a) is only indicated for the Center and Far zones.

Table III. Pollen tube orientation under batch AC electric fields in the center zone. The standard deviation is given in parenthesis.

Electric field (V/cm)	Freq (Hz)	Initial (°)	Final (°)	Difference (°)	Top / Bottom
28.6	100	Does not apply			
10.7	0	Does not apply			
	0.1	13.36 (83.51)	3.43 (92.44)	-9.93 (33.23)	0.00
	1	-10.65 (102.21)	-13.10 (97.82)	-4.43 (37.62)	0.05
	10	17.80 (112.74)	25.27 (103.61)	7.46 (35.02)	-0.07
	100	-8.30 (100.24)	-7.60 (112.07)	0.70 (32.16)	0.10
7.1	0	-5.77 (103.33)	1.19 (101.91)	6.96 (21.23)	-0.04
	0.1	-10.04 (118.63)	-15.75 (120.70)	-5.71 (30.65)	-0.13
	1	5.67 (117.56)	8.67 (114.31)	3.00 (30.32)	0.00
	10	-2.15 (91.64)	-13.31 (76.10)	-11.15 (32.39)	0.08
	100	1.58 (102.76)	-0.47 (104.15)	-2.05 (20.37)	0.01
3.6	0	-4.50 (101.71)	-17.62 (108.21)	-13.12 (11.58)	0.00
	0.1	8.18 (99.08)	7.95 (108.18)	-0.23 (31.77)	-0.09
	1	0.57 (111.15)	-1.57 (117.06)	-2.14 (47.94)	0.14
	10	-4.55 (97.30)	3.18 (99.03)	7.73 (16.72)	0.09
	100	-6.07 (108.68)	-3.53 (110.54)	2.53 (36.58)	0.27
0	0	-3.57 (106.86)	5.86 (103.82)	9.43 (27.70)	-0.07
	Average	-0.56 (103.83)	-1.16 (104.66)	-0.73 (29.69)	0.02

5.2 Effect of Frequency on Pollen Tube Growth

To better assess the relationship between frequency and growth behavior we ran a new data series with field amplitude of 10.7 V/cm, a level that completely inhibited growth in the center zone at zero frequency. The tested frequencies included 10 mHz and 40 mHz, since these correspond to the inherent periodic growth oscillation in *Camellia* tubes (Sanati Nezhad et al., 2013e). The data show that as frequency increased, growth was restored (Figure 5.2). Frequencies below 100 mHz had the same effect as DC, whereas growth is fully re-established above 10 Hz.

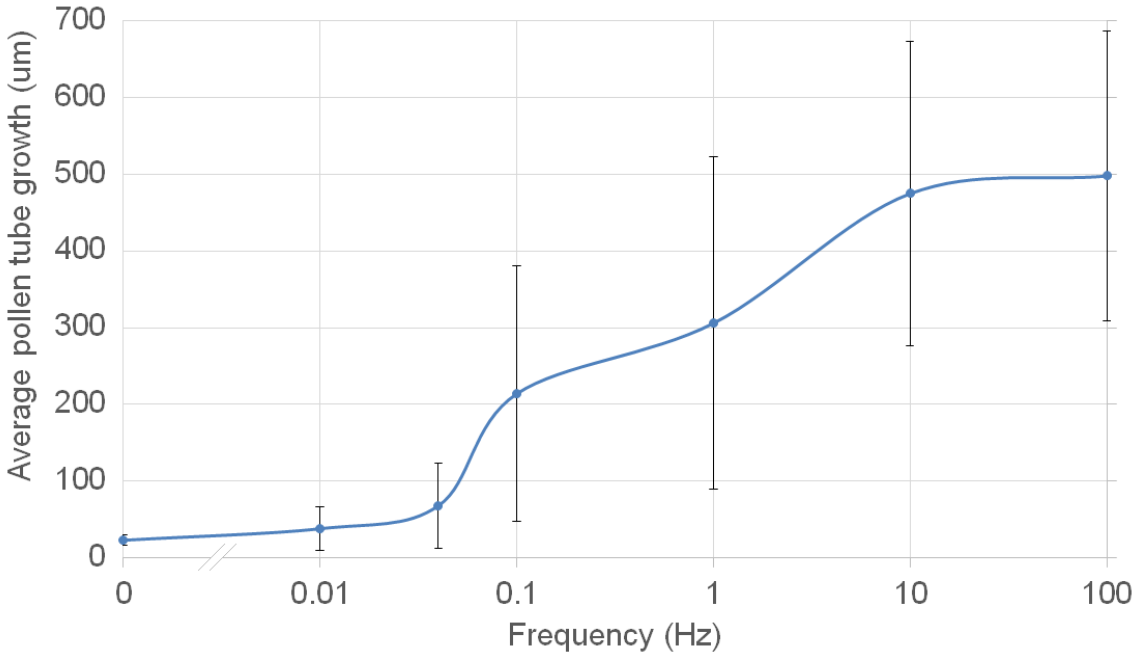

Figure 5.2 Average pollen tube length under an AC electric field in the center zone with a 10.7 V/cm amplitude (n=245). Frequency is plotted in logarithmic scale.

5.3 Effect of the Electrode Material on Pollen Tube Growth

In order to verify possible effects of using different materials for microelectrode fabrication, independent tests with copper and gold were also carried out. A zero-voltage test under no-flow conditions in a batch ELoC built with copper micro-electrodes, instead of aluminium, resulted in pollen not germinating in the center zone. Pollen tubes grew only in the far-zones. However, growth in the central zone was partially restored when culture medium was continuously pumped through the inlet at 15 µl/min. Similar inhibiting effects (18% pollen germination, 29 µm average tube length in center zone) occurred when gold electrodes were used in a zero-voltage test (no-flow). Moreover, no-flow DC tests with gold electrodes were also run with 1 V and 2 V yielding similar growth inhibition. Yet, when an AC electric field (1 V amplitude at 100 Hz) was applied

with gold electrodes (no-flow), growth was promoted dramatically (82% pollen germination, 302 μm average tube length in center zone).

5.4 Discussion

The performance of pollen tubes at higher AC frequencies is remarkable and warrants explanation. The comparison of Figure 3.7b and Figure 5.2 suggests that pollen tube performance in the electric field is related to the conductivity of the culture medium. The frequency-dependency profile of pollen tube growth matches that of medium conductivity. The similarity of the two curves is indicative of a direct correlation between conductivity and pollen tube growth. How medium conductivity influences cell growth will remain to be explored. We hypothesize that this effect is related to the conditions under which the cell is able to uptake ions. Growing pollen tubes take up several ions from the medium, an essential prerequisite for growth (Kühtreiber and Jaffe, 1990; Malhó et al., 1992; Weisenseel et al., 1979). When no electric field is applied, the ions in the medium surrounding the cell move solely by diffusion and possibly by convection. Ions entering the cell through ion channels transit these channels driven by diffusion. When a DC electric field is applied, however, the ions are accelerated directionally. The stronger the field, the more accelerated the ions. According to Figure 3.7c, a DC electric field produces a sustained electric current (which in the culture medium is composed by ions), indicating a continuous flow of ions through the medium. Therefore, there is no ion exhaustion, which could have explained the inhibition of cell growth by lack of ions. We speculate that when the DC electric field is strong enough, the ions are too accelerated to enter ion channels even when these are open. When AC fields are applied on the other hand, not only does the conductivity increase by orders of magnitude (Figure 3.7b),

which means that a considerable amount of ions become now available for uptake; but also the ion movement is likely to be oscillatory rather than unidirectional, which presumably keeps the ions spatially confined to one location that may allow them to enter the ion channels more easily.

Although the complex behaviour of medium conductivity has been acknowledged (Chandra and Bagchi, 2000), this fact has been neglected in virtually all previous studies of pollen tubes. If medium conductivity is reported at all, it is never mentioned at what frequency the measurement was taken (Crombie et al., 1990; Nakamura et al., 1991; Nozue and Wada, 1993; Platzer et al., 1997; Wang et al., 1989). Assuming conventional laboratory equipment, which uses AC fields to measure conductivity, there is an (unintended) mismatch in frequency since experimentation is carried out in DC. Moreover, the ohmic assumption of the growth medium under DC electric fields is just a first approximation since it completely neglects the electrical double layer and its capacitive effect, let alone the complex chemical reactions occurring at the interface of any metal electrode and the electrolyte (Robinson, 1968). Furthermore, the distribution of ions within the medium depends on the geometry of the experimental chamber. Depending on the set-up, the cells could be exposed to different concentrations of ions at different locations in the same testing chamber. This could be particularly significant in the many centimeter-long macroscale chambers usually used in past studies (Crombie et al., 1990; Malhó et al., 1992; Nakamura et al., 1991; Nozue and Wada, 1993; Platzer et al., 1997; Wang et al., 1989). The inconsistency in terms of conductivity determination and experimental conditions might even raise concerns about the levels of current densities reported in studies using the vibrating probe (Kühtreiber and Jaffe, 1990;

Weisenseel et al., 1975, 1979). To summarize, while it is beyond the scope of this discussion to debate the intricacies of the poorly understood electrochemistry of the situation, it is crucial to note that, according to our data, pollen growth is more likely to be influenced by the applied electric field through its effect on conductivity and ion distribution within the medium than by any direct interaction between the exogenous applied field and the endogenous electric field of the cell (Jaffe and Nuccitelli, 1977; Wang et al., 1989) .

Since the toxicity of cells due to potential electrode byproducts has been a concern in other studies (Li and Lin, 2011; Stenz and Weisenseel, 1993), the material of the microelectrodes deserves consideration. To begin with, it must be noted that even though the use of agarose salt bridges in macroscale setups might indeed delay any toxicity effect (Brower and Giddings, 1980; Burgess and Linstead, 1982; Chen and Jaffe, 1979; Malhó et al., 1992; McCaig et al., 2000; McGillivray and Gow, 1986; Nakamura et al., 1991; Peng and Jaffe, 1976; Pu and Zhao, 2005; Rajnicek et al., 1994; Wang et al., 1989; White et al., 1990), this technique does not prevent it. As long as there is a path for ions, the effect of any soluble material detaching from the electrodes remains active. Nonetheless, in a microfluidic device the distance between cells and microelectrodes is significantly reduced. The viability of aluminium as a material for microelectrodes (at least for *Camellia japonica*) was advised previously (Agudelo et al., 2013b) and confirmed in this work with DC and AC zero-voltage tests, which showed that pollen growth in the vicinity of the material was statistically indistinguishable from that located far from the electrodes. However, this is not the case for copper, nor, surprisingly, for gold. Copper caused an inhibiting effect on pollen tube growth that could be restored by continuous

medium flow injection. Even though gold has a low reactivity, it produced growth inhibition at zero, 1V, and 2V. Interestingly, growth was restored when an AC electric field (1 V amplitude at 100 Hz) was applied. The reason for this growth restoration deserves further systematic investigation, but at least these preliminary results suggest that any toxicity effect is not simply produced by the direct contact of the electrodes with the medium since the use of an AC signal alone can promote growth where a DC signal (or no signal at all) inhibits it.

Chapter 6 - Single-Cell Electric Field Application

6.1 Subcellular Electric Field Application

The experiments performed on batches of pollen suggested that the processes of grain germination and pollen tube growth are subject to distinct regulatory mechanisms. We therefore designed an experimental assay in which only the growing region of the pollen tube, not the grain, would be exposed to an electric field. The single-cell ELoC was therefore used to apply electric fields in a highly localized manner, perpendicular to the growth direction (Figure 6.1).

In order to identify the effect on the growth rate of single pollen tubes when a DC electric field is applied only to the tip of the cell, pollen was injected into the single-cell ELoC and left to germinate with no electric field applied. Most of the pollen tubes grew within the main chamber, but a few were successfully directed to the entrance of the microchannels. By the time pollen tubes grew past the microchannels into the electric chamber (2-3 hours after injection), a steady growth rate has already been attained (indicated in Figure 6.2 by the measured growth rate before time-zero).

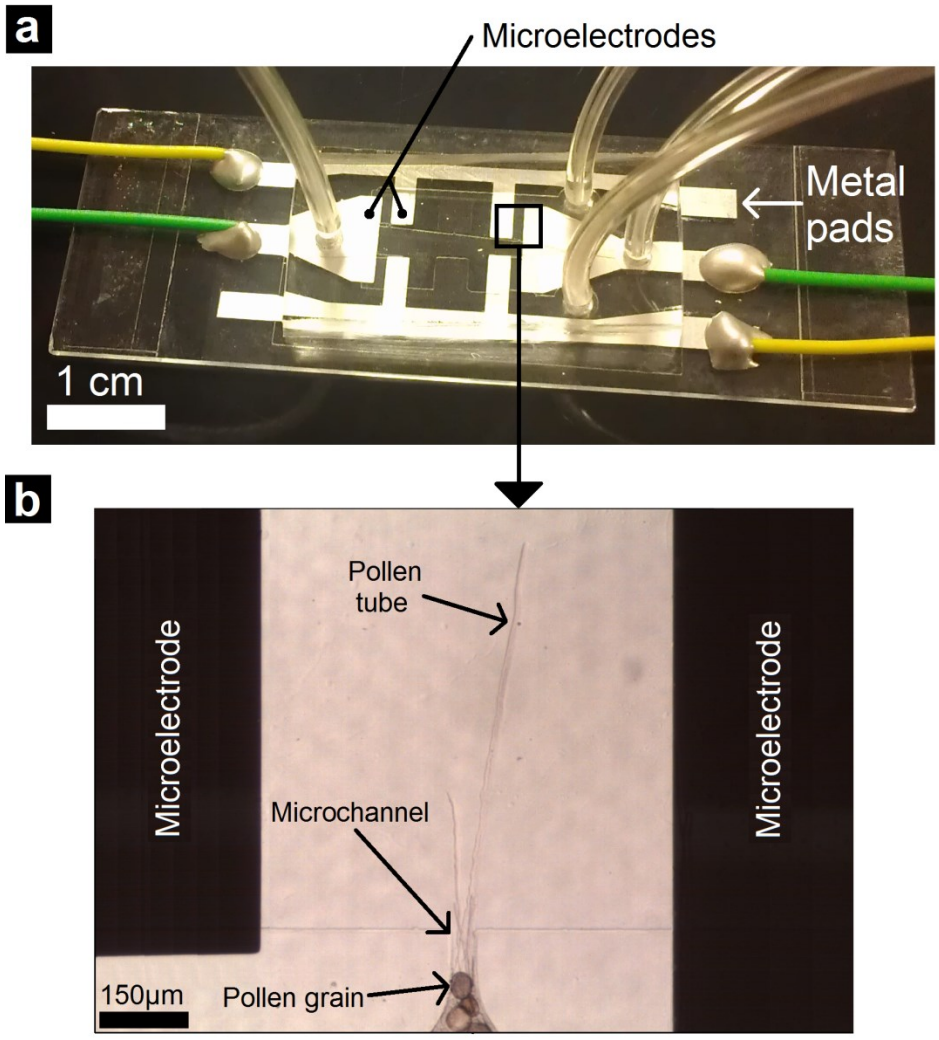

Figure 6.1 Subcellular electric field application. a) Fabricated Single-cell ELoC. b) Trapped pollen grains and exposure of pollen tubes to a local electric field.

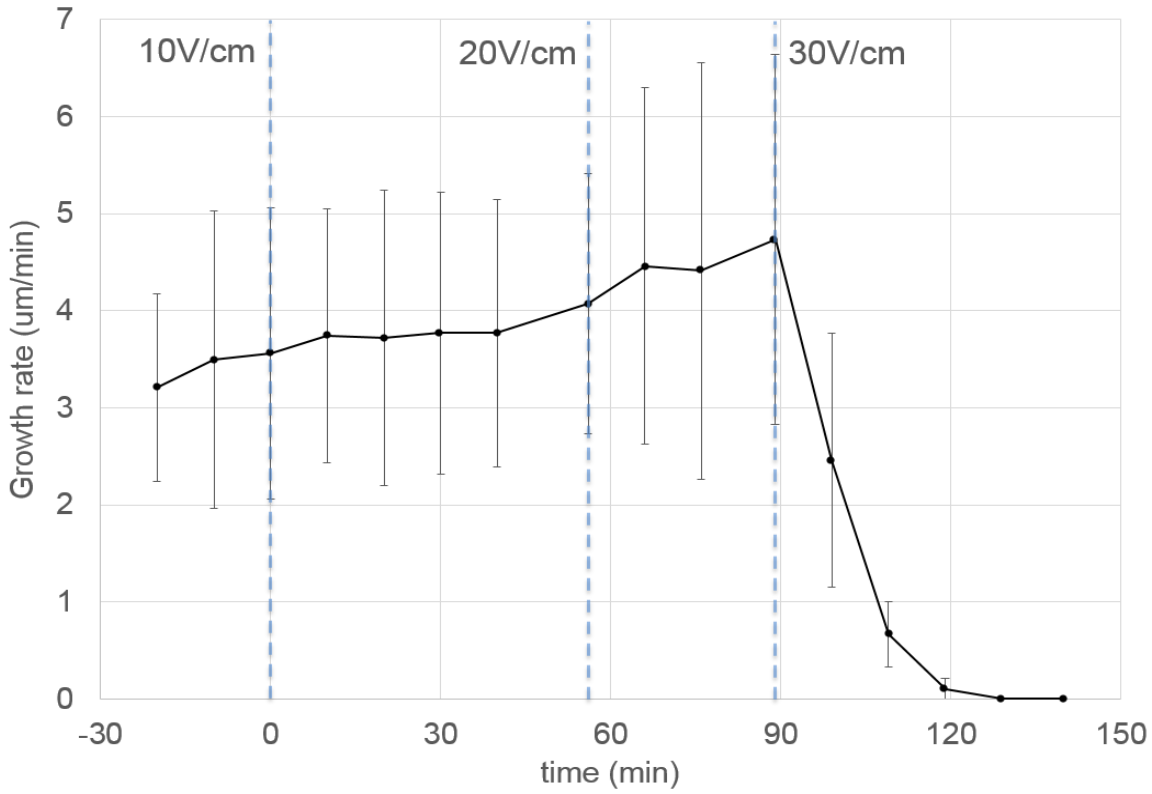

Figure 6.2 Effect of a DC electric field on the instantaneous growth rate of single pollen tubes. Time-zero indicates the instant when the initial electric field is applied. The dashed lines represent the time at which the constant electric field is increased. Error bars represent the standard deviation (n=5).

Once the growing pollen tube tip was well between the microelectrodes, an initial 10 V/cm constant electric field was applied at time-zero during approximately 1 hour. Figure 6.2 shows that the growth rate was essentially unaffected by the 10 V/cm field even though the same field strength caused growth inhibition in the batch configuration. Intriguingly, the growth rate remained relatively steady when the electric field was later increased to 20 V/cm. However, when a 30 V/cm electric field was applied, growth was promptly arrested. As a control we measured the average growth rate of pollen tubes growing in the main chamber (i.e., outside of the influence of the microelectrodes). These

were measured as 3.33 μm/min and 3.65 μm/min (n=6) at t=40 min and t=144 min, respectively, thus indicating stable growth during this stage of pollen tube development.

To assess whether pollen tubes respond in tropic manner upon application of the electric field, the orientation of the pollen tubes was measured. The angle between the growth direction and the electric field lines of each pollen tube were determined just before electric field application (initial angle), and at the end of the test (final angle). The initial angle is always close to 90° since the microchannel is directed perpendicular to the electric field lines, but a deviation from this in the final angle might indicate growth tropism. In average, the difference between the final and initial angles was measured to be 0.66° (n=12), with a standard deviation of 18.24°. These results indicate that pollen tubes essentially maintained their growth direction regardless of the presence of the electric field.

6.2 Pollen Tubes do not Avoid Electric Fields

Since the *Camellia japonica* pollen tubes located within a homogeneous electric field (batch tests) did not exhibit significant reorientation or alignment with respect to the electric field, we wanted to assess whether the tubes would at least sense and respond to a highly localized, micro-sized field. This test would also enable us to determine if a local electric field has the potential to act as an attraction or repulsion cue. To accomplish this, a single-cell ELoC was designed to trap and guide pollen tubes through a short, narrow microchannel (Figure 6.3c). If the pollen tube has any means of detecting the presence of a local high electric field as a negative directional signal, it is reasonable to expect some kind of avoidance mechanism similar to that observed in the response to certain chemical cues such as nitric oxide (Prado et al., 2004). The microchannel was designed to point the

pollen tube directly towards the local field but the microfluidic network offers the tube the option to turn away from it (Figure 6.3c).

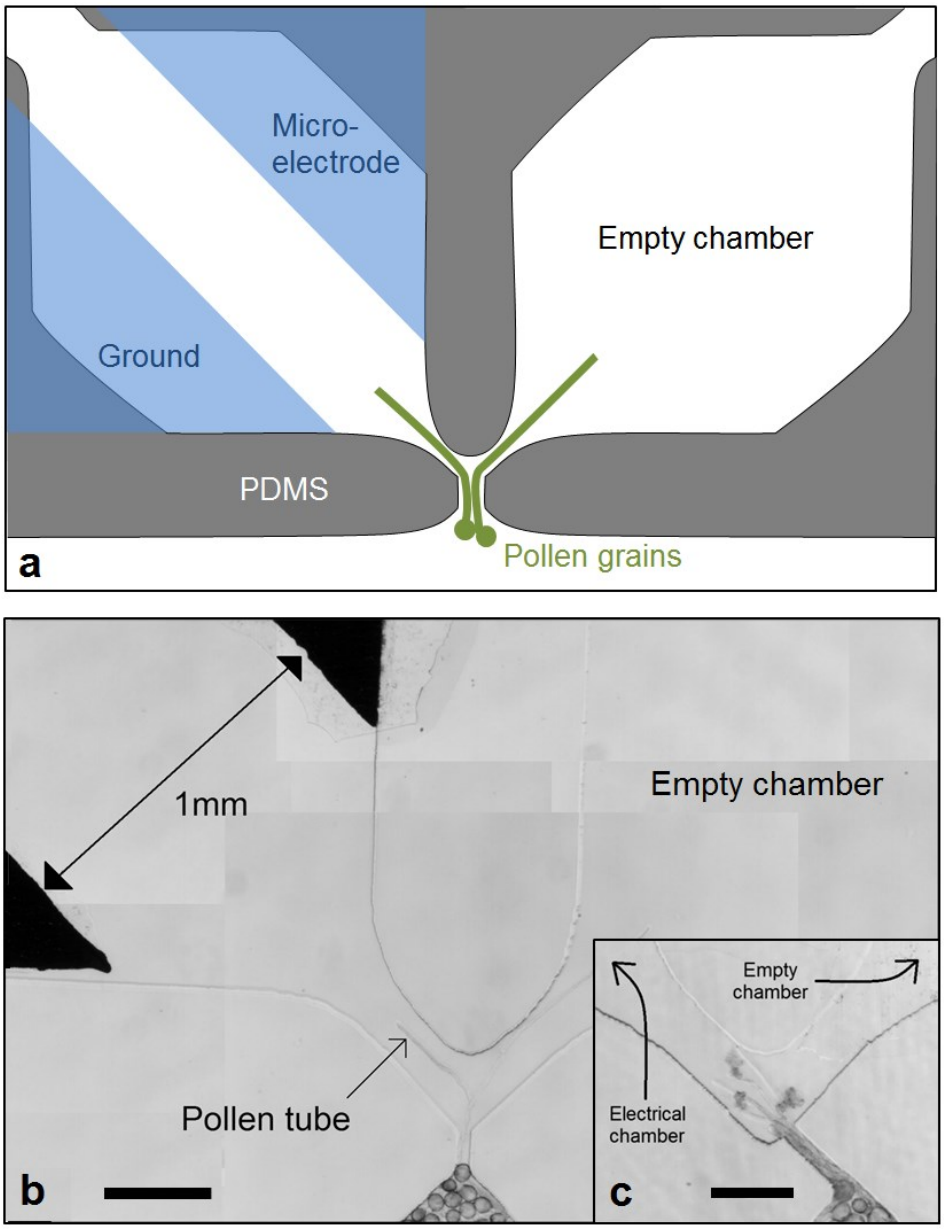

Figure 6.3 Electric field as potential guidance cue. a) Design of a microfluidic network for exposure of single pollen tubes to a local, micron-scale electric field. b) Micrograph showing pollen tubes growing from the microchannel into the chambers while constant voltage of 0.125 V is applied in the left chamber. c) Microchannel points pollen tubes directly towards a local electric field. Scale bar = 200 µm (b,c).

To perform the test, constant voltage between the two microelectrodes in the left chamber was applied once pollen grains were positioned within the device. The field strength was predicted to be highest in the space between the electrodes and to gradually decrease in direction of the microchannel. As the input voltage increases, the influence region of the electric field expands. Experimentation showed that at very high electric fields the effect clearly extended all the way to the microchannel since in this situation pollen tubes traversing the microchannel arrested growth. Therefore the test was conducted at moderate field strength.

In the presence of an intermediate voltage (2V), which produced an electric field in the direction ahead, pollen tubes did not make any attempt to turn away from the field. Despite the increasing field strength they must experience upon approaching, they continued straight and eventually displayed the symptoms established in the batch assay such as bursting or growth arrest.

6.3 Micron-scale Electric Field as Potential Guidance Cue

Since the presence of a local electric field did not produce any clear attraction or repulsion effect on pollen tubes when they were headed straight to an electric field, we modified the single-cell ELoC design to offer the pollen tube a geometrically even choice to further assess the potential role of an electric field as a guidance cue. The microchannel was set to lead to a path fork (Figure 6.3a). Once a pollen tube grows past the microchannel, it is faced with two equally weighted choices: the left branch of the fork leads to an electrical chamber in which an electric field is present (via microelectrodes), whereas the right branch leads to an identically shaped chamber that is not equipped with any electric field. If the presence of the electric field on the left side of

the fork acts as an attractant or repulsive cue, the probability of the tube growing towards this side should be significantly different from 50%. Figure 6.3b illustrates how two pollen tubes negotiate the path fork and grow into the chambers when the applied constant voltage is 0.125 V. Controls consisted in a chamber set identical to the one described but without any microelectrodes in either fork branch. This control was incorporated in the same chip and run simultaneously.

In the presence of an electric field on the left branch of the fork, pollen tubes did not behave differently from the control (Table 2). The probability of a tube to grow towards either fork branch was approximately the same (twosample t-test, P>0.78). For 2.5 V and 3 V no pollen tube grew sufficiently long to elongate beyond the fork and they tended to burst, indicating that the electric field was already too high to allow growth inside the chambers. The absence of an apparent preference at the fork suggests that the presence of a local electric field does not produce any attraction or repulsion effect on pollen tubes.

Table IV. Growth orientation at microchannel fork offering local field at one side. Absolute number of tubes observed (column 2 and 3). The probability of a tube to grow towards or away from the electric field is essentially the same (twosample t-test, P>0.78).

Applied Voltage (V)	Electric field (V/cm)	Towards field	Away from field	Towards field
0.125	1.25	3	3	50%
0.25	2.5	6	4	60%
0.375	3.75	1	1	50%
0.5	5.0	7	6	54%
0.75	7.5	2	2	50%
1.0	10.0	3	2	60%
1.5	15.0	2	1	67%
2.0	20.0	5	7	42%
2.5	25.0	0	0	Does not apply
3.0	30.0	0	0	Does not apply
Total		29	26	54%
Control		33	36	48%

6.4 Discussion

From batch tests, the critical field strength that inhibited pollen growth was approximately 10 V/cm, whereas a strength of 30 V/cm was necessary to prevent pollen tube growth when only the tip was exposed. This suggests that pollen tubes can endure stronger fields than grains. This, in turn, suggests a difference in the ion interaction occurring at the tube compared to that at the grain. In particular, the grain does not necessarily need to be exposed to electric fields to induce growth arrest. Future tests might include applying a localized electric field to the grain only, or to selected parts of the tube. Figure 6.2 also reveals a threshold-like relationship between growth and local applied constant electric field. Growth is not degraded uniformly as the field strength increases, instead there seems to be a threshold above which growth can no longer take place. This switch-like behaviour could potentially be further investigated as a biological detection system (Witters et al., 2014).

As for the significance of electrical cues in the remarkable path finding ability of the pollen tube within the flower pistil, the single-cell tests show that pollen tubes are not attracted nor repulsed by localized electric fields. Pollen tubes do not seem to make any attempt to turn away from the field; instead they just burst or arrest growth. This suggests that electrical cues might not play a significant role in coarse tracking after all, or at least that it is negligible when compared to chemical and possibly mechanical cues. Of course, electric fields do affect pollen tube growth, and in all likelihood the effect can be further investigated by, for instance, applying electric fields to different portions of the pollen tube, something LoC technology readily enables. However, the effect of an electric field as a navigating aid seems to be unlikely in pollen tubes. As long as essential ions are

available for uptake, mechanical and chemical cues seem to dominate guidance. Actually, one may argue that chemistry and mechanics are, at least in part, the effects of electrical phenomena at the atomic scale.

Chapter 7 - Conclusions and Future Work

7.1 Conclusions

A LoC with a structured microenvironment and integrated microelectrodes for the systematic *ex-vivo* application of global and local electric fields to pollen tubes was designed, fabricated, and validated.

We extensively tested various field strengths and types (DC and AC) and correlated *Camellia japonica* pollen tube response with the conductivity of the growth medium surrounding the cells. We tested the application of both global and local fields. Our data reveal significant differences with experiments performed in macroscopic open-assay setups and suggest that the electric field is mediated by ion movement in the medium surrounding the cells rather than by a direct effect on the cell.

The DC batch tests showed that the presence of an electric field inhibited pollen tube growth. However, unlike previous studies, our systematic approach revealed a complex fact: AC fields restored pollen tube growth for frequencies greater than 100 mHz. Importantly, this recovery of growth was achieved under the same strong field strengths (up to 10.71 V/cm) that caused complete growth inhibition at lower frequencies and DC fields. This indicates that pollen cells can in fact tolerate strong electric fields and still perform normal growth—as long as these are applied in form of high frequency AC fields. To our knowledge, this is the first direct comparison of the effect of DC and AC electric fields on the same cell type in any eukaryotic or prokaryotic cell.

Pollen tube tips were exposed to localized electric fields with the aim to provoke an avoidance mechanism. These single-cell tests show that pollen tubes are not attracted nor repulsed by localized electric fields, suggesting that the electrical cue might not play a significant role in pollen tube guidance

This work presented the ELoC as a cost-effective solution for efficient electrical assays on a tip-growing cell in a structured microenvironment. Design challenges for reusability were considered and addressed, resulting in a modular approach: a microfluidic network on a microelectrode substrate. Improvements on the architecture of the microfluidic network for tip-growing cells have also been included, namely the trapezoid-shaped main chamber. The integration of microelectrodes has been described in detail, in particular, fabrication, reusability, and electrical modeling.

7.2 Future Work

There is plenty of room for research as the techniques used in this work can be generalized to any other growing cell and allow for the inclusion or variation of specific features in a systematic manner. For example, changing the microelectrode configuration, modifying the culture medium contents, applying the same tests to another species, devising more involved and ingenious micron-scale tests, among others, might help further elucidate the influence of electric fields on cell growth.

Nevertheless, a few concrete points to tackle next can be mentioned:

- Use fluorescence spectroscopy in conjunction with ELoC in order to monitor the possible rearrangement of internal organelles while the pollen tube is exposed to an electric field.

- Use ratiometric ion imaging in conjunction with the ELoC in order to monitor ion motion while the pollen tube is exposed to an electric field.
- Application of an electric field to the pollen grain only or to parts of the tube only. Conversely, measure endogenous electric fields along the pollen tube as to improve on the vibrating electrode.
- Systematic study of the effect of medium flow on growth direction (without and with an electric field applied).
- Pursue AC fields growth enabling (as opposed to growth restoration) with gold electrodes described in section 5.3.
- Localized tests (along the tube) on cell osmotic pressure dynamics using directed laminar flow of water (without and with an electric field applied).
- Combination of chemical and electrical cues.
- Apply similar tests to neurons.

References

Agudelo, C.G., Sanati Nezhad, A., Ghanbari, M., Packirisamy, M., and Geitmann, A. (2012). A microfluidic platform for the investigation of elongation growth in pollen tubes. J Micromechanics Microengineering. *22*, doi:10.1088/0960-1317/22/11/115009.

Agudelo, C.G., Packirisamy, M., and Geitmann, A. (2013a). Lab-on-a-Chip for studying growing pollen tubes. In: Plant Cell Morphogenesis: Methods and Protocols, Series "Methods in Molecular Biology", eds. Žárský V, Cvrčková F, Springer, pp 237-248.

Agudelo, C.G., Sanati Nezhad, A., Ghanbari, M., Naghavi, M., Packirisamy, M., and Geitmann, A. (2013b). TipChip: a modular, MEMS-based platform for experimentation and phenotyping of tip-growing cells. Plant J Cell Mol Biol. *73*, 1057–1068.

Benkert, R., Obermeyer, G., and Bentrup, FW. (1997). The turgor pressure of growing lily pollen tubes. Protoplasma. *198*, 1–8.

Blasiak, J., Mulcahy, D.L., and Musgrave, M. (2001). Oxytropism: a new twist in pollen tube orientation. Planta. *213*, 318–322.

Boedicker, J.Q., Vincent, M.E., and Ismagilov, R.F. (2009). Microfluidic confinement of single cells of bacteria in small volumes initiates high-density behavior of quorum sensing and growth and reveals its variability. Angew Chem Int Ed. *48*, 5908–5911.

Bove, J., Vaillancourt, B., Kroeger, J., Hepler, P.K., Wiseman, P.W., and Geitmann, A. (2008). Magnitude and direction of vesicle dynamics in growing pollen tubes using spatiotemporal image correlation spectroscopy and fluorescence recovery after photobleaching. Plant Physiol. *147*, 1646–1658.

Brewbaker, J.L., and Kwack, B.H. (1963). The essential role of calcium ion in pollen germination and pollen tube growth. Am J Bot. *50*, 859–865.

Brower, D.L., and Giddings, T.H. (1980). The effects of applied electric fields on Micrasterias. II. The distributions of cytoplasmic and plasma membrane components. J Cell Sci *42*, 279–290.

Burgess, J., and Linstead, P.J. (1982). Cell-wall differentiation during growth of electrically polarised protoplasts of *Physcomitrella*. Planta. *156*, 241–248.

Campetelli, A., Bonazzi, D., and Minc, N. (2012). Electrochemical regulation of cell polarity and the cytoskeleton. Cytoskeleton. *69*, 601–612.

Chandra, A., and Bagchi, B. (2000). Frequency dependence of ionic conductivity of electrolyte solutions. J Chem Phys. *112*, 1876–1886.

Chebli, Y., and Geitmann, A. (2007). Mechanical principles governing pollen tube growth. Funct Plant Sci Biotechnol. *1*, 232–245.

Chen, T.-H., and Jaffe, L.F. (1979). Forced calcium entry and polarized growth of Funaria spores. Planta. *144*, 401–406.

Cheung, A.Y., Wang, H., and Wu, H.M. (1995). A floral transmitting tissue-specific glycoprotein attracts pollen tubes and stimulates their growth. Cell. *82*, 383–393.

Cooper, J.R., Qin, Y., Jiang, L., Palanivelu, R., and Zohar, Y. (2009). Microsystem-based study of pollen-tube attractants secreted by ovules. In: IEEE 22nd International Conference on MEMS 2009, pp. 208–211.

Crombie, C., Gow, N.A., and Gooday, G.W. (1990). Influence of applied electrical fields on yeast and hyphal growth of *Candida albicans*. J Gen Microbiol. *136*, 311–317.

Bou Daher, F., and Geitmann, A. (2011). Actin is involved in pollen tube tropism through redefining the spatial targeting of secretory vesicles. Traffic. *12*, 1537–1551.

Fayant, P., Girlanda, O., Chebli, Y., Aubin, C.-É., Villemure, I., and Geitmann, A. (2010). Finite element model of polar growth in pollen tubes. Plant Cell. *22*, 2579–2593.

Feijó, J.A., Malhó, R., and Obermeyer, G. (1995). Ion dynamics and its possible role during in vitro pollen germination and tube growth. Protoplasma. *187*, 155–167.

Feijó, J.A., Sainhas, J., Hackett, G.R., Kunkel, J.G., and Hepler, P.K. (1999). Growing pollen tubes possess a constitutive alkaline band in the clear zone and a growth-dependent acidic tip. J Cell Biol. *144*, 483–496.

Geitmann, A., and Palanivelu, R. (2007). Fertilization requires communication: signal generation and perception during pollen tube guidance. Floric Ornam Biotechnol. *1*, 77–89.

Gossot, O., and Geitmann, A. (2007). Pollen tube growth: coping with mechanical obstacles involves the cytoskeleton. Planta. *226*, 405–416.

Gray, J., Chaloner, W.G., and Westoll, T.S. (1985). The microfossil record of early land plants: advances in understanding of early terrestrialization. Philos Trans R Soc Lond B Biol Sci. *309*, 167–195.

Holdaway-Clarke, T.L., and Hepler, P.K. (2003). Control of pollen tube growth: role of ion gradients and fluxes. New Phytol. *159*, 539–563.

Ishikawa, H., and Evans, M.L. (1990). Electrotropism of maize roots role of the root cap and relationship to gravitropism. Plant Physiol. *94*, 913–918.

Jaffe, L.F., and Nuccitelli, R. (1977). Electrical controls of development. Annu Rev Biophys Bioeng. *6*, 445–476.

Jones, T. (1995). Electromechanics of particles. Cambridge University Press. 288p.

Kristen, U., and Kappler, R. (1995). The pollen tube growth test. In: In Vitro Toxicity Testing Protocols, Series "Methods in Molecular Biology", Springer Protocols, *43*, pp. 189–198.

Kühtreiber, W.M., and Jaffe, L.F. (1990). Detection of extracellular calcium gradients with a calcium-specific vibrating electrode. J Cell Biol. *110*, 1565–1573.

Langdon, P.G., Barber, K.E., and Morriss, S.H.L.-C. (2004). Reconstructing climate and environmental change in northern England through chironomid and pollen analyses: evidence from Talkin Tarn, Cumbria. J Paleolimnol. *32*, 197–213.

Li, J., and Lin, F. (2011). Microfluidic devices for studying chemotaxis and electrotaxis. Trends Cell Biol. *21*, 489–497.

Lush, W.M. (1999). Whither chemotropism and pollen tube guidance?. Trends Plant Sci. *4*, 413–418.

Malhó, R. (1998). Pollen tube guidance–the long and winding road. Sex Plant Reprod. *11*, 242–244.

Malhó, R. (2006). The Pollen Tube: a cellular and molecular perspective. Springer-Verlag Berlin Heidelberg. 295p.

Malhó, R., Feijó, J.A., and Pais, M.S.S. (1992). Effect of electrical fields and external ionic currents on pollen-tube orientation. Sex Plant Reprod. *5*, 57–63.

Marsh, G., and Beams, H.W. (1945). The orientation of pollen tubes of *Vinca* in the electric current. J Cell Comp Physiol. *25*, 195–204.

Mascarenhas, J.P., and Machlis, L. (1964). Chemotropic response of the pollen of *Antirrhinum majus* to Calcium. Plant Physiol. *39*, 70–77.

McCaig, C.D., Sangster, L., and Stewart, R. (2000). Neurotrophins enhance electric field-directed growth cone guidance and directed nerve branching. Dev Dyn. *217*, 299–308.

McCaig, C.D., Rajnicek, A.M., Song, B., and Zhao, M. (2005). Controlling cell behavior electrically: current views and future potential. Physiol Rev. *85*, 943–978.

McGillivray, A.M., and Gow, N.A.R. (1986). Applied electrical fields polarize the growth of mycelial fungi. J Gen Microbiol. *132*, 2515–2525.

Melling, A. (1997). Tracer particles and seeding for particle image velocimetry. Meas Sci Technol. *8*, 1406–1416.

Messerli, M.A., Danuser, G., and Robinson, K.R. (1999). Pulsatile influxes of H^+, K^+ and Ca^{2+} lag growth pulses of *Lilium longiflorum* pollen tubes. J Cell Sci. *112*, 1497–1509.

Messerli, M.A., Créton, R., Jaffe, L.F., and Robinson, K.R. (2000). Periodic increases in elongation rate precede increases in cytosolic Ca^{2+} during pollen tube growth. Dev Biol. *222*, 84–98.

Michard, E., Alves, F., and Feijó, J.A. (2009). The role of ion fluxes in polarized cell growth and morphogenesis: the pollen tube as an experimental paradigm. Int J Dev Biol. *53*, 1609–1622.

Morgan, H., and Green, N. (2003). AC electrokinetics: colloids and nanoparticles. Research Studies Press. 360p.

Nahmias, Y. (2009). Methods in bioengineering: microdevices in biology and medicine. Artech House.

Nakamura, N., Fukushima, A., Iwayama, H., and Suzuki, H. (1991). Electrotropism of pollen tubes of camellia and other plants. Sex Plant Reprod. *4*. 138–143.

Nozue, K., and Wada, M. (1993). Electrotropism of *Nicotiana* pollen tubes. Plant Cell Physiol. *34*, 1291–1296.

Okuda, S., and Higashiyama, T. (2010). Pollen tube guidance by attractant molecules: LUREs. Cell Struct Funct. *35*, 45–52.

Palanivelu, R., and Preuss, D. (2000). Pollen tube targeting and axon guidance: parallels in tip growth mechanisms. Trends Cell Biol. *10*, 517–524.

Parre, E., and Geitmann, A. (2005). Pectin and the role of the physical properties of the cell wall in pollen tube growth of Solanum chacoense. Planta. *220*, 582–592.

Peng, H.B., and Jaffe, L.F. (1976). Polarization of fucoid eggs by steady electrical fields. Dev Biol. *53*, 277–284.

Pierson, E.S., Miller, D.D., Callaham, D.A., Shipley, A.M., Rivers, B.A., Cresti, M., and Hepler, P.K. (1994). Pollen tube growth is coupled to the extracellular calcium ion flux and the intracellular calcium gradient: effect of BAPTA-type buffers and hypertonic media. Plant Cell. *6*, 1815–1828.

Platzer, K., Obermeyer, G., and Bentrup, F.-W. (1997). AC fields of low frequency and amplitude stimulate pollen tube growth possibly via stimulation of the plasma membrane proton pump. Bioelectrochem Bioenerg. *44*, 95–102.

Prado, A.M., Porterfield, D.M., and Feijó, J.A. (2004). Nitric oxide is involved in growth regulation and re-orientation of pollen tubes. Development. *131*, 2707–2714.

Pu, J., and Zhao, M. (2005). Golgi polarization in a strong electric field. J Cell Sci. *118*, 1117–1128.

Rajnicek, A.M., McCaig, C.D., and Gow, N.A. (1994). Electric fields induce curved growth of *Enterobacter cloacae*, *Escherichia coli*, and *Bacillus subtilis* cells: implications for mechanisms of galvanotropism and bacterial growth. J Bacteriol. *176*, 702–713.

Robinson, D.A. (1968). The electrical properties of metal microelectrodes. Proc. IEEE. *56*, 1065–1071.

Robinson, K.R. (1985). The responses of cells to electrical fields: a review. J Cell Biol. *101*, 2023–2027.

Robinson, K.R., and Messerli, M.A. (2003). Left/right, up/down: the role of endogenous electrical fields as directional signals in development, repair and invasion. BioEssays. *25*, 759–766.

Sanati Nezhad, A., and Geitmann, A. (2013). The cellular mechanics of an invasive lifestyle. J Exp Bot. *64*, 4709–4728.

Sanati Nezhad, A., Naghavi, M., Packirisamy, M., Bhat, R., and Geitmann, A. (2013a). Quantification of cellular penetrative forces using lab-on-a-chip technology and finite element modeling. Proc Natl Acad Sci. *110*, 8093–8098.

Sanati Nezhad, A., Naghavi, M., Packirisamy, M., Bhat, R., and Geitmann, A. (2013b). Quantification of the Young's modulus of the primary plant cell wall using Bending-Lab-On-Chip (BLOC). Lab Chip. *13*, 2599–2608.

Sanati Nezhad, A., Ghanbari, M., Agudelo, C.G., Packirisamy, M., Bhat, R.B., and Geitmann, A. (2013c). PDMS microcantilever-based flow sensor integration for Lab-on-a-Chip. IEEE Sens J. *13*, 601–609.

Sanati Nezhad, A., Ghanbari, M., Agudelo, C.G., Naghavi, M., Packirisamy, M., Bhat, R.B., and Geitmann, A. (2013d). Optimization of flow assisted entrapment of pollen grains in a microfluidic platform for tip growth analysis. Biomed Microdevices. *16*, 23–33.

Sanati Nezhad, A., Packirisamy, M., Bhat, R., and Geitmann, A. (2013e). In vitro study of oscillatory growth dynamics of *Camellia* pollen tubes in microfluidic environment. IEEE Trans Biomed Eng. *60*, 3185–3193.

Sawidis, T., and Reiss, H.-. D. (1995). Effects of heavy metals on pollen tube growth and ultrastructure. Protoplasma. *185*, 113–122.

Spanjers, A.W. (1981). Bioelectric potential changes in the style of Lilium longiflorum Thumb. after self- and cross-pollination of the stigma. Planta. *153*, 1–5.

Sperber, D. (1984). Das Wachstum pflanzlicher Zellen und Organe im magnetischen und elektrischen Feld. Konstanzer Dissertationen. Hartung-Gorre.

Sperber, D., Dransfeld, K., Maret, G., and Weisenseel, M.H. (1981). Oriented growth of pollen tubes in strong magnetic fields. Naturwissenschaften. *68*, 40–41.

Stahlberg, R. (2006). Historical overview on plant neurobiology. Plant Signaling and Behavior. *1*, 6–8.

Stenz, H.-G., and Weisenseel, M.H. (1993). Electrotropism of maize (*Zea mays L.*) roots. Plant Physiol. *101*, 1107–1111.

Vanapalli, S.A., Duits, M.H.G., and Mugele, F. (2009). Microfluidics as a functional tool for cell mechanics. Biomicrofluidics. *3*. doi:10.1063/1.3067820.

Velve-Casquillas, G., Le Berre, M., Piel, M., and Tran, P.T. (2010). Microfluidic tools for cell biological research. Nano Today. *5*, 28–47.

Wang, P., and Liu, Q. (2010). Cell-based biosensors: principles and applications. Artech House. 271p.

Wang, C., Rathore, K.S., and Robinson, K.R. (1989). The responses of pollen to applied electrical fields. Dev Biol. *136*, 405–410.

Weisenseel, M.H., and Jaffe, L.F. (1976). The major growth current through *Lily* pollen tubes enters as K^+ and leaves as H^+. Planta. *133*, 1–7.

Weisenseel, M.H., Nuccitelli, R., and Jaffe, L.F. (1975). Large electrical currents traverse growing pollen tubes. J Cell Biol. *66*, 556–567.

Weisenseel, M.H., Dorn, A., and Jaffe, L.F. (1979). Natural H^+ currents traverse growing roots and root hairs of barley (*Hordeum vulgare L.*). Plant Physiol. *64*, 512–518.

White, R.G., Hyde, G.J., and Overall, R.L. (1990). Microtubule arrays in regenerating *Mougeotia* protoplasts may be oriented by electric fields. Protoplasma. *158*, 73–85.

Whitesides, G.M. (2011). What Comes Next?. Lab Chip. *11*, 191–193.

Witters, D., Sun, B., Begolo, S., Rodriguez-Manzano, J., Robles, W., and Ismagilov, R.F. (2014). Digital biology and chemistry. Lab Chip. *14*, 3225–3232.

Wulff, H.D. (1935). Galvanotropismus bei Pollenschläuchen. Planta. *24*, 602–608.

Yetisen, A.K., Jiang, L., Cooper, J.R., Qin, Y., Palanivelu, R., and Zohar, Y. (2011). A microsystem-based assay for studying pollen tube guidance in plant reproduction. J Micromechanics Microengineering. *21*. doi:10.1088/0960-1317/21/5/054018

Zeijlemaker, F.C.J. (1956). Growth of pollen tubes in vitro and their reaction on potential differences. Acta Bot Neerlandica. *5*, 179–186.

Ziaie, B., Baldi, A., Lei, M., Gu, Y., and Siegel, R.A. (2004). Hard and soft micromachining for BioMEMS: review of techniques and examples of applications in microfluidics and drug delivery. Adv Drug Deliv Rev. *56*, 145–172.

Zonia, L., Cordeiro, S., Tupy, J., and Feijó, J.A. (2002). Oscillatory chloride efflux at the pollen tube apex has a role in growth and cell volume regulation and is targeted by inositol 3,4,5,6-Tetrakisphosphate. Plant Cell. *14*, 2233–2249.

Appendix A - PDMS-based Bendable 2D Load Sensor Integration for Lab-on-a-Chip

A.1 Introduction

The proposed 2D Load sensor provides a low-cost, reliable solution to accurately measure a load in a 2D domain noninvasively. Additionally, operation can be performed in a bent configuration. The sensor operates in both static and dynamic conditions. Since the device is made with standard microfabrication techniques it can be easily integrated into MEMS devices or designed for stand-alone operation.

A.2 Design Principle

The proposed 2D load sensor makes use of a set of distributed load cells. A load cell consists of a planar microfluidic chamber and a pair of sensing microelectrodes. The chamber is patterned in a soft polymer which forms the top layer that is to interact with the load. Figure A.1 shows the structural design of the proposed 2D load sensor with four (4) load cells. Each load cell is filled with a conductive fluid which makes for a nominal electrical resistance value between a pair of microelectrodes. When load is applied from the top, the cell shape is deformed, effectively reducing the volume of the cell as the ceiling gets pushed downwards. Such reduction in volume results in less conductive fluid inside the chamber, which increases the nominal electrical resistance of the cell. Then, by monitoring the value of this electrical resistance, the cell load intensity can be measured. Since there is a corresponding electrical resistance for every load condition, then the

sensor operates in both static and dynamic regimes. Furthermore, since electrical dynamics is considerably faster than mechanical dynamics then the sensor output follows closely the applied load dynamics. Also, the transduction of the mechanical load to electrical signals greatly facilitates the data acquisition. Figure A.2 shows a designed load cell with its electrical simulation.

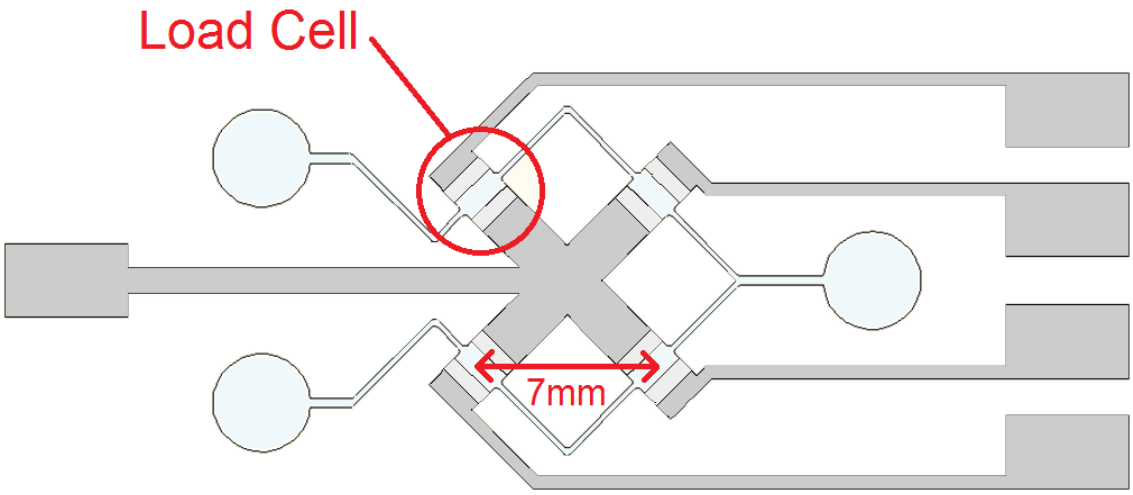

Figure A.1 Schematic representation of the 2D load sensor with four (4) load cells. Gray filled pattern represents the electrical layer whereas the light blue pattern represents the microfluidic network

If only one cell were to be used then only information on the intensity of the load would be available. A direct relationship can be found that relates the applied load to the cell shape deformation and ultimately to the fluid electrical resistance. However, if more than one cell is employed then information on the position of the load can be derived. For instance, by comparing the relative intensity between two adjacent cells one can deduce the intensity and location of a concentrated load along the straight line that connects them. Therefore, in order to measure a load in one axis several cells can be put in a linear configuration. The amount of cells is determined by the range and resolution required in both space and intensity, and by the effective area of the applied load which can be

concentrated or distributed. This concept can be easily extended to 2D by employing a matrix of cells. The design presented in this work makes use of four (4) load cells in a square configuration as a case study, which is the basic unit of a 2D matrix arrangement. Nonetheless, the number of cells is by no means limited to four; on the contrary, the use of more complex configurations is particularly encouraged by the planar microfabrication techniques at hand which are capable of handling very small features sizes and is only restrained by the complexity of the electrical routing.

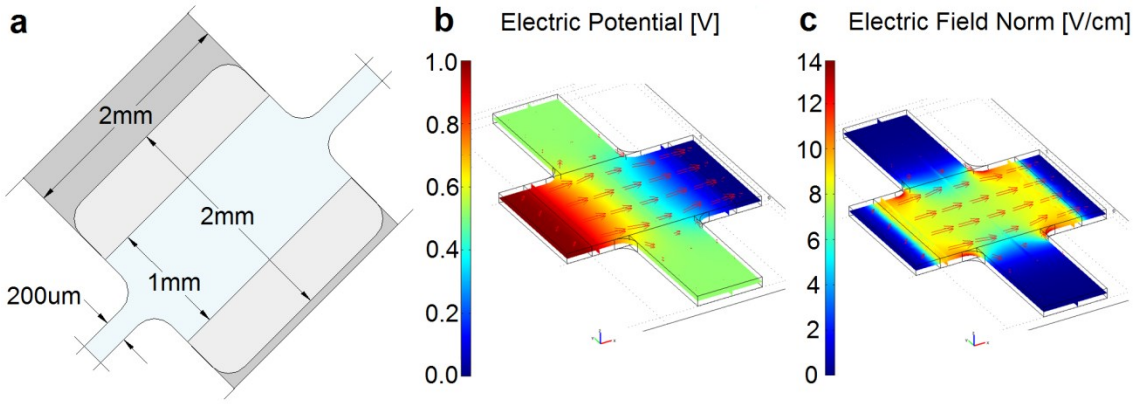

Figure A.2 The Load Cell. a) Schematic. b) Simulated voltage distribution when 1V is applied between the microelectrodes. c) Simulated electric field when 1V is applied.

The microfluidic network is composed of one inlet, two outlets, load cells, and fluid interconnections paths as shown in Figure A.1. The conductive fluid used is saline water, which is an inexpensive and ubiquitous electrolyte. The conductivity determines the nominal load cell resistance and can be easily set by the quantity of salts dissolved. Depending on the sensitivity of the electrical equipment to be used for data acquisition, the conductivity can be set to a value that ensures a suitable range of measurement. It is noted that only AC signals are applied to the load cell in order to avoid the occurrence of electrolysis, which would be inevitable should DC signals be used. Furthermore, electrolysis not only adds undesired electrical currents, contaminating the electrical

output signal, but also affects the electrode/electrolyte interface since it may chemically etch or deposit material on the microelectrodes, and hence deteriorate the sensor performance and durability. It is also noted that saline water conductivity, as with any other electrolyte, has a nonlinear dependency on the frequency. Fortunately, once a suitable setting is chosen, operation of the load sensor is ensured.

A.3 Sensor Fabrication

For rigid sensors, the electrical pattern can be reproduced on a Printed Circuit Board (PCB) using well known circuit manufacturing techniques, which offers an inexpensive and more accessible alternative to common conductive layer deposition techniques. The microfluidic network can then be attached to the PCB substrate to complete the sensor fabrication. Figure A.3 shows a PCB-based fabricated sensor and the experimental setup used to test it. The exact load sensor dimensions are shown in Figure A.4. It is noted that the PDMS bulk height h (Figure A.4) is critical in the sensor design since it plays an important role in the sensitivity and range of operation of the load sensor.

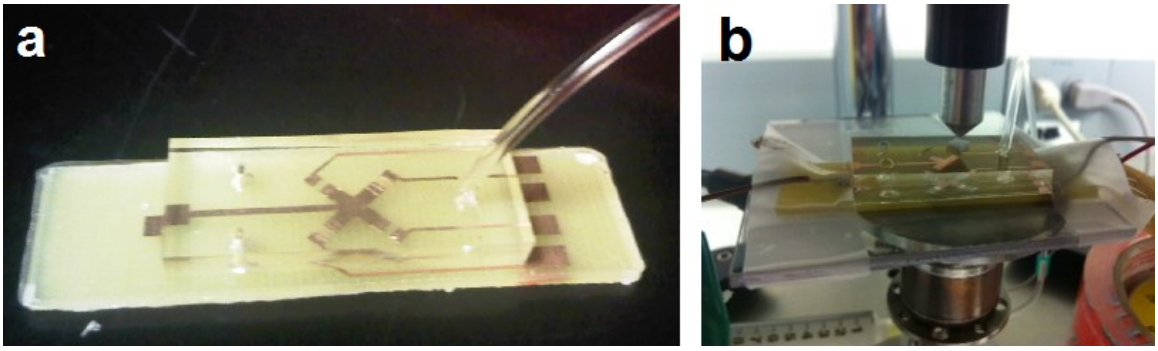

Figure A.3 PCB-based rigid sensor. a) Fabricated sensor. b) 2D load sensor under test while a concentrated force is being applied.

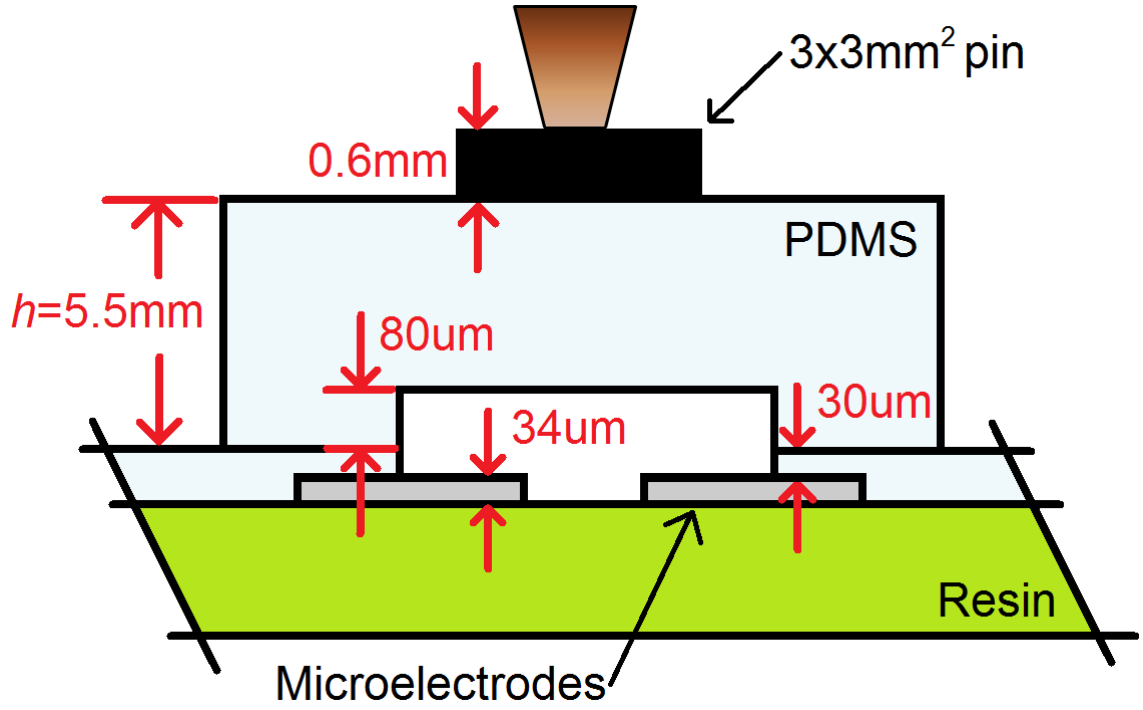

Figure A.4 Front view of a single load cell.

On the other hand, a bendable sensor can be obtained by employing a suitable thin film metal layer on a PDMS substrate. This sensor can be fabricated using the techniques described in chapter 3. Figure A.5 shows a fabricated bendable sensor in operation while being subjected to a bent configuration.

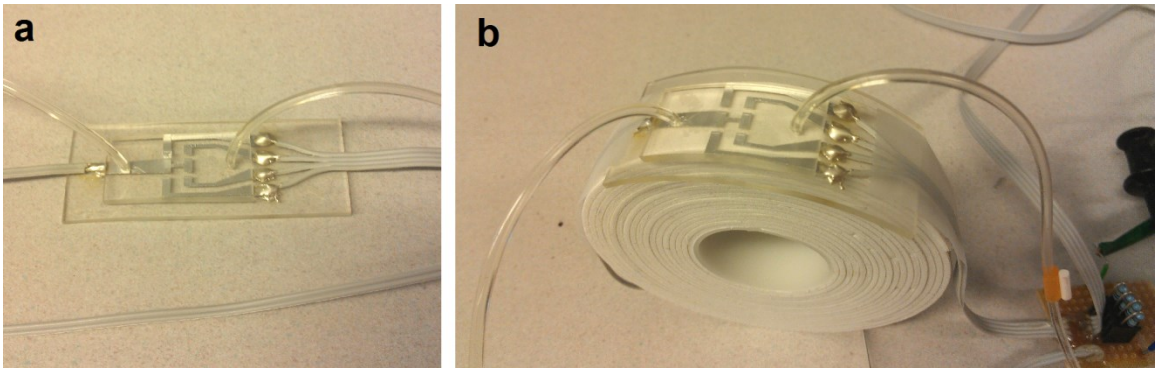

Figure A.5 PDMS-based bendable sensor. a) Fabricated sensor. b) 2D load sensor in a bent configuration.

A.4 Experimental Results

An experimental setup was used to test the proposed 2D load sensor by means of a Bose ElectroForce® device. Using a DAQ (NI PCI-6225), the converted electrical signals are next digitalized and recorded using LabVIEW software. The Bose ElectroForce® device uses a conical-shaped aluminum indenter to apply a concentrated force of desired intensity. The sensor was tested by applying a concentrated force at different locations (Figure A.6). A step force of 10N was applied in all cases. The applied reference input to the sensor is a sinusoidal of amplitude 8V and frequency 20Hz. Figure A.6 shows how the output signals from each load cell correlate well in intensity depending on the location of the applied load. Based on the electrical output of the load cells, an algorithm can be used to determine the exact position and intensity of the applied load.

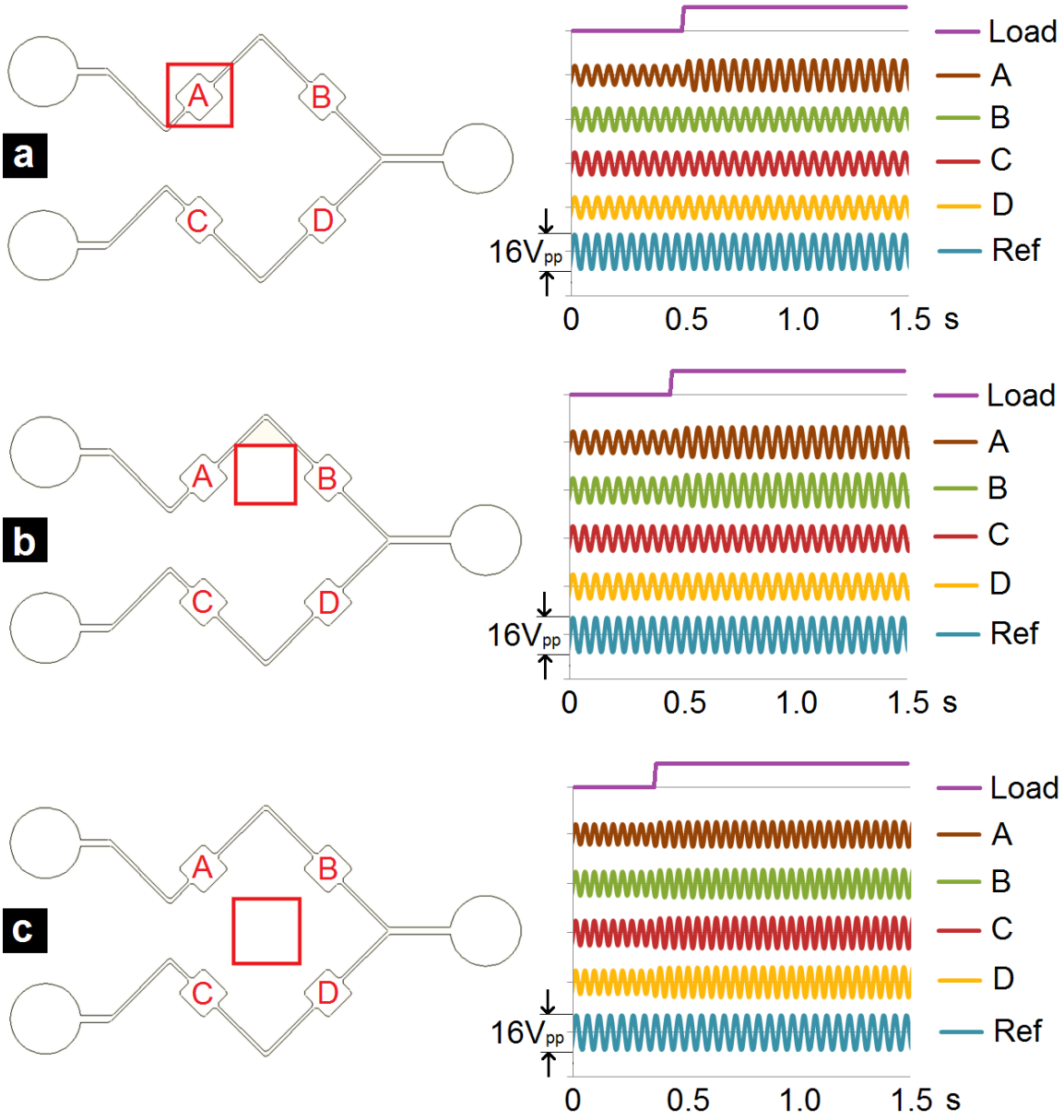

Figure A.6 2D sensor testing. Localized loads of 10N a) directly on a load cell, b) between two load cells, and c) in the center of a matrix of load cells.